

NATIONAL UNIVERSITY OF SCIENCES & TECHNOLOGY
COLLEGE OF ELECTRICAL AND MECHANICAL ENGINEERING,
RAWALPINDI, PAKISTAN



**A Numerical and Experimental Investigation of “Open-hole
Compression” testing method for 3D woven fibre reinforced polymeric
composites**

By

Mr. Muhammad Kamran

MS-64 (Mechanical Engineering)

(2010-NUST-MS-PhD-Mech-22)

**Thesis submitted to the Department of Mechanical Engineering, National
University of Sciences and Technology, College of Electrical and Mechanical
Engineering, Rawalpindi, Pakistan in partial fulfillment of the requirements for
the degree of Masters of Science in Mechanical Engineering**

Thesis Supervisor

Dr. Rizwan Saeed Choudhry



**In the name of Allah
The most beneficent and The most Merciful**

CERTIFICATE OF COMPLETENESS

It is hereby certified that the dissertation submitted by NSMuhammad Kamran, Reg No.2010-NUST-MS-PhD-Mech-22, Titled: A Numerical and Experimental Investigation of “Open-hole Compression” testing method for 3D woven fibre reinforced polymeric composites has been checked/reviewed and its contents are complete in all respects.

Supervisor's Name: **Dr. RizwanSaeedChoudhry** Signature: _____

Date: _____

DECLARATION

I hereby declare that this thesis is entirely and purely my own work and based on my personal efforts and intellect under the guidance and supervision of my thesis supervisor

“Dr. RizwanSaeedChoudhry”

All the sources used in this thesis are properly cited and no portion of this thesis is an act of plagiarism. This work is purely done for the fulfillment of requirements for aforementioned degree in respective department. No part of this thesis is submitted for any other application for any degree or qualification in this or any other university, degree awarding or non-degree awarding college or institute.

Signature: _____

Muhammad Kamran

ACKNOWLEDGMENT

I would like to thank Almighty Allah; whose guidance lead this work to be completed in time and whose blessings and benevolent help kept me sheltered all the time. I would like to express my sincere gratitude to my advisor Dr. RizwanSaeedChoudhry for continuous support, for his patience, motivation, enthusiasm, and immense knowledge. His guidance helped me in all the time of research and writing of this thesis.

Besides my advisor, I would like to thank the rest of my thesis committee members Dr S. WaheedulHaq, Dr. Aamer A. Baqai, and Dr. S. Kamran Afaqfor their encouragement and insightful comments.

I would like to thank my beloved parents and family, who always guided me in right manner and whose endless effort and support made it possible for me, to be, what I am today. I would not forget to thank my dear friends like Mr. HaroonIqbal Mr. ShehzadAslam and MrYasir Abbas for always being there for me. I have been fortunate to have met and work with many wonderful people likeDrLaraib, Mr. WaleedMirza, Mr. TalhaSolaija, Mr. Salman Siddiqui, MrMaaz Hassan, MrFahad Hassan, MrAbid, MrRizwan-ul-Haq, MrZulfiqar, Mr Kamran Nazir, MrSharjeelandMrKhurram who made my time at college enjoyable and whose continuous encouragement made it possible for me to reach all the way to this point.

Last but not the least my sincere thanks go to National Composites Certification and Evaluation Facility (NCCEF), University of Manchester, UK and HITEC University, Taxila for providing me continuous technical support to accomplish my task. In addition I would also like to acknowledge the financial support of DFID, UK and British Council as part of the DelpHE project “Capacity building for enhancing R&D in composite materials”. This enabled me to obtain valuable training at NCCEF, University of Manchester, UK.

Muhammad Kamran kayani

13, Sep, 2013

ABSTRACT

3D composites due to high delamination resistance are replacing the laminated composites in many applications. Messier-Dowty's landing gear strut for Boeing 787, JSF inlet duct and Snecma motor's aero-engine fan blade are some of the high profile aerospace applications of 3D woven composites. Holes are unavoidable in aerospace applications and can significantly affect the structural strength of any material and 3D composites are no exception. Currently ASTM D6484, an open-hole compression standard test method developed for 2D composites is being used for measuring the notched compressive strength of 3D woven composites. Since this test method was developed for 2D composites it is arguable whether the standard should be applied as it is for 3D composites. Thus, the aim of this project is to understand the failure stress state of OHC specimens by using FE and experimental techniques. To achieve this objective, ABAQUS 6.10 a commercial FE package is used to simulate the standard open-hole compression test so that the stress state in the specimen near the point of failure can be studied in detail. FE Models were built from three different types of elements i.e. the conventional shell, continuum shell and solid elements. These models are validated by simulating the OHC testing of 2D continuous fiber-reinforced carbon/epoxy composites for which the experimental results are taken from the literature. It was found that solid elements provided better results and with these elements it was also straight forward to implement the fully orthotropic material definition required for modeling the behavior of 3D composites. Thus these were then used to study the failure modes of 2D and 3D GFRP woven composites. Experimental work on 2D and 3D woven GFRP OHC composite specimens was performed partially at NCCEF (National Composites Certification and Evaluation Facility), University of Manchester, UK and HITEC University, Pakistan.

Detailed numerical and experimental study has shown that the damage modes developed in 2D and 3D GFRP woven composites were analogous. Similarly, magnitudes of longitudinal, transverse and in-plane stresses were observed in both composites. On the contrary, out of plane stresses were found significantly higher in 3D woven composites as compared to 2D woven composites due to 3rd directional reinforcement i.e. the z-yarns, however this increase in out of plane stress is not so significant as to cause change in dominant damage mode.. Conclusively, ASTM D6484 an open-hole compression standard test method was found reliable testing technique for 3D woven composites.

TABLE OF CONTENTS

1.1	Background.....	14
1.1.1	What are 3D woven composites?	14
1.1.2	Advantages of 3D woven composites over 2D laminates.....	14
1.1.3	Applications of 3D textile composites	14
1.1.4	Problem	15
1.2	Review of modeling strategies	15
1.3	Need.....	16
1.3.1	Manufacturing Defects	17
1.3.2	Structural complexities.....	18
1.3.3	Fibre architecture.....	18
1.3.4	Out of plane properties	18
1.3.5	Inter-laminar properties.....	19
1.4	Objective.....	19
1.4.1	Extent of damage prediction	19
1.4.2	Inhomogeneous stress concentration.....	19
1.4.3	Singularity of Inter-laminar stress state	19
1.4.4	Kinking.....	20
1.4.5	Effects of geometric parameters.....	20
1.4.6	Dominant Failure mode.....	20
1.4.7	Percent bending	20
1.4.8	Loading configuration effects	21
1.4.9	High standard deviations	21
1.4.10	Size of RVE.....	21
1.4.11	Test parameters	21
1.5	Methodology.....	22
1.5.1	FE macro-mechanical model.....	23
1.5.2	Experimental work	23
1.6	Scope	23

2.1	Introduction	24
2.2	Open-hole compression	24
2.2.1	Point stress criterion	24
2.2.2	Average stress criterion	25
2.3	Compressive testing of composite materials	25
2.3.1	Multidirectional laminated composites (UD).....	25
2.3.2	Woven composites	28
2.4	Mechanical modeling of composites	32
2.4.1	Numerical modeling.....	32
2.4.2	Experimentation	33
2.5	Concluding remarks.....	35
3.1	Introduction	37
3.2	Numerical modeling	38
3.2.1	Multidirectional carbon fibre reinforced laminated composite.....	38
3.2.2	2D and 3D woven GFRP composites.....	50
3.3	Experimentation.....	52
3.3.1	Panel fabrication.....	52
3.3.2	Fibre volume fraction determination.....	52
3.3.3	Specimen preparation	52
3.3.4	Hole preparation	52
3.3.5	Stacking sequence	52
3.3.6	Thickness scaling	53
3.3.7	Failure load determination	54
3.3.8	Damage analysis and microscopy	54
3.4	Concluding remarks.....	55
4.1	Introduction	56
4.2	Multidirectional (UD) carbon fibre composites	56
4.2.1	Stress analysis of a laminated CFRP composite	56
4.2.2	Damage analysis.....	65
4.3	2D and 3D woven GFRP composite.....	73

4.3.1	Experimental results.....	73
4.3.2	Numerical findings.....	79
4.4	Concluding remarks.....	88
5.1	Introduction	89
5.2	Comparison of 2D and 3D woven composites	89
5.3	Limitations.....	90
5.3.1	Numerical modeling.....	90
5.3.2	Experimental work	91
5.4	Future recommendations	91
	Publication	94

LIST OF FIGURES

Figure 1: Methodology.....	22
Figure 2: Failure modes of the specimen	34
Figure 3: Hierarchal approach of FE modeling.....	38
Figure 4: Loading condition (Front and rear sides of the specimen).....	39
Figure 5: X-symmetric BC (i.e. symmetric in 1 direction)	39
Figure 6: Y-symmetric BC (i.e. symmetric in 2 direction)	39
Figure 7: $U_3=0$, BC (Front and rear sides of the specimen).....	40
Figure 8: $UR_1=UR_2=UR_3=0$ BC (Front and rear sides of the specimen)	40
Figure 9: Compressive stress vs. number of elements (conventional shell model).....	44
Figure 10: Compressive strain vs. number of elements (conventional shell model).....	44
Figure 11: Longitudinal displacement vs. number of elements (conventional shell model)	45
Figure 12: Compressive stress vs. number of elements (continuum shell model).....	46
Figure 13: Compressive strain vs. number of elements (continuum shell model).....	46
Figure 14: Longitudinal displacement vs. number of elements (continuum shell model).....	47
Figure 15: Compressive stress vs. number of elements (solid model)	48
Figure 16: Compressive strain vs. number of elements (solid model)	48
Figure 17: Longitudinal displacement vs. number of elements (solid model)	49
Figure 18: Path selected to study the difference of stress state in 2D and 3D composite.....	51
Figure 19: Support fixture assembly	54
Figure 20: A zoomed view of longitudinal compressive stress variation near the hole at ply-14(Conventional shell model).....	58
Figure 21: A zoomed view of longitudinal compressive stress variation near the hole at ply-14(Continuum shell model).....	59
Figure 22: Longitudinal compressive stress variation near the hole (Solid model)	59
Figure 23: A zoomed view of longitudinal compressive stress variation near the hole (Solid model)	60
Figure 24: A zoomed view of transverse stress variation near the hole at ply-14(Conventional shell model).....	61
Figure 25: A zoomed view of transverse stress variation near the hole at ply-14 (Continuum shell model).....	61
Figure 26: A zoomed view of transverse stress variation near the hole (Solid model)	62
Figure 27: A zoomed view of in-plane stress variation near the hole at ply-14 (Conventional shell model).....	62
Figure 28: A zoomed view of in-plane stress variation near the hole at ply-14 (Continuum shell model)	63
Figure 29: A zoomed view of in-plane stress variation near the hole (solid model).....	63

Figure 30: A zoomed view of through thickness stress variation near the hole (solid model).....	64
Figure 31: Results of compressive fibre failure at ply-2. A zoomed view near the hole.....	67
Figure 32: Results of compressive fibre failure at ply-4. A zoomed view near the hole.....	68
Figure 33: Results of compressive fibre failure at ply-1. A zoomed view near the hole.....	68
Figure 34: Results of compressive matrix failure at ply-16. A zoomed view near the hole.....	69
Figure 35: Results of compressive matrix failure at ply-2. A zoomed view near the hole.....	70
Figure 36: Results of tensile matrix failure at ply-1. A zoomed view near the hole	70
Figure 37: Results of tensile matrix failure at ply-4. A zoomed view near the hole	71
Figure 38: A zoomed view of maximum normalized stress failure near the hole	72
Figure 39: A zoomed view of von-Mises failure near the hole	72
Figure 41: Load displacement curves of 2D woven GFRP composite specimens	75
Figure 42: Load displacement curves of 3D woven GFRP composite specimens	75
Figure 43: Stress strain diagram of 2D woven GFRP composite specimens	76
Figure 44: Stress strain diagram of 3D woven GFRP composite specimens	76
Figure 45: Damaged specimens of 2D woven GFRP composites-A zoomed view	77
Figure 46: Damaged specimens of 2D woven GFRP composites- Zoomed views are taken by using overhead projector	78
Figure 47: Damaged specimens of 3D woven GFRP composites-A zoomed view	78
Figure 48: Damaged specimens of 3D woven GFRP composites- Zoomed views are taken by using overhead projector	78
Figure 49: Longitudinal stress variation along path-1.....	79
Figure 50: Longitudinal stress variation along path-2.....	80
Figure 51: Longitudinal stress variation along path-3.....	80
Figure 52: Longitudinal stress variation along path-4.....	81
Figure 53: Transverse stress variation along path-1	81
Figure 54: Transverse stress variation along path-2.....	82
Figure 55: Transverse stress variation along path-3	82
Figure 56: Transverse stress variation along path-4.....	83
Figure 57: Through thickness stress variation along path-1	83
Figure 58: Through thickness stress variation along path-2.....	84
Figure 59: Through thickness stress variation along path-3	84
Figure 60: Through thickness stress variation along path-4.....	85
Figure 61: In-plane stress variation along path-1	85

Figure 62: In-plane stress variation along path-2	86
Figure 63: In-plane stress variation along path-3	86
Figure 64: In-plane stress variation along path-4	87
Figure 65: Effect of hole diameter variation on OHC strength of 3D woven GFRP composites.....	87

LIST OF TABLES

Table 1: Standards currently used for the testing of 3D FRP composites	17
Table 2: Element type used to develop FE models	37
Table 3: Dimensions of the specimen	39
Table 4: Engineering constants required to define material models	41
Table 5: Mesh convergence results of conventional shell model	43
Table 6: Mesh convergence results of continuum shell model	45
Table 7: Mesh convergence results of solid model	47
Table 8: Experimental results of UD carbon fibre composite	49
Table 9: Strength properties of UD carbon fiber lamina	50
Table 10: Material Properties of GFRP composite	51
Table 11: Specimen dimensions	52
Table 12: Thickness details of 3D specimens	53
Table 13: Thickness details of 3D specimens	53
Table 14: Ply by ply results of conventional and continuum shell element models for UD carbon fibre laminate	57
Table 15: Results of solid element model for UD carbon fibre laminate	57
Table 16: Maximum longitudinal compressive stress in different models	58
Table 17: Maximum transverse stress in different models	60
Table 18: Output variables available in ABAQUS for Hashin damage	66
Table 19: Results of output variables for prediction of damage initiation	66
Table 20: Failure loads of 3D specimens	73
Table 21: Failure loads of 2D specimens	74

CHAPTER 1: INTRODUCTION

1.1 Background

3D composites have been developed as smart structural materials for multi-directional loading and impact applications [1]. Introduction of bias yarns in transverse (out of plane) direction not only increases their through thickness properties but also significantly improves the delamination resistance [1]. Following is the introduction of 3D woven composites, benefits of 3D woven composites over 2D laminated composites, applications of 3D composites and the problems which are being facing by the industry about the testing techniques of 3D composites.

1.1.1 What are 3D woven composites?

A preforming process will be known as 3D weaving if yarns are supplied from two or more perpendicular directions. The process also involves the insertions of one or more sets of yarns into other sets of yarns. Therefore, the fabrics produced from this technique will have 3D shape and the yarns will be in three or more directions [2].

1.1.2 Advantages of 3D woven composites over 2D laminates

Some of the major advantages of 3D woven composites over 2D laminates are as under;

- 3D weaving is capable of producing near-net-shape preforms which significantly reduces the material cost and handling time.
- 3D weaving products can give complex integrated structures which tend to have better mechanical properties.
- In 3D composites, through-thickness properties variation could be possible by controlling the amount of fibres in 3rd direction.
- 3D woven composite have high impact failure resistance and low velocity impact failure resistance as 3rd directional reinforcement absorbs significant amount of impact stresses. This improves the post-impact mechanical response of 3D woven composites as compared to 2D laminates.
- 3D woven composites have higher failure strains as compared to 2D laminates.
- 3D woven fabrics have very good formability as they have very low shear moduli's.

1.1.3 Applications of 3D textile composites

Some of the high profile applications of 3D textile composites are as under [2,3];

- Aircraft fuselage panels
- Aircraft brakes

- JSF inlet duct and
- Biteam's beam

1.1.4 Problem

Manufacturer's demand of 3D composites is increasing day by day due to their high strength to weight ratios and cost effective products. Recently, industry has put a serious demand of 3D woven composites for manufacturing of high end applications such as aerospace (fairings), military (Body armors), automotive etc. but moving from 2D to 3D composites is not straight forward due to fundamental differences in mechanics [4]. Similarly, standardized testing methodologies are needed for 3D composites because the most commonly used coupon testing standards such as CRAG, ASTM and MIL standards (MIL-HDBK-17) are not able to provide reliable testing techniques for 3D composite materials [5].

To adopt 3D composites as working materials researchers are forced to use the 2D testing standards for testing of 3D composites. This leads towards faulty prediction of mechanical properties of composite materials. Therefore, there is a need to highlight the problems in existing testing standards/practices being followed and to identify the standards on which immediate work can be carried out with a view to develop specific standards for testing 3D composites.

1.2 Review of modeling strategies

Number of modeling strategies has been developed to determine the mechanical properties of 2D and 3D composites. As this work mainly consists of numerical analysis so basic understanding about these techniques is mandatory. Following is the review of basic modeling strategies.

Crimp Model also known as **Fiber inclination model (FIM)** was developed to determine the elastic properties of 2D woven composites and is being used for 3D woven composites. The model is based on classical laminate theory (CLT) i.e. a unit cell approach is used in which undulating yarns are considered as piece-wise straight [6]. Similarly, **Fabric Geometry Model (FGM)** is also based on unit cell approach and is being used for 3D woven composites. In this approach, unit cell is further segregated into sub-cells where each sub-cell represents one fiber bundle. Furthermore, compliance matrix of each sub cell is generated and added to evaluate the elasticity of whole unit cell. In this regard, Samer et al. observed that these techniques are not suitable for shear-moduli prediction therefore they proposed a modified FGM in which each yarn system was considered as a combination matrix and a yarn layer [7].

Effective Response Comparison (ERC) is a representative volume/macro-cell based technique for determining the properties of angle interlock weaves. In this model, macro-cell is divided into elements known as unit cells whose stiffness is calculated by using fiber tow geometry and constituent's stiffness. Microscopic stiffness of macro-cell is then determined by using the load sharing relations between the unit cells[8].

FEM based unit cell approach are available for prediction of stiffness properties of 3D composites e.g. μ -Tex-10 and mTex-20.

BINMOD code is a numerical technique for modeling the fibre reinforced composites. In this approach, line elements are used to model the fiber tow axial properties and effective medium elements are used to model the shear and transverse properties of composite. The technique can also be used for handling interlock weaves, nonlinear effects, progressive failure and large strains[9,10].

WEAVE is a numerical technique for determining the stiffness properties of 3D composites i.e. orthogonal interlock, layer to layer and through the thickness. The program initially selects the micromechanical model on the basis of elastic constants of pre-impregnated tows by using the fiber and matrix properties, and then performs the laminate analysis for prediction of macroscopic stiffness[10].

TEXCAD is developed for calculating the elastic properties of 2D weaves but it is also able to model 3D interlock weaves by using unit cell approach. This software has the capabilities to better predict the non linear stress strain and shear response of yarns. Conclusively, it can include the effect of wrinkling and straightening of yarns at different sections and also able to model the progressive damage [11].

TEXCOMP, CCM-TEX, Mosaic models, Orienting averaging models, Mixed iso-strain and iso-stress models, Inclusion model, Finite element model etc are the different modeling strategies being employed to determine the properties of 3D composites [1,12]. All of these techniques are used to calculate the stiffness coefficients, elastic constants, binder effects of 3D composites etc. but are not able to predict the stress state developed within the specimen of 3D composite.

1.3 Need

3D woven composites are being demanded by high profile applications so it is need of time that there must be testing standards which can provide true measures of properties of these materials for design and analysis. There are still no proper testing standards for 3D composites as these are relatively new materials and it is only now that there wide spread use

is being anticipated. Another hurdle in developing these standards is the difficulty of correctly modeling the internal stress state due to a given loading.

Standards currently available and being used for the testing of 3D composites are the same as that used for the 2D composites [12]. Some of the methods that are currently employed are shown in the table 1 [13,14]

Table1: Standards currently used for the testing of 3D FRP composites

Test Method	Property Measured	Measured Property
D 3039	In-Plane Tensile	Tensile strength
D 3410	In-Plane Compression	Compressive strength
D 3518	In-Plane Shear	Shear strength, Shear modulus, Stress-strain response
D 4255	In-Plane Shear	Shear strength, Shear modulus, Stress-strain response
D 5379	Out-of-Plane Shear	Inter-laminar shear strength, Inter-laminar shear modulus
D 790	Laminate Flexural	Flexural strength, Flexural modulus, Flexural stress-strain response
D6484	OHC strength	Open-hole compressive strength

These methods do not necessarily generate the desired stress state within the specimen and consequently may show higher magnitudes of standard deviations and coefficient of variance. This may lead towards the faulty prediction of structural properties [12].

Higher values of standard deviations in measuring properties of various composites indicate that testing methods in Table 2 may not be reliable and should not be used e.g. states that 3D specimens all failed in crushing (CRAG short beam shear test)[12].

Some common problems due to which 2D standards cannot be used for the testing of 3D composites are discussed as under;

1.3.1 Manufacturing Defects

Adoption of 2D weaving machines and devices for manufacturing of 3D preforms create extensive fibre crimp & waviness which damages the properties i.e. stiffness, strength etc of the fabric so the understanding about how the properties of the 3D preforms vary by changing their manufacturing techniques is mandatory [1].

3D woven composites have various geometric variations due to the several process windows being adopted by the manufactures in the introduction of the bias yarn as

reinforcement. Complexity of interlacing and interweaving yarns in three directions cause significant variation and in homogeneity within the structure which then introduces the local displacement fields [14].

During the determination of rate dependent compression response of 3D woven composites M. Pankow reported that there is a strain non uniformity within the composite due to the local displacement fields which in turn deviate the values of stress which make the results unreliable[15].

It can be concluded that, manufacturing flaws may introduce the local displacement fields which affects the strain uniformity and may be the cause of faulty results. Thus, there must be different testing standards for 3D woven composites which can include the effect of tolerances in geometrical parameters involved within the structure.

1.3.2 Structural complexities

Out of plane fibres improves the out of plane tensile and shear strength but reduce in-plane properties which affects the failure modes [16]. This happens due to high fibre crimp in warp direction which may introduce new failure mode in compression i.e. compressive fibre failure of 3D composites occur at an angle with respect to 2-axis due to high crimp in warp direction [12]. Crimp due to complex interlacing of yarns not only reduces the fibre volume fraction of the composite (max. Up to 55%) but also creates in-homogeneity of local displacement fields [3]. These complexities makes the understanding ambiguous for a particular test due to combined failure modes involved in 3D woven composites e.g. Wen-Shyong Kuo [17] reported that yarns at different orientations behave differently in response of loading. Warp and weft yarns come under a shear force and binder yarn will be under tensile and compressive load.

Several modifications have been made to ensure the dominant mode of failure is e.g. Yu.Mtarnopol'ski proposed extra notches through specimen width in Iosipescu shear test method to make the specimen failure possible in pure shear mode[18].

1.3.3 Fibre architecture

There is a significant micro-structural difference between 2D and 3D composites. Large size unit cell of 3D composites may be the cause of variation in stress state than 2D composites. [19].

1.3.4 Out of plane properties

CRAG short beam shear method is not able to quantify the difference between the failure modes of 2D and 3D composites. Similarly, out-of-plane test is not able to give true

out-of plane strength of 3D material due to adhesive failure between specimens and loading cylinders [12].

1.3.5 Inter-laminar properties

Two procedures are currently used for improvement of through-thickness properties i.e. by adding secondary fibre reinforcement in the direction perpendicular to in-plane reinforcement (i.e. z-pinning, stitching) and by changing the orientation of primary fibres reinforcement with respect to secondary fiber reinforcement i.e.3D weaving. Integrally woven structures (e.g. I-beams, T-beams, sandwich structures) significantly have higher damage tolerance and skin-core delamination resistance than 2D composites but lower interlaminar shear strength [1].

1.4 Objective

Testing standards e.g. short beam shear, open-hole compression etc have already been developed for tape laminates and are being used for 3D composites. These standards are not able to give the desired failure stress state in 3D composites due to their complex weave architecture.

Many researchers have used 2D standards for the testing of 3D composites but they faced some common problems. Some of these problems which may relate with OHC testing standard are discussed as under;

1.4.1 Extent of damage prediction

OHC strength is considered to be the strength of the composite with some damage [20]. This definition not clearly indicates that how much damage of the composite will be considered during the compressive strength prediction of the composite.

1.4.2 Inhomogeneous stress concentration

Inhomogeneous material properties of composites make the stress concentration complex near the boundaries of the hole which makes difficult to predict the initiation and propagation of failure and also affect the overall prediction of OHC strength of the specimen [21].

1.4.3 Singularity of Inter-laminar stress state

Stress concentration of large magnitude near the hole regime may not be able to initiate the damage in the presence of small magnitude of singularity of interlaminar stress

state. Even one half of the typical crack makes it difficult to exactly predict the compressive properties of the composite due to the relaxation of stress at the interface caused by singularity[20, 21].

1.4.4 Kinking

Budiansky et al in kinking theory has neglected the effect of bending resistance of fibres and analyze that initial fibre waviness and shear yield strength are the dominating parameters upon which FRP compressive strength depends [22]. They also found it difficult to exactly predict the degree of initial fibre waviness of composite.

1.4.5 Effects of geometric parameters

Sathiamoorthy et al. in 1997 observed that by decreasing the hole diameter from 3 mm to 0.3 mm compressive strength increases up to 20%. They also states in couple stress theory that fibre bending resistance and notch strength increases as the hole diameter decreases[22]. Thus, there is a need of standardizing the hole diameter to get the OHC strength of the particular composite.

1.4.6 Dominant Failure mode

Argon et al. observed that, compressive strength of long fiber laminated composites is less than tensile strength due to plastic micro buckling which occurs as a dominant failure mode in compressive loading. Compressive axial stress is the cause of fibres rotation and matrix shear which then creates the strain hardening effect within the matrix region. This strain hardening ultimately induces the instability in the structure which then initiates and propagates the micro buckle within the composite [22].

1.4.7 Percent bending

Percent bending may increase within the fibres due to unsuitable length of the specimen. During compressive loading, length of the specimen must be critically decided otherwise it may cause mixing of failure modes [3]. Mathematical formulation for percentage bending is;

$$B_y = \frac{\epsilon_f - \epsilon_b}{\epsilon_f + \epsilon_b} * 100 \leq 10\%$$

Where, B_y = percent bending in specimen

ϵ_f = indicated strain from front transducer

ϵ_b = indicated strain from back transducer

1.4.8 Loading configuration effects

Hatta et al. during the testing of compressive behavior of laminated composites observed that higher magnitude of loading create the shear stress concentration at the end of the specimen which may be the cause of end kink development [23].

1.4.9 High standard deviations

The application of standards developed for the testing of 2D laminated composites to 3D composites gives significantly high coefficient of variance values and standard deviations in compressive loading which readily make the available mechanical property values and correction factors unreliable [12]. Standard size of specimen Ideally, failure initiates from the hole of the specimen in open-hole compression test and it is well known fact that if width to diameter ratio of hole is not of critical value on which the pure compressive failure occurs, failure initiation region may shift towards the ends of the hole or towards the side of loading i.e. before the edge of the hole [24].

1.4.10 Size of RVE

Instrumentation such as strain gauge size affects the measured properties due to the difference in the size of RVE of 2D and 3D composites. RVE of 3D composites is larger than 2D composites which may affect the results. Hence, optimum size of strain gauge is necessary for better prediction of properties [16].

1.4.11 Test parameters

Test parameters such as end tab sizes, gripping mechanism, loading etc are different for different composites. These parameters need to be modified for testing of 3D composites [25].

Loading configuration which includes loading method, fixtures adjustment, loading speed and orientation of fibres developed for tape laminates may not be applicable to 3D composites due to the complexities within the yarns arrangement of 3D woven composites [3].

All of these problems suggest that if we want to get the desired failure mode in 3D composites, these tests are needed to be modified. Thus, in this work 2D OHC standard i.e. ASTM D6484 will initially be used to validate the loading and boundary conditions used in FE model and then this model will be used to analyze the failure stress state of 3D composites.

Conclusively, objective of this work is to provide a roadmap to researchers working in the area of development of testing standards for 3D woven composites so that they would be able to develop a reliable testing standard for 3D composites.

1.5 Methodology

Whitney et al used fracture mechanics based mathematical models i.e. characteristic distance approach and numerical methods i.e. FEA approach to predict the properties of laminated composites [26]. They found that numerical modeling techniques offer much more flexibility and robustness. These techniques can easily be employed to complex geometries i.e. ply by ply analysis of laminated composite structures.

Pure experimental approach towards the understanding of internal stress state of 2D and 3D specimens is not considered cost effective and is also time consuming. Due to efficient response of numerical models, this work is mainly focused on FE modeling of 2D and 3D composites. These models will be validated with experimental results. Complete strategy of development of this model is shown and discussed as under;

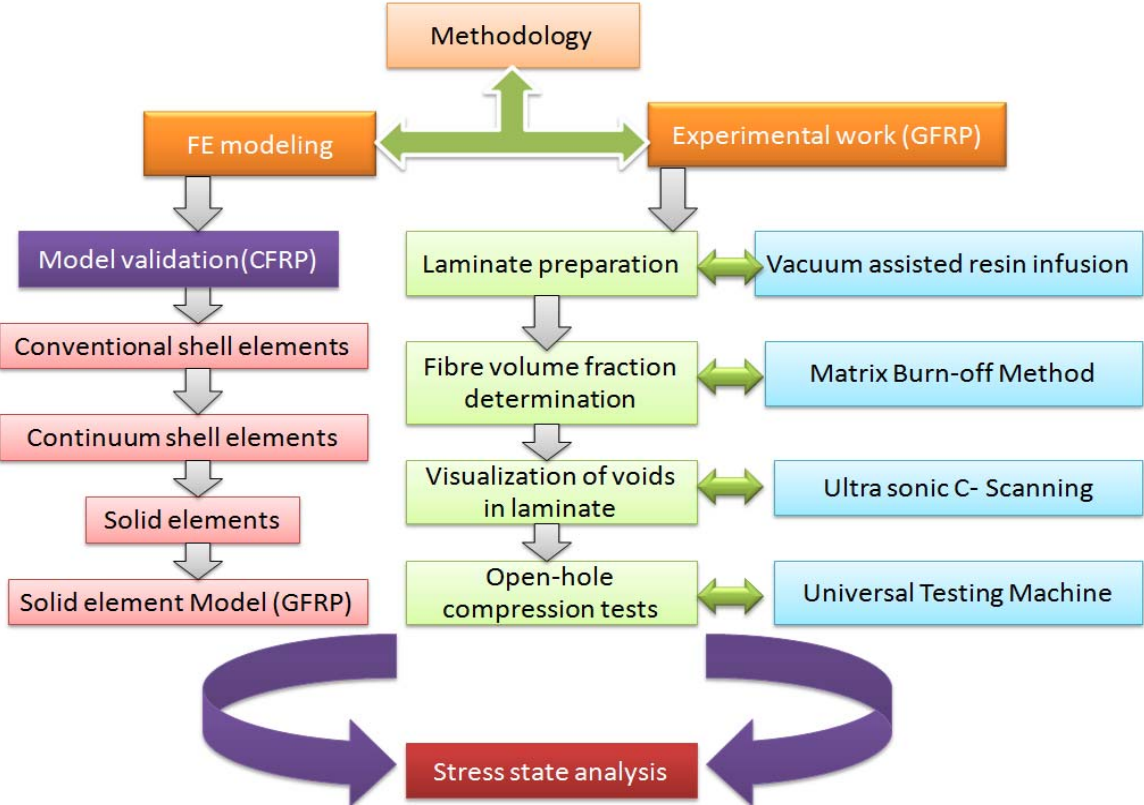


Figure 1: Methodology

1.5.1 FE macro-mechanical model

3D macro-mechanical model with orthotropic material definition is developed to validate the loading and boundary conditions of ASTM D6484 standard. ABAQUS 6.10, a commercial FE package is used to develop the model. Models made of conventional shell, continuum shell and solid type elements with carbon fibres as input material properties is validated with experimental results [27]. The model with solid elements provided best results and is used to study the internal stress state of 2D and 3D woven GFRP composites.

1.5.2 Experimental work

Experimental work was performed on 2D and 3D woven GFRP OHC composite specimens at NCCEF, University of Manchester, UK and HITEC University, Taxila, Pakistan. The centre has extensive facilities for producing 3D composite, manufacturing specimens and testing. Tests were carried out according to ASTM D6484 standard to get the OHC strength of the specimens.

1.6 Scope

The work is limited to FE analysis of the stress state in 3D composites by simulating the ASTM D6484 testing standard using orthotropic homogenous material definition. Based on this analysis initial recommendations will be made about the suitability of this testing standard for application to 3D composites or otherwise. Since no attempt is being made to model the progressive failure and the heterogeneous nature of the materials involved therefore the results from this study can only be considered as preliminary results for building a more detailed model that can be taken up in future by a PhD student in the department.

CHAPTER 2: LITERATURE REVIEW

2.1 Introduction

In this chapter, numerical and experimental findings of various researchers in determining the open-hole compressive (OHC) strength of UD, 2D and 3D fibre reinforced polymeric composites will be discussed. To achieve this purpose, detailed literature survey has been carried out in which the influence of notch/hole size on compressive strength of composites was studied. In particular, the effect of fibre architecture (i.e. 2D and 3D woven) on compressive strength of notched composites will be discussed. Moreover, the standard procedures which have been used to investigate the numerical and experimental OHC strength of composites will be discussed. Therefore the aim is to study numerical and experimental findings of various researchers about the effect of fibre architecture on OHC strength of composites.

2.2 Open-hole compression

Holes in mechanical structures are unavoidable and significantly reduce the structural strength. This occurs due to stress concentration near the hole which generally causes the failure. Stress concentration mainly occurs due to highly localized stresses at the root of notch and is usually analyzed by calculating the stress concentration factor (SCF) near the hole. SCF is defined as the ratio between maximum stress (max) at hole and nominal stress (nom).

$$K_T = \frac{\text{max}}{\text{nom}}$$

In isotropic materials, it is easy to determine the SCF by using tangential stress at two ends of the diameter of the hole and the nominal stress developed within the specimen [28] but it's a cumbersome task to evaluate the SCF in composites. Some of the techniques which are currently being employed for the determination of stress concentration in composites are explained as under;

2.2.1 Point stress criterion

When a stress is developed away from a certain distance d_0 from the hole becomes equal or exceeds the value of the strength of un-notched laminate, failure occurs. The particular distance d_0 is independent from the laminate geometry and the stress distribution within the laminate. This behavior is considered as a material property. This indicates the critically stressed point within the material from where the failure initiation may occur [26].

2.2.2 Average stress criterion

When the value of an average stress over a distance a_0 ahead the hole approaches the strength of an un-notched laminate, failure occurs. This particular distance a_0 is considered as a material property and indicates the initiation of crack within the laminate due to the presence of intense stresses [26].

Several attempts have been made by researchers to determine the suitable technique for evaluating the SCF for FRPC's but still there is no closed form solution available for finding the stress concentration factor of finite width orthotropic plates. SCF of composites having low orthotropic ratios are closer to each other but with increasing orthotropic ratios SCF's are not remain closer to each other. Conclusively, SCF of the composites varies with the variation of orthotropic nature of the materials [29]. In addition experimental results show that the measured notch sensitivity for composites ($1/K_T$) is lesser than the value calculated theoretically or from linear elastic FE analysis of orthotropic laminates.

As discussed earlier that, the aim of this work is to determine the reliability of 2D standard open-hole compression test for estimating the OHC strength of 3D woven composites. To achieve this purpose, a detailed literature survey of analytical and experimental techniques of UD, 2D and 3D composites has been made and presented as under;

2.3 Compressive testing of composite materials

Compression testing of composite materials results in deformations in matrix, fiber (fiber misalignment) and matrix fiber interface. In case of UD, 2D and 3D composites, extensive work has been carried out to estimate failure mechanisms particularly formation of kink bands and buckling. In this regard, microscopic analysis has also been made to predict the compressive properties and to understand the damage modes of the composites. The influence of fibre break due to compression or discontinuity on its surrounding undamaged fibres and the influence of fibre-matrix interfacial properties appear to be the major problems in determining the compressive properties of the composites.

Some of the observations which have been made by different researchers during compression testing of laminated and woven composites are discussed as under;

2.3.1 Multidirectional laminated composites (UD)

Failure initiation of notched laminated fiber reinforced composite plate loaded under uni-axial compression was observed by using non-empirical procedure. In this study, it was presumed that failure in notched laminates mainly occurs near the hole due to the presence of kink band. To understand this localized damage initiation near the hole, surface strain gages

were placed remote from the notch and were found unaffected from the initial kink band. ABAQUS, a commercial FE package was then used to analyze this localized damage. Progressively decreasing modulus of matrix and a non uniform pre-buckling stress field was analyzed and observed that these gradients are mainly based on size of the notch. Therefore, it was concluded that the analysis was sufficient to characterize the kink band development and also able to lead the accurate prediction of load carrying capacity of composite plates. Good agreement was seen between experimental work and FE analysis [30].

Peijs et al studied the microscopic compressive response of UD carbon fibre composites. The aim was to study the influence of fibre damage in compression on surrounding fibres and on fibre/matrix interfacial properties. Experimental and numerical results have shown that compressive response is the dominant parameter which controls the compressive failure of high modulus carbon fibre composites. Furthermore, fibre failure in shearing has indicated the higher stress transfer rate in compression. Therefore, it was concluded that compressive stress is linear to strain at low strains and deviation increases as the stress level increases [31].

Suemasu et al performed a thorough numerical and experimental study to investigate the open-hole compressive damage initiation and evolution of quasi-isotropic composite laminates. Experimental work was carried out on OHC testing fixture proposed by National Aerospace Laboratory (NAL III) and it was concluded that the limited size of damage initiates unstably which then propagates the stable damage on further increase of compressive load [24].

Saha et al performed the open-hole compression tests by using the testing setup of Institute for Aerospace Research. Effect of hole size on compressive strength of E-glass fiber/isophthalic polyester resin matrix pultruded composite sheet material was investigated. Higher strains were observed at the hole edges by increasing the hole diameter. It was also observed that the compressive fibre damage initiates due to delamination. Furthermore, delamination, fiber micro buckling and shearing of layers were seen to be the major compressive failure mechanisms [32].

Poon et al performed the experimental work and numerical simulations to investigate the damage evolution in compressively loaded open-hole laminates. Narmco IM6/5245C was used to prepare the specimens and the tests were performed on MTS testing machine with a testing fixture of Institute for Aerospace Research. It was concluded that compressive damage initiates at 90% of the ultimate failure load. Furthermore, it was concluded that strain to initial failure decreases as the number of plies increased within the laminate [33].

Wang et al used ASTM standard D695 and Boeing Specification Support Standard BSS 7260 to determine the OHC strength of AS4/3501-6 quasi-isotropic laminate. A shell

element model was used to simulate the progressive damage approach. The model was validated by using characteristic distance approach on the specimens. A good agreement was observed between numerical and experimental results [34].

Fiber micro-buckling, kinking, longitudinal cracking and fiber failure are the major damage modes in compression. All of these modes depend upon various environmental or loading factors which may act individually or in combination. Analytical modeling of these damage modes often use the assumption that the specimen is under uni-axial compression. This assumption may lead faulty results as it is observed that the failure stress state of damaged specimens is not purely compressive and may depend upon various factors such as load introduction, stress concentration and other deformation modes [35].

Lee et al has carried out the experimental work to study the effect of notch size, ply and laminate thickness on compressive strength of the quasi isotropic laminate. Kinking and fibre micro-buckling was observed as the dominant failure modes. It was concluded that, notch size is the most important parameter in determining the compressive strength of notched composites. It was also concluded that increment in notch size significantly reduces compressive strength of open-hole composite layup [36].

Basu et al has carried out the experimental work to determine the effect of multi-axial stress on compressive strength of fibre-reinforced lamina. It was concluded that the shear stress acting against the compressive stress in axial direction can significantly increase the compressive strength of the composite [37].

Williams et al observed compressive failure/yielding of reinforced fibres, longitudinal splitting of matrix (due to the Poisson ratio effects), shearing failure of laminate, interfacial debonding of matrix and fibres, matrix yielding and fibre splitting as the dominant failure modes in longitudinal compressive loading of FRP composites [38].

Shih et al observed fibre kinking as the dominant failure mode of FRPCs under compressive loading which occurs due to fibres misalignment in loading direction. Compressive loading affects the localized regions of the composite in such a way that fibre bundles in localized region may get tilted or slightly moved at some angle. This initiates kink band within the laminate which later cause the large shearing deformation within the matrix [39].

Kumar et al observed fibre micro-buckling as the buckling of axial tows embedded inside the matrix and kinking as the highly localized buckling of axial fibres. Kinking initiates on the application of peak compressive load and then plastically damages the region nearby [40].

Shu et al observed that in-plane shear stress concentration significantly reduces the normalized OHC strength of the composites as it causes delamination within plies. Delamination is a well known failure mode in composites which occurs due to high interlaminar shear stresses and, can lead to subsequent matrix shearing and kink bands in adjacent plies [41, 63]. To reduce the effect of delamination on OHC strength of composites, Masters et al suggested to improve the damage tolerance of laminated composites by interleaving (Interleaving is the introduction of thin layer of tough, ductile polymer or adhesive between the plies to increase the fracture toughness) [42].

Waas et al observed that high out of plane stresses can shift the dominant mode of failure of OHC specimens as low magnitude of matrix/ interfacial fracture toughness invites fibre micro-buckling [43]. Similarly, Fleck et al. observed that OHC strength depends upon the relative magnitudes of elastic stiffnesses and shear yield strength of the material [44].

Waters et al. observed that specimens with low thickness have high average compressive stress so thick composite structures may not necessarily fail at same stress as those of thin composites. Thickness being used in testing of laminate may affect the overall strength of composite [45].

Whitney et al observed that if width of plate is infinite, stress concentration factor near the hole get independent of hole size. However, if the width of the plate is finite, stress concentration factor increases with the increment of hole size [26].

Schultheisz et al observed that it is difficult to determine the compressive properties of UD composites due to their high stiffness, high strength and anisotropic behavior. Several analytical and numerical models have been developed to validate the experimental results but still there are discrepancies which have not been resolved by the researchers. This indicates that there is still a need to improve the testing methodology which should be specifically true for estimating the location and mode of damage as it relates to stress concentration within the specimens [46].

2.3.2 Woven composites

Mohamed et al observed complex weave architecture as one of the major problems in developing the failure criteria for 3D textile composites because it makes difficult to understand the damage modes of these composites [4]. Similarly, Fleck et al observed that the tensile strength and modulus of woven laminates is less than multidirectional fabric laminates due to fibre crimp. On the other hand, they observed the advantage of woven composites over laminated composites that these composites can provide balanced properties in 0^0 and 90^0 directions. Multidirectional laminated composites can also be used for getting balanced and

better properties but these fabrics take much more time in fabrication than those of woven[47].

Estimating properties of 3D woven composites need special attention due to their high profile aerospace applications e.g. Landing strut gear of BOEING etc .Therefore, this work is dedicated to 2D and 3D woven composites and mainly focused on OHC strength of 3D woven composites.In this regard, detailed literature survey of numerical and experimental techniques used on 2D and 3D woven composites has been made. Findings are as under;

2.3.2.1 2D Woven composites

Zako et al performed a detailed numerical study on woven fabrics and observed that the compressive loading is the cause of stress concentration at geometrical discontinuities such as holes, reduced cross section, discontinuities etc within the structure. Stress raiser such as hole significantly increases the magnitude of peak stress and is used to determine the OHC strength of the composites. Moreover, presence of imperfections within the laminate creates stress gradient zones which develop the tri-axial stress state within the specimen [48].

Carvalho et al has performed the extensive numerical simulations and experimental work to study the compressive damage of randomly stacked and orderly stacked laminates of orthogonal 2D woven composites. It was concluded that the failure mechanisms of both specimens are significantly different. In ordered stacked laminates, in addition to matrix cracking and kinking, delamination due to significant yarn bending was found[49].

Kaleemulla et al has performed numerical and experimental work to examine the effect of fibre content and notch size on OHC strength of plain-woven glass fabric composite. ANOVA (Analysis of variance) technique was used to validate the experimental work. Affect of fibre content, fibre orientation and notch size on OHC strength of the laminate was evaluated and it was concluded that the OHC strength of the laminate increases as the fibre content increases within the laminate. Similarly, it was also concluded that the OHC strength of the laminate reduces as the hole size increases [50].

2.3.2.2 3D Woven composites

Brandt et al. compared conventional 3D woven composites with 3D orthogonal woven composites and it was found that the compressive strength of 3D orthogonal woven composite is significantly higher than that of a conventional 3D woven composite. Main reason of this behavior is the crimp free geometry i.e. absence of undulation within yarns. Later, the effect of 3rd directional reinforcement(z yarn fiber) on the compression strength of 3D woven composite was studied and it was concluded that proportion z yarn fiber has small effect on compressive properties of composites with low z yarn volume fraction. It was also

concluded that the compressive properties of 3D woven composites showed a significant improvement compared with 2D woven composites [51].

Compression and compression after impact (CAI) tests on 3D woven composites were performed and it was concluded that the compressive strength of through thickness reinforced composites was half than 2D woven laminates [52]. It was also concluded that CAI strength of 3D composites is twice than 2D laminates. This improvement in compressive properties is mainly due to high interlaminar strength provided by through-the-thickness reinforcement. The main reason of decrease in compressive strength for 3D composites is explained by Mouritz. According to Mouritz et al, fibre misalignment is not the only parameter which reduces the compressive properties of 3D composites but matrix rich regions because matrix rich channels can reduce fibre volume fraction in each in-plane yarn which increases the stress concentration within the matrix around the fibers and reduces the lateral support. Therefore longitudinal fibers are more susceptible to compressive failure [53].

Gu et al did a systematic study to understand the influence of through the thickness yarn size on compressive strength of 3D orthogonal woven composites. No delaminations were observed during experimentation and it was concluded that all the samples were failed under shear. This indicated the significance of shear strength analysis. It was also analyzed that the compressive strength of 3D orthogonal woven composites decreases as the z yarn size increases [54].

Fleck et al studied the influence of fibre architecture on compressive strength of the 2D and 3D woven composites. Tests were carried out on notched as well as un-notched specimens and fibre micro-buckling was observed as a dominant failure mode in compression. Crack bridging model and infinite kinking band model were used to predict the notched and un-notched strength of the composites. It was concluded that plastic micro-buckling of the axial load bearing fibres is the dominant failure mode in notched as well as in un-notched specimens. Fibre misalignment was observed as the major cause of low compressive properties of woven composites [47].

Cox et al studied the behavior of angle interlock woven polymeric composites under uni-axial compression. Kink band formation in load bearing axial tows was observed as a dominant failure mode. Initial fibre misalignment, intersection of load bearing tows and through-thickness reinforcing tows were observed as the major cause of kink band initiation within the composite. It was concluded that these geometric flaws may reduce the macroscopic stiffness and strength of the composite but are able to distribute the failure throughout the specimen which minimize the chance of catastrophic damage [55]. Furthermore, Cox et al studied the compressive failure mechanisms of 3D woven composites and observed kinking as the most important failure mechanism. Kink bands initiate and distort the weft yarns and then propagate towards z-yarns due to contact pressure created in z-yarns. This causes

formation of two kink bands within narrow region. Therefore, it was concluded that the delamination can also create kink band, although it is limited but it can separate the specimen into layers which may cause buckling in warp and weft fibres[56].

Microscopic analysis and post mortem sectioning of 3D woven interlock composite specimens under uni-axial compression shows that the dominant failure mode is kink band formation in load bearing fibres. Initial fibre misalignment, buckling and lateral loads on stuffer yarns are the main geometrical flaws which may initiate the kink band. All of these non-uniformities within the structure significantly reduce the critical loads for kink band formation which then decreases the strength of the composite. On the contrary, these geometrical flaws increase the strains to ultimate failure by distributing the damage throughout the specimen [55].

Cox et al performed a systematic analysis to evaluate the compressive properties of layer to layer angle interlock, through the thickness angle interlock and orthogonal woven composites. In this study, delamination was observed in different laminas of the 3D composites. It was concluded that if the z-yarn strength is effective enough to restrain the delamination fracture, Euler buckling will be considered neglected due to properties of above mentioned 3D woven composites ,otherwise buckling caused by delamination will give catastrophic failure [55].

Fleck et al studied the failure propagation of notched 2D and 3D woven fibre reinforced composite specimens by using traveling microscope on side face of the specimen. SEM (Scanning electron microscopy) of the damaged specimens was also performed and it was concluded that the micro-buckling of the warp tows near the hole causes failure. Therefore, it was also concluded that compressive strength of 2D woven notched specimens is higher than 3D woven notchedspecimens[47].

The above mentioned literature review have clearly shown that thereis no dedicated standard available for evaluating the compressive properties of 3D woven composites. Till now, 2D standards are being used to evaluate theopen-hole compressive properties of 3D woven composite materials. It has also highlighted that in general the mechanisms of failure for 3D fibre reinforced composites are different from 2D fibre reinforced composites. Therefore, a detailed numerical and experimental work is needed to study the stress state developed within notched3D woven composite specimens.

2.4 Mechanical modeling of composites

Mechanical properties of 3D woven composites should be evaluated before they can be used in manufacturing industry. This objective can be met by adopting one of the two possible approaches.

- Building validated analytical models to determine mechanical properties and failure mechanisms in composite materials.
- Building large database of experimental results to estimate the elastic properties.

2.4.1 Numerical modeling

2.4.1.1 Why FE modeling?

The aim of analytical and numerical modeling of textile composites is to predict their mechanical properties. Marrey et al observed that the complex weave architecture of textile composites is the major problem in developing the reliable analytical approach to predict the properties at micro structural level. They also concluded that, recently proposed research techniques such as variational boundary methods and rule of mixture approximations are not capable of predicting these properties due to oversimplification. Hence, a computationally efficient FEA model can be used to cater the complexity of the composite at a reasonable cost of accuracy [57]. Similarly, Tan et al observed that the complex microstructure of textile composites makes their understanding ambiguous which creates difficulty in modeling these composites by using theoretical techniques. They also suggested, finite element approach (FEA) to be an efficient and powerful tool for predicting mechanical properties of these composites [58].

2.4.1.2 Review of FE analysis

Waas et al used finite element approach (FEA) to build a micromechanical model for predicting the failure initiation of the notched composite laminates loaded in compression. Experimental study was carried out to investigate the compressive failure mechanisms in uniply laminates. Geometric parameters of FE model were taken from experimental analysis and failure was observed as a narrow kink band near the hole edge. In FE analysis, failure was restricted to a distance within one half of the hole radius. For this purpose, a small rectangular area near cutout edge in which kink band occurs is analyzed. Stress analysis was made by using the available closed form solutions for orthotropic laminates and observed good agreement between experimental work and FE analysis [30].

Nurhaniza et al used ABAQUS, commercial FE software to model the compressive properties of E-glass UD composite. The aim was to quantify the ultimate failure load, elastic

response and compressive properties of the composite by using stress-strain curves. It was concluded that the numerical simulations show a good agreement with experimental results i.e. the percentage error was in between 10-25% [59].

Schuecker et al has implemented the FE model to study the progressive damage of open-hole compression specimens of fiber reinforced polymeric laminates. The aim was to study the damage evolution and propagation within the laminate. It was concluded that the experimental results of damage prediction have shown a good agreement with load displacement curves [60].

Rao et al used ABAQUS to simulate the notched and un-notched quasi isotropic laminate specimens for compressive strength. Failure loads and stiffnesses were modeled in the analysis and a good agreement was found between experimental work and numerical simulations [61].

H. J. Lin et al studied the failure strength of woven glass roving composite specimens with different hole sizes. FE based model along with Hashin strength criterion was used to perform the stress state analysis of the specimens. Good agreement was observed between the experimental results and numerical simulations [62].

Conclusively, currently available numerical models are not able to predict the relationship between fibre volume fraction and OHC strength of material but can provide a reasonable approximation with an error of 10-20%. In order to achieve better results, Piggott et al suggested the empirical formulae approach which can only be obtained through detailed experimentation.

2.4.2 Experimentation

In this section, the failure modes of standard open-hole compression test method are discussed. It also includes the precautionary measures which should be taken care of during experimentation.

2.4.2.1 Damage modes

The acceptable failure modes of standard OHC specimens are shown in fig.2 and are discussed as under [63]

- (a) **LGM** (Lateral gauge middle): Compressive failure of laminate which occurs across the centre of the hole due to the kinking and buckling of the 0^0 dominated ply.

- (b) **AGM** (Angled gauge middle): Laminate failure occurs due to compression at the hole but the remnants of the other plies cross the centre line of the hole. This failure is the dominated matrix failure due to effect of 45° ply.
- (c) **MGM** (Multimode gauge middle): Failure of laminate occurs at the hole due to the occurrence of multiple failure modes on various plies

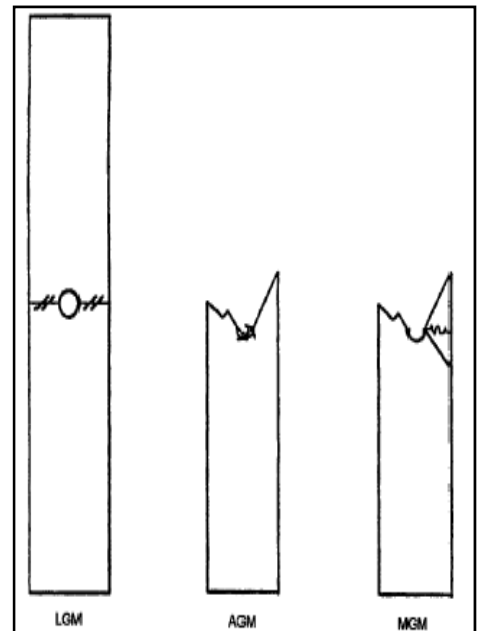


Figure 2: Failure modes of the specimen

2.4.2.2 Precautionary measures

Factors which may affect the overall strength of notched composites include constituent materials, methods of material fabrication, accuracy of lay-up, laminate stacking sequence and overall thickness, specimen geometry, (including hole diameter, diameter-to-thickness ratio, and width-to-diameter ratio), specimen preparation (especially of the hole), specimen conditioning, environment of testing, specimen alignment and gripping, loading procedure, speed of testing, time at temperature, void content, and volume percent of reinforcement[63]. Some of these factors are needed to be discussed and are as under;

2.4.2.2.1 Panel fabrication

Argon et al observed imperfections in fibres significantly reduce the OHC strength of FRP composites. He also stated that imperfections not only introduce during curing of the laminate but also appears during manufacturing of the prepreg/composite [64]. Thus, panel fabrication technique is one of the important factors in this test to avoid erratic placement of fibres.

2.4.2.3 Fibre volume fraction

Kozey et al determined the linear relationship between fibre volume fraction and compressive strength of the multidirectional (UD) laminate [65]. Thus, fibre volume fraction of the laminate must be properly determined to better predict the compressive properties of the composite.

2.4.2.4 Specimen preparation

Suitable machining processes with reasonable tolerance limits must be adopted to get the standard specimen configurations because negligence in machining may cause delamination, undercuts etc within the specimens [63].

2.4.2.5 Specimen geometry

OHC strength measurement results may vary due to change in specimen width to diameter ratio (which should be maintained at 6 in test)[63]. Therefore, specimen dimensions were taken according to standard test method to avoid faulty prediction.

2.4.2.6 Hole preparation

Sathiamoorthy et al observed that OHC strength increases as the hole diameter decreases and faulty hole preparation may cause early damage initiation and lead the specimen to early rupture [22]. Similarly, Saha et al. observed that longitudinal splitting and delamination increases as the hole diameter increases. This may cause sharp stress concentration near the hole and increase the force carrying capacity of specimen as well as calculated strength[32]. Therefore, to avoid all such problems, specimens must be properly drilled.

2.4.2.7 Stacking sequence

Coefficient of mutual influence between adjacent layers and mismatch of poisson's ratio may cause high interlaminar normal and shear stresses at free edges of laminated composites [66]. To avoid this problem, plies must be properly stacked.

2.4.2.8 Thickness scaling

Waters et al. observed that specimens with low thickness have high average compressive stress so thick composite structures may not necessarily fail at same stress as those of thin composites. In other words, thickness being used in testing of laminate may affect the overall strength of composite[32].

2.5 Concluding remarks

Literaturereview has clearly shown that there is no dedicated standard available for evaluating the compressive properties of 3D woven composites. Till now, 2D standards are being used to evaluate the OHC properties of 3D woven composite materials. High standard deviations and coefficient of variance values were observed by using these standards.

Therefore, a detailed numerical and experimental work is needed to achieve the desired stress state within notched 3D woven composite specimens.

CHAPTER-3: METHODOLOGY

3.1 Introduction

This chapter describes the FE model development of OHC test specimen by using ABAQUS 6.10, a commercial FE package. Open-hole compression test method is used to determine the OHC strength of FRP composite materials. ASTM standard D6484 is used to develop the FE model for the determination of OHC strength of 2D laminated FRP composite materials.

ABAQUS/CAE is used to create model geometry, generate mesh and for applying loading and boundary conditions, and ABAQUS/STANDARD is used to perform the analysis. One of the fundamental problems faced during this study was that the literature giving experimental results of OHC strength of 3D composites is almost non-existent. Due to practical constraints of resources the experimental results obtained during this study were also not available during the start of the work. Thus in order to have sufficient confidence in the results of FE analysis, an approach was developed to validate present FE model. In this approach, experimental data was obtained by the work of Wang et al [34]. In their work, experimentation was carried out on UD carbon fiber composites to evaluate the compressive failure load of the specimen. These results were compared with presently developed FE model to validate its loading and boundary conditions. In presently developed FE model, conventional shell, continuum shell and solid element approaches are used as shown in Table 2. Results from each model are compared with experimental data. Upon validation of existing FE model, solid elements are then used to evaluate the OHC response of 2D and 3D woven GFRP composites.

Table 2: Element type used to develop FE models

Element types	Element name	Geometric Features	Output stress parameters
Conventional shell	S4R	Four node built in quadrilateral shell element	S11, S22, S12
Continuum shell	SC8R	Eight node built in quadrilateral shell element	S11, S22, S12
Solid	C3D8R	Eight node built in 3D stress element	S11, S22, S33, S12, S13, S23

3.2 Numerical modeling

FE modeling is mainly divided into two major stages i.e. validation by using multidirectional carbon fibre properties (i.e. UD lamina) and actual stress state analysis by using 2D and 3D woven glass fibre reinforced polymeric (GFRP) composite properties.

3.2.1 Multidirectional carbon fibre reinforced laminated composite

Analytical modeling approaches which are currently being used to study the compressive response of laminated composites in longitudinal direction are either based on micro-buckling or kinking of fibres. In actual, both of these phenomena occur simultaneously to cause failure. Therefore, these approaches cannot be simply implemented to get the desired results.

In order to validate the experimental results of compressive failure load of multidirectional carbon fibre laminates with FE model hierarchical modeling approach is used. In this approach, 2D conventional shell, 2D continuum shell and solid element models are implemented to validate the loading and boundary conditions of standard OHC test method i.e. ASTM D6484 as shown in fig 3. Modeling details are as under;

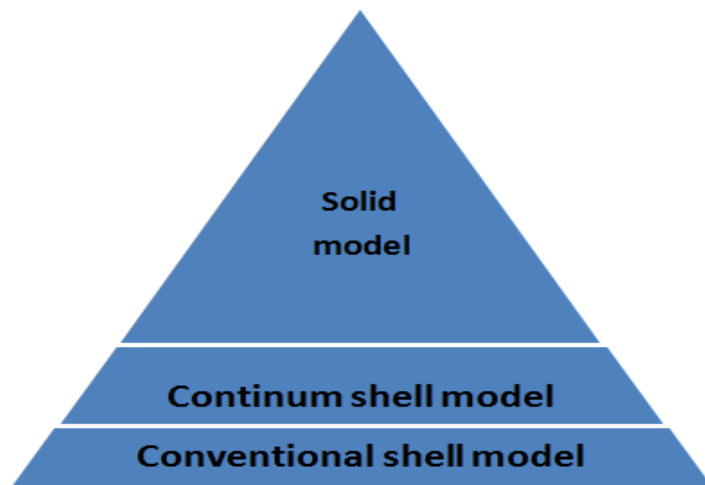


Figure 3: Hierarchal approach of FE modeling

3.2.1.1 Part geometry

ABAQUS/CAE is used to model the part geometry in which global coordinate axes (XYZ) correspond with the model's 1, 2 and 3 directions. However, due to geometrical symmetry of the specimen only quarter model is made. Specimen dimensions are taken from literature [34] and are shown in table 3.

Table 3: Dimensions of the specimen [34]

Parameter	Dimensions
Length	305(mm)
Thickness	2.08(mm)
Width	38.1(mm)
Hole diameter	6.35mm

3.2.1.2 Loading conditions

A uniform surface traction load is applied up to the length of 80mm on both sides of the specimen. Red color in fig. 4 shows the regions under load.

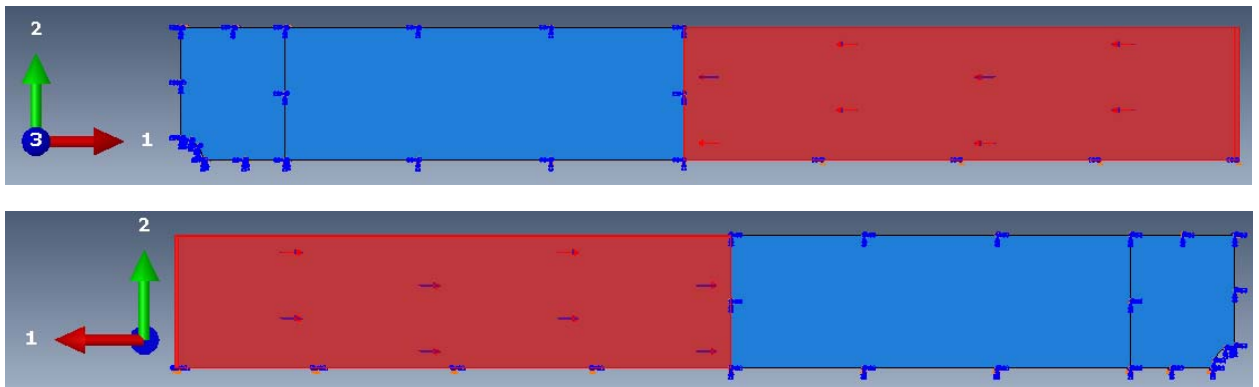


Figure 4: Loading condition (Front and rear sides of the specimen)

3.2.1.3 Boundary conditions

Due to symmetry only quarter of the specimen is modeled and symmetric boundary conditions are applied on two planes i.e. X-symmetric and Y symmetric as shown in fig. 5 & 6.

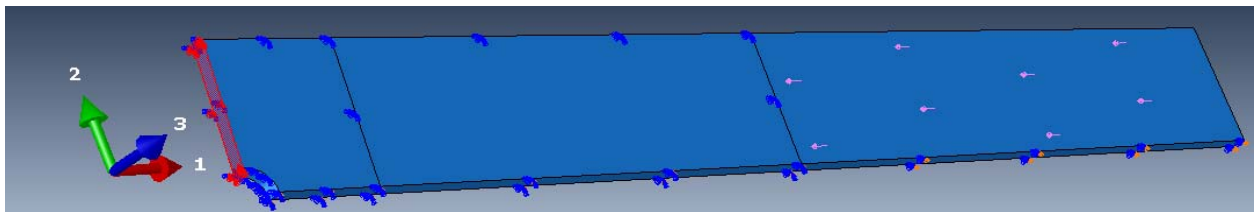


Figure 5: X-symmetric BC (i.e. symmetric in 1 direction)

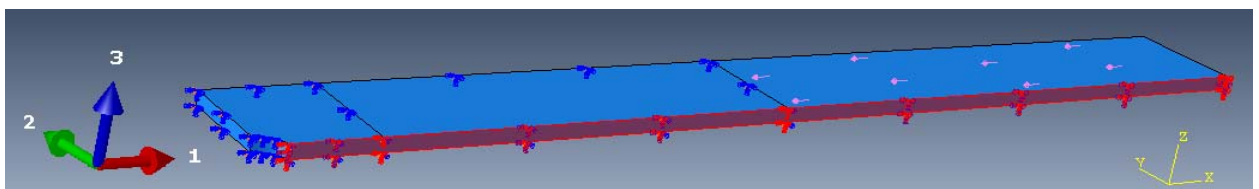


Figure 6: Y-symmetric BC (i.e. symmetric in 2 direction)

Zero out of plane displacement and constrained rotational motion are the boundary conditions which are applied on the specimen and are shown in fig. 7 & 8 respectively.

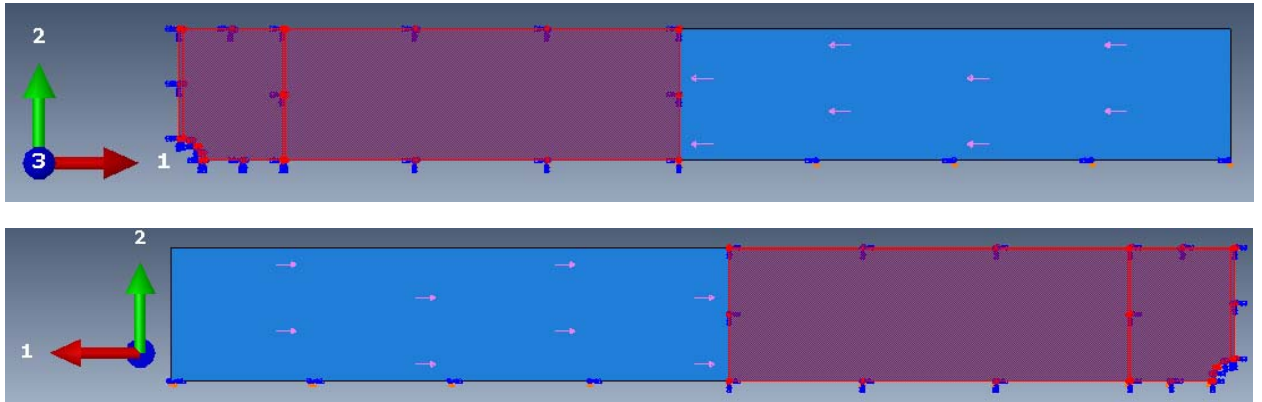


Figure 7: $U_3=0$, BC (Front and rear sides of the specimen)

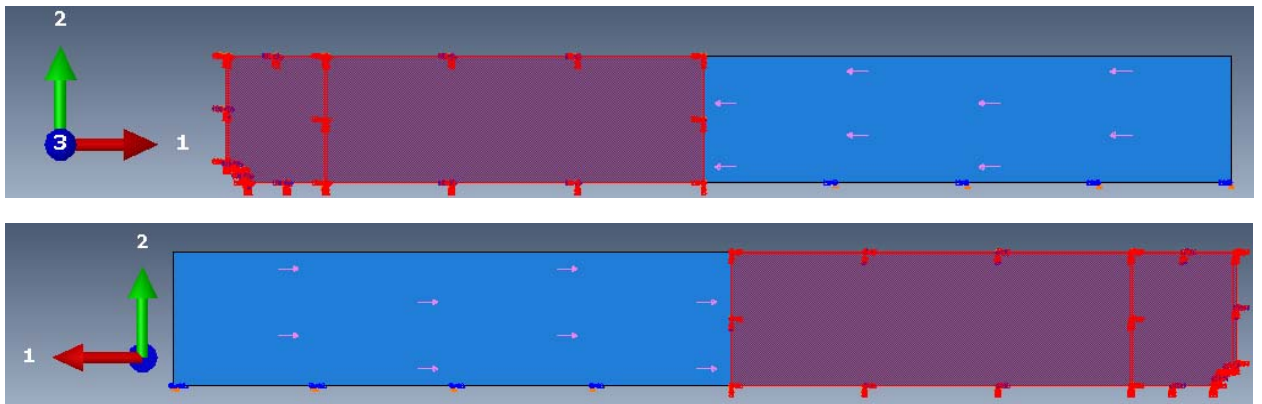


Figure 8: $UR_1=UR_2=UR_3=0$ BC (Front and rear sides of the specimen)

Out of plane displacement is constrained to avoid bending and buckling within the specimen. All the rotations are constrained near the hole to avoid kinking and buckling phenomenon within the specimen.

3.2.1.4 Material model

Wang et al used UD carbon/epoxy (AS4/3501-6) prepreg tape with layup sequence of $[45\ 0\ -45\ 90]_2$, areal weight of $150\ \text{gm}^{-2}$, fibre volume fraction of 0.63 and nominal ply thickness of 0.13mm to evaluate the compressive failure load[34]. For defining such model, Lamina type material with elastic mechanical properties was used to define 2D conventional and 2D continuum shell elements in ABAQUS 6.10. Orientation and properties to laminates have been defined in ABAQUS using **Composite Layup**. On the other hand, nine engineering constants were needed to define solid material model. Engineering constants needed to define these models are presented in table 4.

Table 4: Engineering constants required to define material models [34]

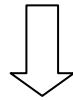
Input material constants	Conventional shell	Continuum shell	Solid
E1(GPa)	142	142	142
E2(GPa)	10.3	10.3	10.3
E3(GPa)	-----	-----	5.15 *
V12	0.27	0.27	0.27
V13	-----	-----	0.155 *
V23	-----	-----	0.155 *
G12(GPa)	7.2	7.2	7.2
G13(GPa)	-----	-----	3.6 *
G23(GPa)	-----	-----	3.6*

Note: * represents assumed values

3D & 2D stress strain equations which are used to calculate the stresses and strains on various locations of the laminates are as under;

$$\begin{bmatrix} E11 \\ E22 \\ E33 \\ E23 \\ E13 \\ E12 \end{bmatrix} = \begin{bmatrix} \frac{1}{E1} & \frac{-v21}{E2} & \frac{-v31}{E3} & 0 & 0 & 0 \\ \frac{-v12}{E1} & \frac{1}{E2} & \frac{-v32}{E3} & 0 & 0 & 0 \\ \frac{-v13}{E1} & \frac{-v23}{E2} & \frac{1}{E3} & 0 & 0 & 0 \\ 0 & 0 & 0 & \frac{1}{G23} & 0 & 0 \\ 0 & 0 & 0 & 0 & \frac{1}{G13} & 0 \\ 0 & 0 & 0 & 0 & 0 & \frac{1}{G12} \end{bmatrix} \begin{bmatrix} S11 \\ S22 \\ S33 \\ S23 \\ S13 \\ S12 \end{bmatrix}$$

(Solid model: 3D stress strain equations for orthotropic materials)



$$\begin{bmatrix} E11 \\ E22 \\ E12 \end{bmatrix} = \begin{bmatrix} \frac{1}{E1} & \frac{-v12}{E1} & 0 \\ \frac{-v12}{E1} & \frac{1}{E2} & 0 \\ 0 & 0 & \frac{1}{G12} \end{bmatrix} \begin{bmatrix} S11 \\ S22 \\ S12 \end{bmatrix}$$

(Conventional shell and continuum shell models: 2D stress strain equations for UD lamina)

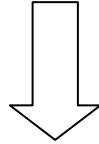
Where, $E_1, E_2, E_3, G_{12}, G_{13}, G_{23}, V_{12}, V_{13}$ and V_{23} are the engineering constants.

$S_{11}, S_{22}, S_{33}, S_{23}, S_{13}$ & S_{12} and $E_{11}, E_{22}, E_{33}, E_{23}, E_{13}$ & E_{12} are the applied stresses and resultant strains respectively.

3D stress strain equations are reduced to 2D stress strain equations due to plane stress assumption of conventional shell and continuum shell element models. Similarly, transformation matrix is used to evaluate the stresses on angled plies of conventional shell and continuum shell element models as shown below [67].

$$\begin{bmatrix} S_{xx} \\ S_{yy} \\ S_{xy} \end{bmatrix} = \begin{bmatrix} c^2 & s^2 & -2cs \\ s^2 & c^2 & 2cs \\ cs & -cs & c^2 - s^2 \end{bmatrix} \begin{bmatrix} S_{11} \\ S_{22} \\ S_{12} \end{bmatrix}$$

Where, $c = \cos\theta, s = \sin\theta$



(Transformation matrix)

3.2.1.5 Meshing

2D conventional shell, 2D continuum shell and solid elements are used to generate the mesh and to analyze the failure stress state of the specimen. 2D conventional shell elements and 2D continuum shell have the plane stress assumption and are not able to predict the through thickness response. Similarly, 2D conventional shell elements are not capable of capturing transverse shear effects as well but continuum shell elements due to 3D geometry can predict the transverse shear response. In contrast, solid elements can capture through thickness and transverse shear response as well.

3.2.1.5.1 Element type

As explained earlier, for meshing purpose, three FE models are developed each having one of elements mentioned in table 2.

S4R (2D conventional shell) elements are used to model thin shell problems in which material lines normal to the surface remains straight and normal throughout the deformed region i.e. transverse shear strains are considered to be zero i.e. $\gamma = 0$. SC8R (2D continuum shell) elements are capable of efficiently evaluating the displacements, stresses and strains at reduced integration points by including the effect of stiffness degradation. SC8R elements are also able to identify the effects of transverse shear stiffness. On the contrary, C3D8R (solid) elements can examine transverse shear effects as well as through thickness effects [68].

Structured mesh technique with quad-dominated element shape is used to generate the mesh. A very fine mesh near the hole is generated to get better results while still ensuring computational efficiency by having larger elements in areas with non-steep stress / strain gradients.

3.2.1.5.2 Mesh convergence

In FEmodeling, accurate solution is usually achieved by refining the mesh results. Mesh refinement is usually achieved by increasing the mesh density of the region which is under investigation. On the other hand, this sufficiently increases computational time.

In this work, a grid independence study of the specimens with higher mesh density near the hole was performed of all the three models i.e. 2D conventional shell, 2D continuum shell and solid. The aim was to get the convergedFE solution.To meet this objective, mesh convergence of longitudinal stress S11, longitudinal strain E11 and longitudinal displacement, was made. Thus, the results reported here are for converged mesh and it was observed that by further refining the mesh, the results do not change substantially.Results of 2D conventional shell (Table 5, Fig. 9, 10 & 11), 2D continuum shell (Table 6, Figure 12, 13 & 14) and solid element (Table 7, Figure 15,16 & 17) models along with graphs are as under;

Table 5: Mesh convergence results of conventional shell model

Serial no.	No. of elements	Compressive stress, S11 (MPa)	Compressive Strain, E11	Displacement, U1
1	14325	205.24	0.001403	8.82E-35
2	16299	210.92	0.001443	8.00E-35
3	18404	213.4	0.001461	6.86E-35
4	20454	219.58	0.001505	6.74E-35
5	20475	220.2	0.001509	6.26E-35
6	20794	220.4	0.001511	6.13E-35
7	20986	222.01	0.001522	6.00E-35
8	22000	223.9	0.001535	5.48E-35
9	22875	226.5	0.001554	4.87E-35
10	25425	228.73	0.001569	4.90E-35
11	26315	228.4	0.001567	5.15E-35
12	29170	228.42	0.001567	5.15E-35

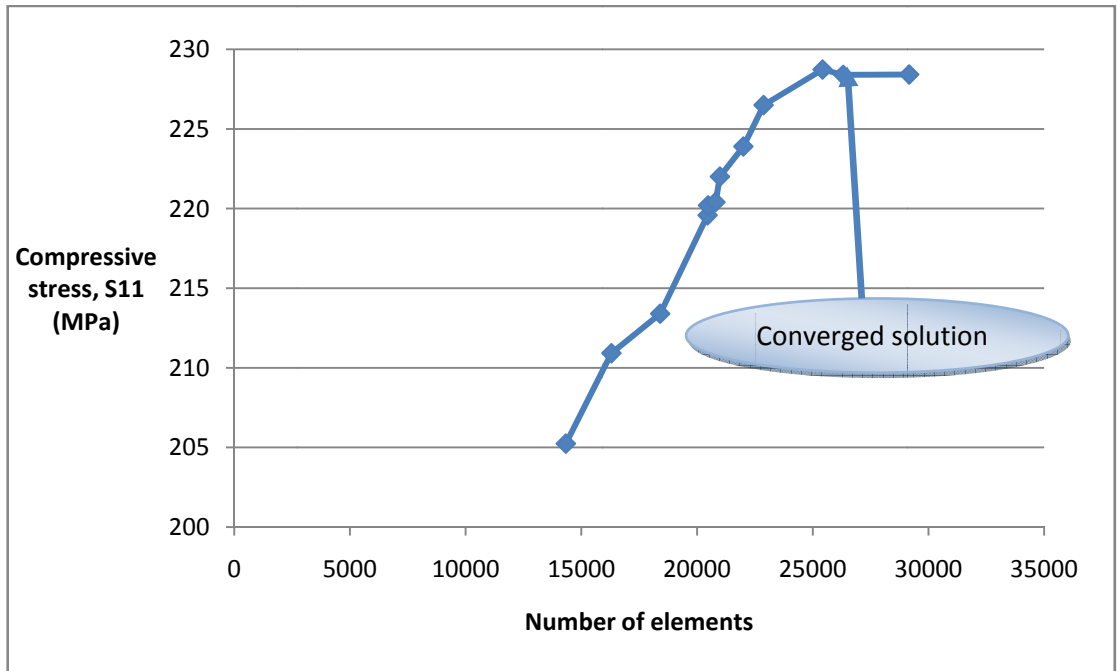


Figure 9: Compressive stress vs. number of elements (conventional shell model)

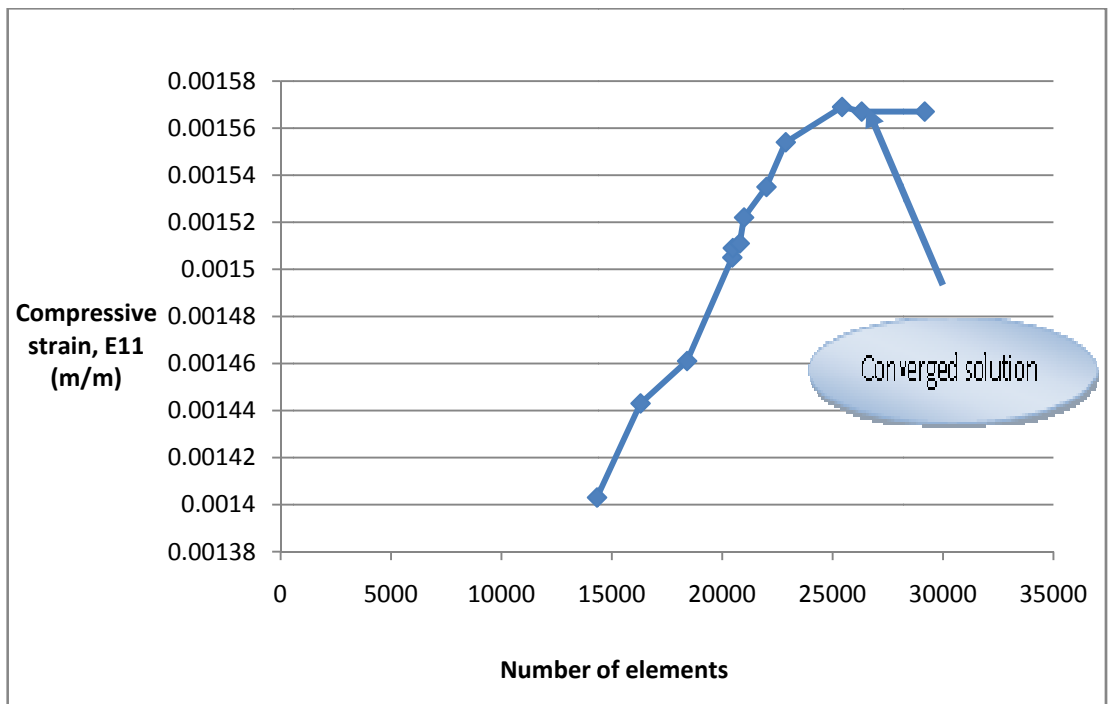


Figure 10: Compressive strain vs. number of elements (conventional shell model)

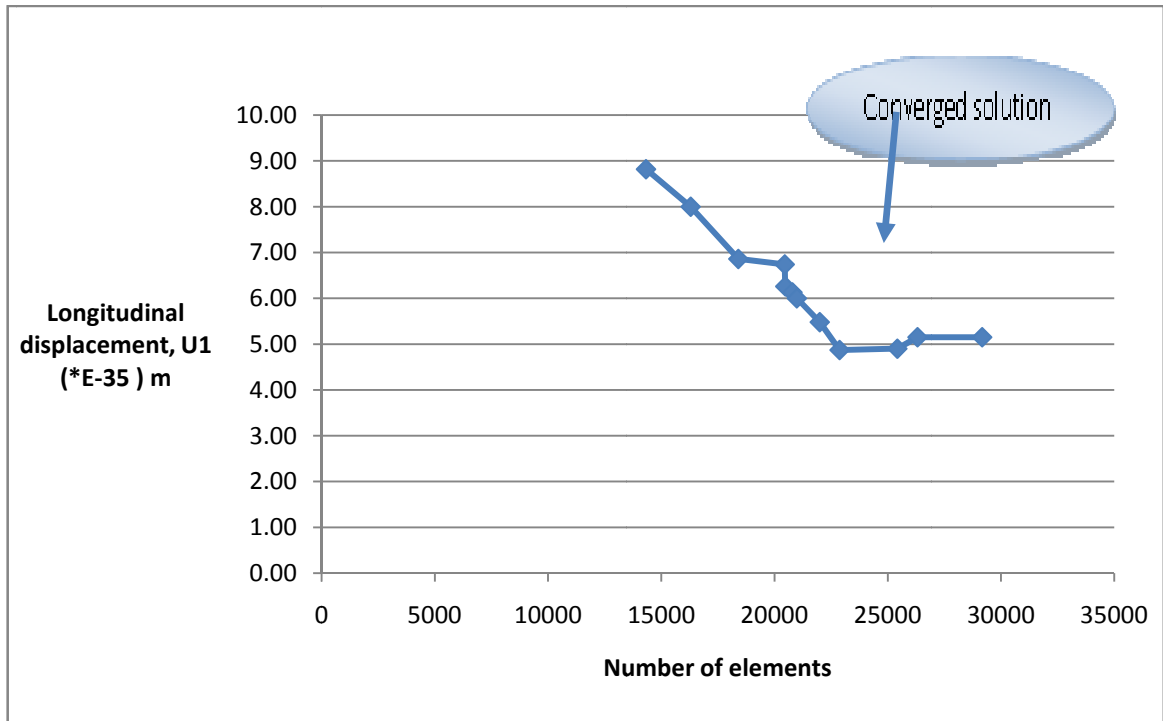


Figure 11: Longitudinal displacement vs. number of elements (conventional shell model)

Table 6: Mesh convergence results of continuum shell model

Serial no.	No. of elements	Compressive stress, S11 (MPa)	Compressive Strain, E11	Displacement, U1
1	9988	220	0.001487	8.02E-35
2	10650	223.8	0.001511	7.34E-35
3	12800	226.7	0.001531	6.78E-35
4	14722	227	0.001537	6.29E-35
5	16472	229.7	0.001552	5.88E-35
6	18050	230.7	0.001559	5.52E-35
7	18988	232.8	0.001573	5.19E-35
8	20948	234.6	0.001585	4.90E-35
9	23008	236.1	0.001595	4.64E-35
10	23958	236.12	0.001595	4.64E-35
11	25383	236.121	0.00159551	4.65E-35

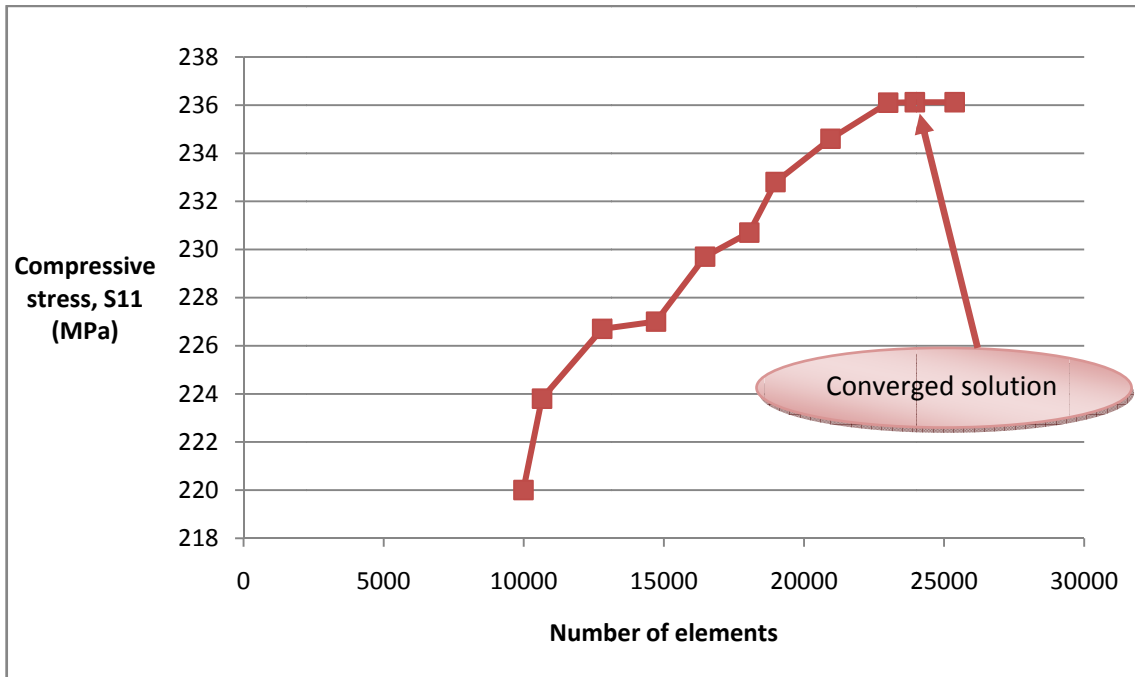


Figure 12: Compressive stress vs. number of elements (continuum shell model)

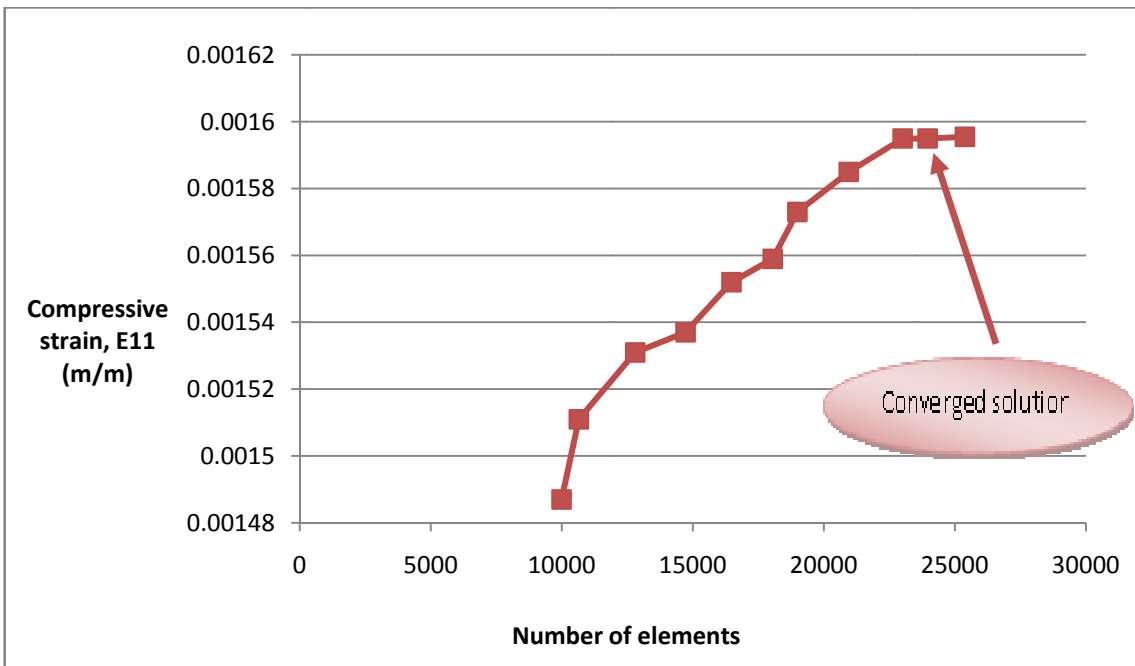


Figure 13: Compressive strain vs. number of elements (continuum shell model)

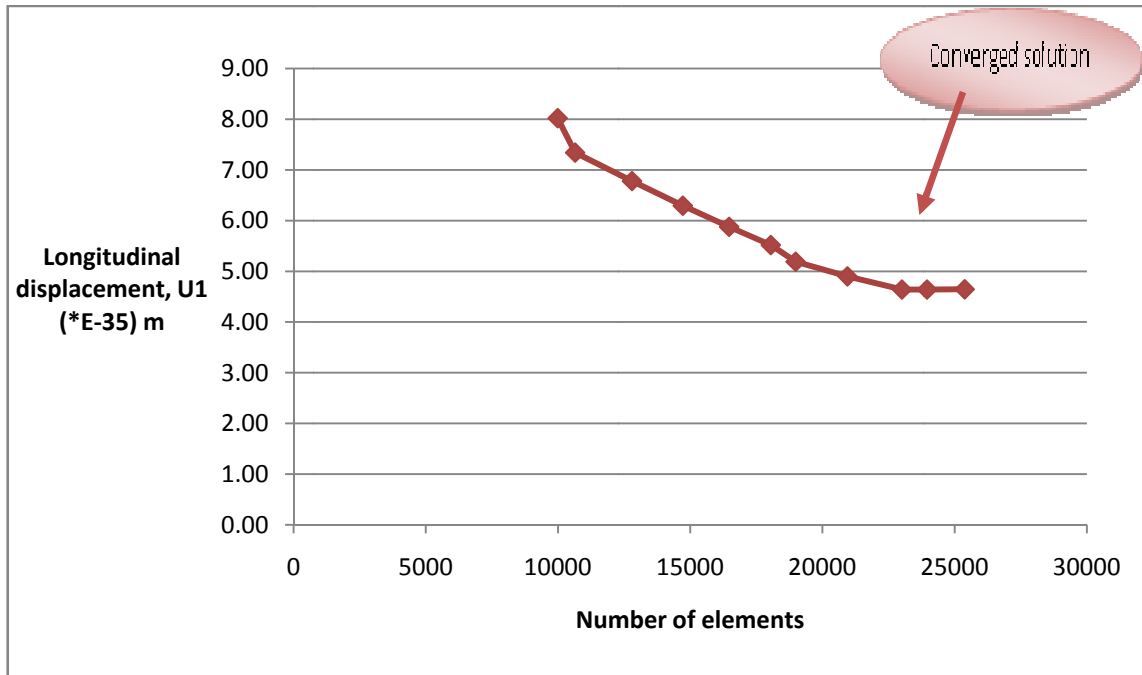


Figure 14: Longitudinal displacement vs. number of elements (continuum shell model)

Table 7: Mesh convergence results of solid model

Serial no.	No. of elements	Compressive stress (S11),MPa	Compressive Strain (E11)	Displacement,U1
1	62100	700	0.004899	1.38E-35
2	66750	711	0.00497	1.31E-35
3	75150	729	0.005107	1.19E-35
4	76800	730	0.005109	1.19E-35
5	83700	738.6	0.00517	1.13E-35
6	89160	741.8	0.005192	1.11E-35
7	96030	746.5	0.005226	1.08E-35
8	105150	746.5	0.005226	1.08E-35
9	110850	746.5	0.005226	1.08E-35

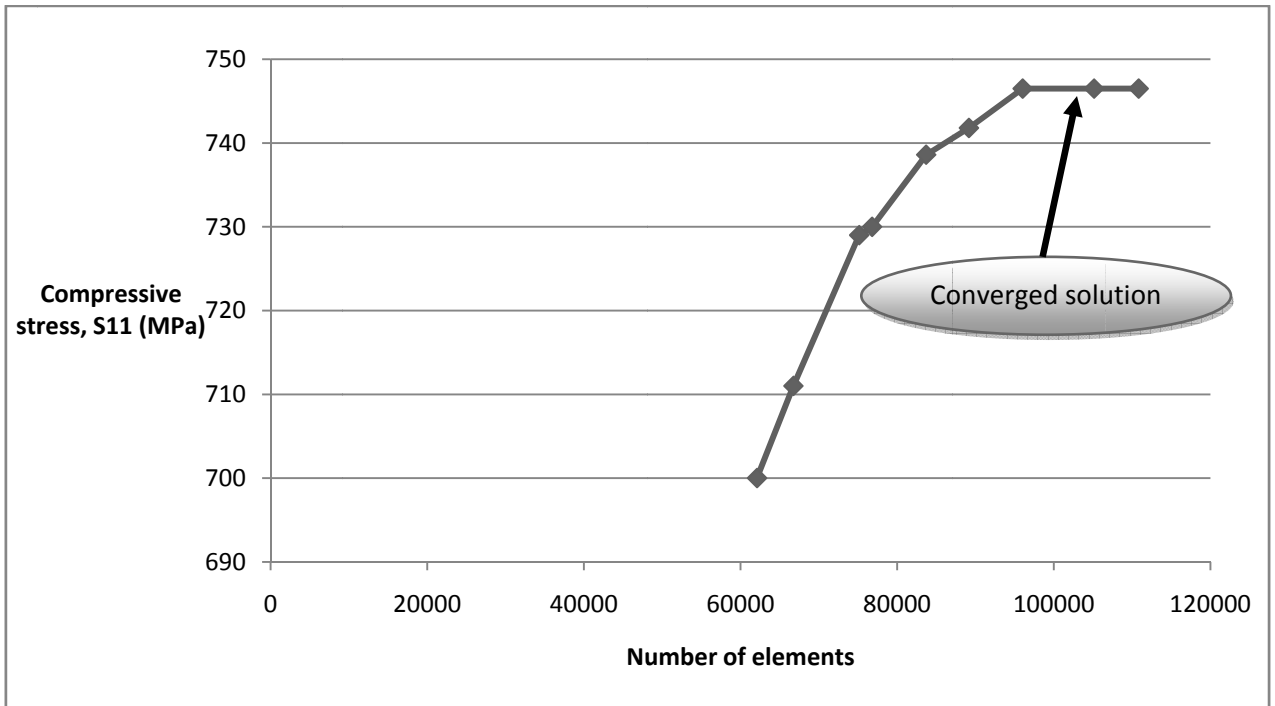


Figure 15: Compressive stress vs. number of elements (solid model)

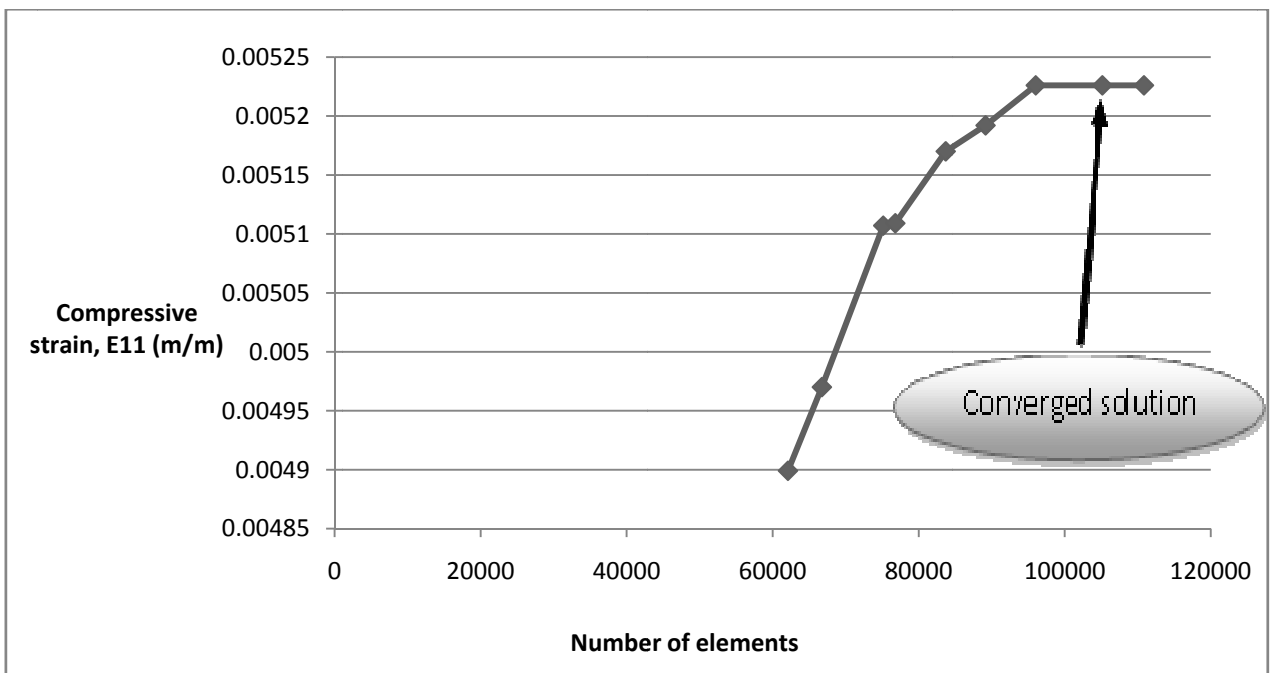


Figure 16: Compressive strain vs. number of elements (solid model)

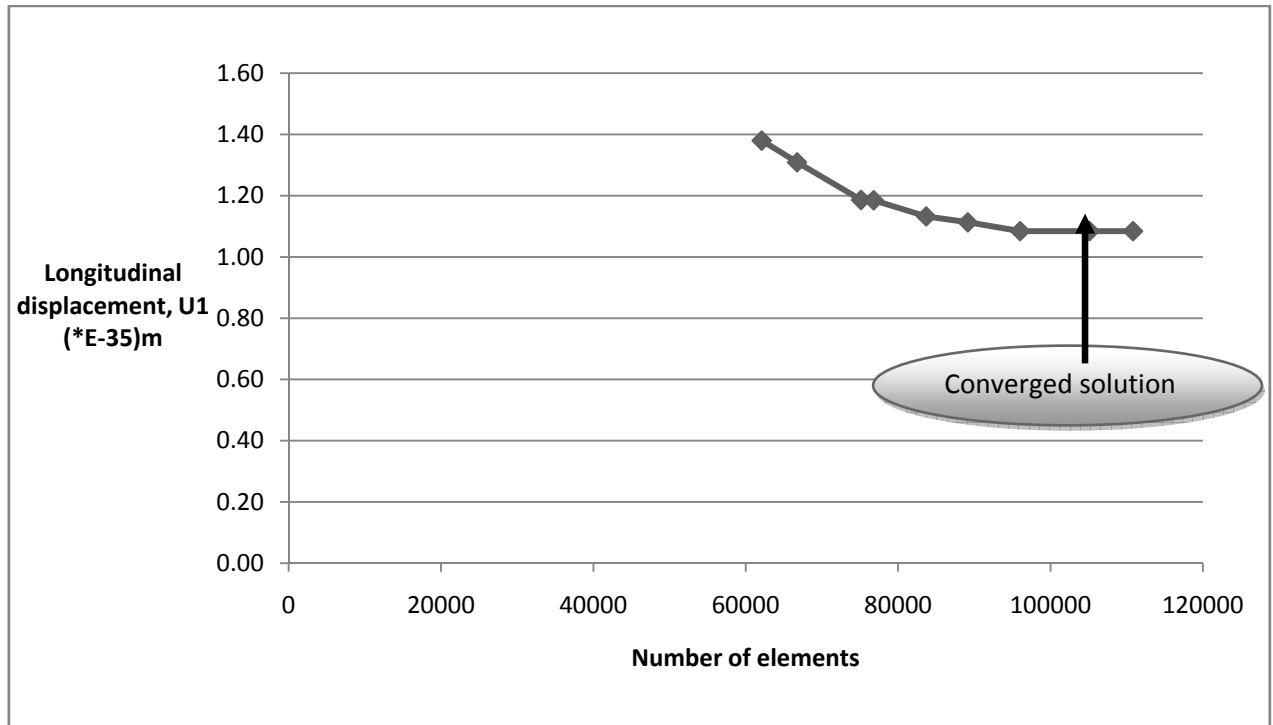


Figure 17: Longitudinal displacement vs. number of elements (solid model)

3.2.1.6 Experimental results of UD carbon fibre composite

In work of Wang et al. experimentation was performed on Instron 1185 screw driven test machine at room temperature/dry condition to determine the OHC strength of the carbon/epoxy (AS4/3501-6) prepreg tape [34]. Results are shown in table 6.

Table 8: Experimental results of UD carbon fibre composite [34]

Hole size	Number of replicates	Average peak load	Average net strength	Standard deviation
6.35mm	4	26.3 kN	398.2 MPa	1.1 kN

3.2.1.7 Damage prediction

In this section, the aim is to numerically simulate the damage initiation of all the three models i.e. conventional shell, continuum shell and solid and to validate the compressive failure load with experimental results. Failure modeling without understanding the stress state within the specimen is impossible. Therefore, there must be a criterion by using which one would be able to explain the composite failure. FRP composite mainly comprise of two constituents i.e. matrix and fibre. Both of these components have their own modulus and

strength values so to examine the overall strength of the composite it is important to understand the overall properties required of both the constituents separately and in combined form as well.

In this work, Hashin damage criteria will be used to examine the damage initiation in conventional and continuum shell element models. Similarly, Von misses, maximum normal stress and Tresca criteria's will be used to evaluate the damage produced within the solid element model.

In order to model Hashin failure criteria in Abaqus 6.10, Lamina type material properties are needed and are presented in Table 9 [34].

Table 9: Strength properties of UD carbon fiber lamina

Strength properties	Values (MPa)
Longitudinal tensile, σ_{1T}	2280
Longitudinal compressive, σ_{1c}	-1440
Transverse tensile, σ_{2T}	57
Transverse compressive, σ_{2c}	-228
Shear, τ_{12}	71

3.2.2 2D and 3D woven GFRP composites

FE models with 3D orthotropic material properties were made to visualize the internal stress state of 2D and 3D woven GFRP composite specimens. The aim was to compare the failure stress state of 2D and 3D woven GFRP composite specimens by applying the actual compressive failure load on both models. Following procedure was followed for the development of FE models:

- 1)-Guidelines from ASTM D6484 standard were taken to define geometric parameters of the specimen
- 2)-Fleck et al observed that compressive strength mainly depends upon material properties of the composite i.e. upon relative magnitude of elastic stiffness and shear yield strength [69]. Therefore, input material properties of 2D and 3D woven (angle interlock) GFRP composites were used to define the material model. Some of them were experimentally determined at University of Manchester and remaining were taken from literature [70]. Tabulated material properties of 2D and 3D woven GFRP composites are shown below:

Table 10: Material Properties of GFRP composite [71,72 and73]

Input material parameters	3D(Woven)	2D(Woven)
E1 (GPa)	23*	22.9*
E2 (GPa)	23*	22.3*
E3 (GPa)	10	10.8
□ 12	0.12	0.104
□ 13	0.28	0.155
□ 23	0.28	0.155
G13 (GPa)	8	3.57
G12 (GPa)	8	3.8
G23(GPa)	8	3.8

*represents assumed values.

3) -Loadings and boundary conditions were taken from ASTM standard D6484.

4)-Failure loads of 2D and 3D woven GFRP composite specimens were experimentally determined at University of Manchester, UK and HITEC University, Pakistan.

5) - Solid elements, C3D8R were used for meshing of the models.

6) - In post processing, four different regions near the hole were created to study the stress state variation between 2D and 3D woven GFRP composite specimens. The aim was to understand the compressive failure modes of these specimens by analyzing the longitudinal, transverse and in plane stresses developed within the models. These paths are shown in fig.18 which is as under;

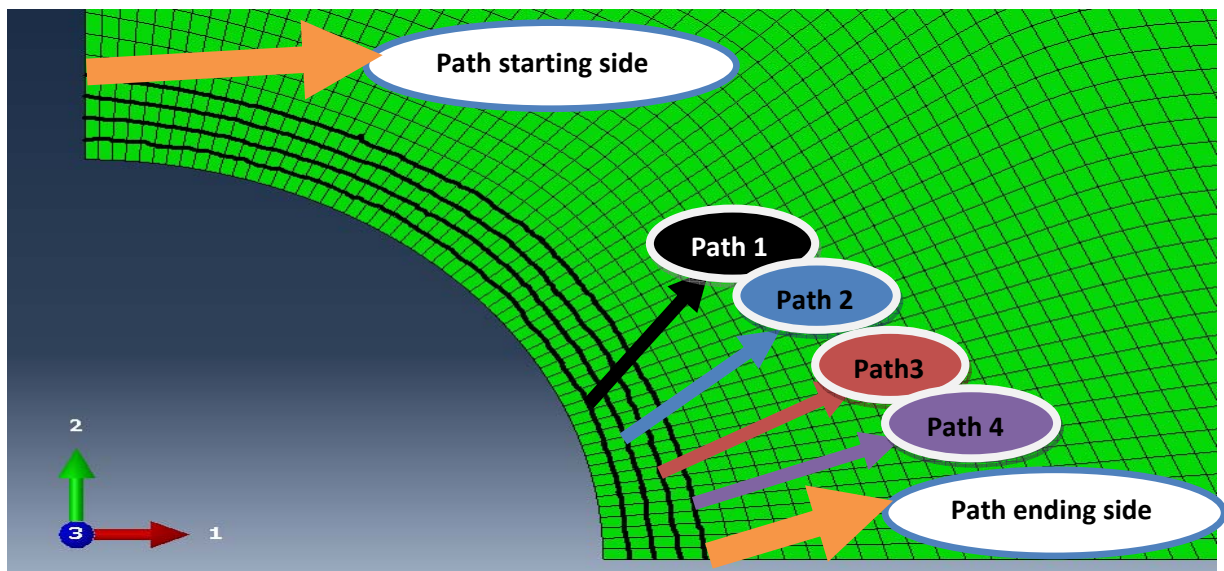


Figure 18: Path selected to study the difference of stress state in 2D and 3D composite

3.3 Experimentation

Experimental work was carried out at NUST, Pakistan, University of Manchester, UK and HITEC University, Pakistan. A dedicated standard open-hole compression test method i.e. ASTM D6484 was used for the testing of 2D and 3D woven GFRP composites. Details of the standard testing procedure which were adopted are as under;

3.3.1 Panel fabrication

Vacuum assisted resin infusion (VARI) technique was used to prepare the laminate of 2D plain and 3D angle interlock woven glass fabric with epoxy resin. The panels were of uniform thickness and flat geometry. Fabrication was performed in NCCEF, University of Manchester, UK.

3.3.2 Fibre volume fraction determination

Guidelines of ASTM D 3171 standard test method were used to determine the fibre volume fraction of the panel. Matrix burn-off method was adopted and it was concluded that 60% fibre content, 35% resin content and 5% voids were present in the laminate.

3.3.3 Specimen preparation

Suitable machining processes were adopted to get the standard specimen dimensions (i.e. within reasonable tolerance limits) as shown in table 11. Standard guidelines were adopted to achieve the desired parameters. In particular, when cutting the specimens from plates to avoid delamination, undercuts etc.

Table 11: Specimen dimensions [63]

Parameter	Dimensions(mm)
Length	300±0.25
Width	36±0.25
Thickness range	3 to 5
Nominal thickness	2 to 4
Hole diameter	6to 9

3.3.4 Hole preparation

Specimens were properly drilled according to ASTM D6484 standard with hole diameter of 6mm.

3.3.5 Stacking sequence

Plies were properly stacked.

3.3.6 Thickness scaling

Thickness of the specimens was achieved according to the standard requirements. Thickness details of 2D and 3D woven GFRP composite specimens are shown in table 12 & 13.

Table 12: Thickness details of 3D specimens

3D Specimens	Top	Middle	Bottom	Mean
1	2.13	1.85	1.91	1.963333
2	1.91	1.76	1.65	1.773333
3	1.81	1.94	1.94	1.896667
4	1.72	1.89	2.02	1.876667
5	1.92	1.77	1.76	1.816667
6	1.75	1.79	1.94	1.826667

Table 13: Thickness details of 3D specimens

2D Specimens	Top	Middle	Bottom	Mean
1	2.01	2.03	1.98	2.006667
2	1.91	1.79	1.85	1.85
3	1.8	1.83	1.78	1.803333
4	1.83	1.82	1.84	1.83
5	1.84	1.9	1.94	1.893333

3.3.6.1 Loading procedure

Hydraulic grip loading was used to measure the OHC strength of composites. Fixture was located at grip jaws and was held in test machine by keeping the specimen in the direction of loading. Outer portion of grips were tightened up to the length of 80mm to hold the specimen tightly. Compression through shear load was then applied at the grips which induce the compressive stress state within the specimen. This shifts the stress concentration regime towards the hole and specimen ruptures as the ultimate load approaches. The specimen with fixture details is shown in fig.19.

During loading of the specimen, following precautionary measures were adopted to get the desired results.

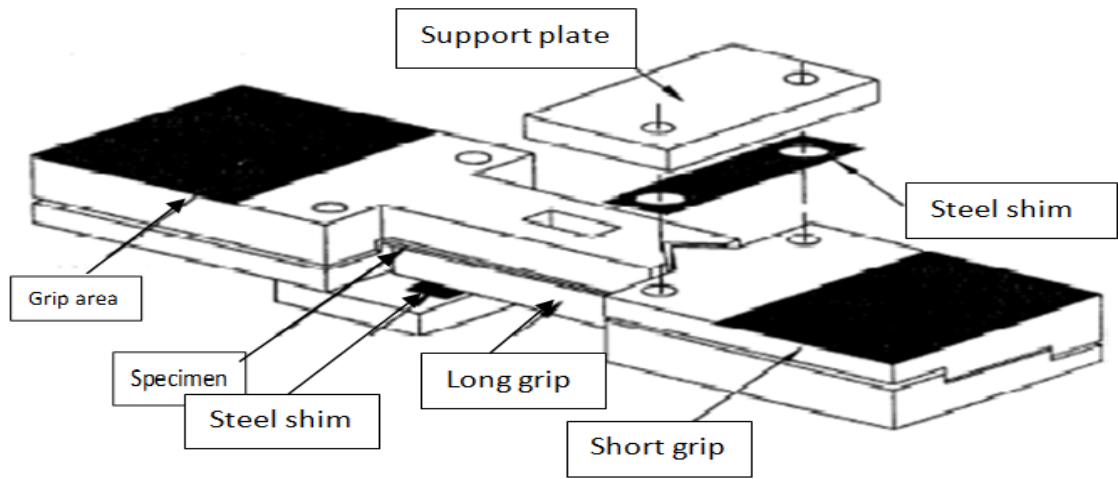


Figure 19: Support fixture assembly

- (a) Loading was in appropriate limits.
- (b) Bolts were tightened accurately before the application of hydraulic pressure on grips.
- (c) Gap between the support plates and long grip portion of the support fixture was properly checked to avoid buckling within the specimen.
- (d) Gap between the gage section and long grip portion of the support plates was in prescribed tolerance limit.
- (e) Specimen was loaded till the magnitude of force was reached to maximum and then drops off up to 30%.

3.3.7 Failure load determination

Tests were carried out on Universal Testing Machine at HITEC University, Taxila. In experimentation, the aim was to evaluate the failure loads of 2D and 3D woven GFRP composite specimens in order to visualize failure modes of 2D and 3D composites.

3.3.8 Damage analysis and microscopy

A detailed microscopy of damaged specimens was carried out at NUST (College of EME), Pakistan. The aim was to visualize the failure modes and to compare the failure modes of 2D and 3D woven GFRP composite specimens.

3.4 Concluding remarks

Three types of FE macro-mechanical models were developed (i.e. Conventional shell, Continuum shell & Solid) to analyze the stress state developed within the specimen. Stress, strain and displacement convergence was performed to minimize the effect of mesh size on results. In the mean while, 2D and 3D woven GFRP composite specimens were tested to get the stress-strain and load displacement curves of the specimens. Failure loads and failure stresses of 2D and 3D specimens were also evaluated. The results of these simulations and experiments will be discussed in next chapter.

CHAPTER 4: RESULTS AND DISCUSSIONS

4.1 Introduction

In this chapter, FE models are validated with experimental results of UD carbon fibre composites. Longitudinal, transverse, in-plane and out of plane stresses are analyzed, and a good agreement is observed in numerical and experimental results. After that, a detailed damage analysis is carried out by using Abaqus built-in criteria. Hashin damage criteria is used to analyze the damage initiation of conventional and continuum shell element models. On the other hand, Hashin criterion cannot be simply implemented on solid element model therefore Abaqus built-in criteria for isotropic materials are used to get the reasonable approximation of failure initiation. Solid element model provided better results as it can capture out of plane response of composites. Therefore, it is decided to use 3D solid element model to analyze the stress state developed in 2D and 3D woven GFRP composite materials. Failure loads are taken from experimental results to compare the actual failure stress state of 2D and 3D woven GFRP composite specimens.

As mentioned in chapter 3 that four different paths are created near the hole to examine and compare the actual stress variation near the hole. Longitudinal, transverse, in-plane and out of plane stresses of 2D and 3D composites are compared on all paths and it is observed that the trends of all stresses are similar except out of plane stress. Moreover, it is also observed that the failure loads of 3D composites are lower than 2D composites.

A detailed microscopic analysis is also carried out to identify the failure modes of 2D and 3D woven GFRP composite specimens.

4.2 Multidirectional (UD) carbon fibre composites

4.2.1 Stress analysis of laminated CFRP composite

Numerical investigation of compressive failure of carbon fibre composite specimen under the application of failure load has been made by using three types of models. The three models differ in terms of underlying material model and the choice of elements used. The three type of models employed the conventional shell, continuum shell and solid element models respectively. Uni-directional CFRP laminate was modeled using the conventional and continuum shell element models and the material definition type selected in ABAQUS was of type lamina which represents a plane stress orthotropic material definition. The ply stacking sequence was specified using the section definition defined using the composite layup tool.

This allows for investigation of ply by ply stress-strain results. Similarly, solid element model with 3D orthotropic material properties was also built to get the better approximation of stress strain response of the laminate. Results are shown in table 14 & 15.

Tabulated results were taken from the same node at the hole vicinity for all the three models. The aim was to get the basic understanding of stress variation along different axis of the specimen.

Table 14: Ply by ply results of conventional and continuum shell element models for UD carbon fibre laminate

Ply layup		Conventional shell model			Continuum shell model		
Sequence	Angle	S11	S22	S12	S11	S22	S12
1	45	228.4	28.7	39.6	640.4	37.15	78.92
2	0	620.9	6.74	22.25	1127	5.015	44.03
3	-45	398.3	20.89	39.67	434.2	43.2	79.01
4	90	54.18	42.08	22.5	36.51	73.86	44.16
5	45	228.4	28.7	39.6	652.3	35.85	79.1
6	0	620.9	6.74	22.25	1126	5.763	44.29
7	-45	398.3	20.89	39.67	658.2	35.2	79.19
8	90	54.18	42.08	22.5	44.02	73.69	44.41
9	90	54.18	42.08	22.5	45.9	73.65	44.48
10	-45	398.3	20.89	39.67	397.1	45.1	79.33
11	0	620.9	6.74	22.25	1125	6.72	44.6
12	45	228.4	28.7	39.6	673.1	33.57	79.42
13	90	54.18	42.08	22.5	53.42	73.49	44.73
14	-45	398.3	20.89	39.67	375.9	46.19	79.51
15	0	620.9	6.74	22.25	1123	7.572	44.86
16	45	228.4	28.7	39.6	685	32.28	79.6

Table 15: Results of solid element model for UD carbon fibre laminate

Model type	S11 (max)	S22(max)	S33(max)	S12(max)	S13(max)	S23(max)
Solid	699.7	33.34	6.617	8.94	1.87	0.00166

Failure modes of OHC specimen are ambiguous due to anisotropic nature of composite materials. Complex stress field around the hole may cause failure mode mixing i.e. mixture of longitudinal, transverse and shear stress concentration leads to rupture. In this section, effect of such stresses will be discussed one by one;

4.2.1.1 Longitudinal compressive stress, S11

Failure initiation was indicated in conventional and continuum shell element models at plies 2,3,6,7,10,11,15 &16 and 1,2,3,5,6,7,10,11,12,14,15 &16 respectively because

maximum longitudinal compressive stress was observed higher than the experimental failure stress. Similarly, in solid element model, higher magnitude of longitudinal compressive stress than the actual failure stress indicates the failure initiation.

Longitudinal compressive stress is observed as a dominant stress among all stresses which may initiate damage near the hole. In conventional and continuum shell element models, different magnitude of longitudinal stress at different plies is observed near the hole. Thus, the results which are closer with experimental values will be discussed i.e. ply 14 as shown in table 16. Fig. 20, 21, 22 & 23 show the results of longitudinal compressive stress variation along the length of the specimen in conventional shell, continuum shell and solid element models respectively.

Table 16: Maximum longitudinal compressive stress in different models

Model type	S11, MPa (max)
Conventional shell(ply-14)	398.3
Continuum shell(ply-14)	375.9
Solid	699.7
Experimental	398

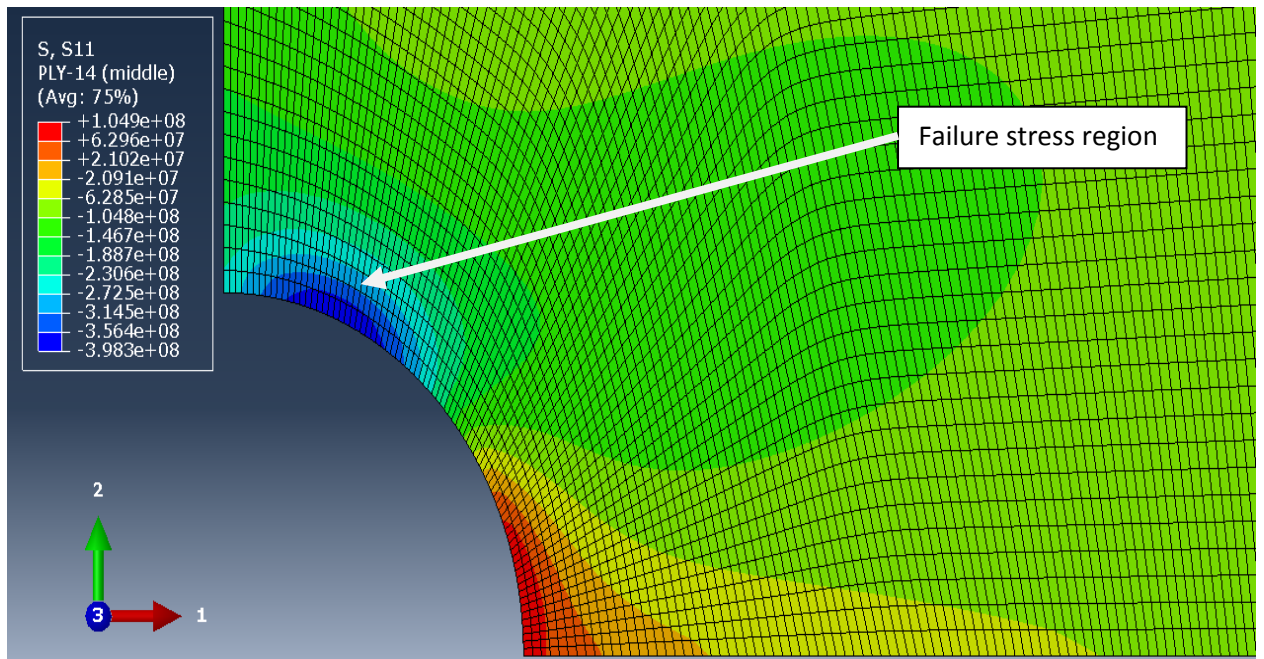


Figure 20: A zoomed view of longitudinal compressive stress variation near the hole at ply-14(Conventional shell model)

Fig. 20 is a closer view of longitudinal compressive stress variation near the hole vicinity of 2D conventional shell element model. Negative magnitude of S11 indicates that the stresses are compressive and blue region indicates the highest stress concentration regime.

In all models, compressive stress concentration appears to be in safe limits (i.e. below 398 MPa) at maximum portion of specimen but its magnitude was higher near the hole than compressive strength of the composite (i.e. 398 MPa) as shown in fig. 20, 21, 22 & 23. This indicate that the damage initiation will occur at hole vicinity as it is the area of maximum stress concentration. In other words, higher the stresses near the hole severe will be the damage. Therefore, it was concluded that the magnitude of longitudinal compressive stress in all models were closer to each other and a good agreement was observed between numerical and experimental results.

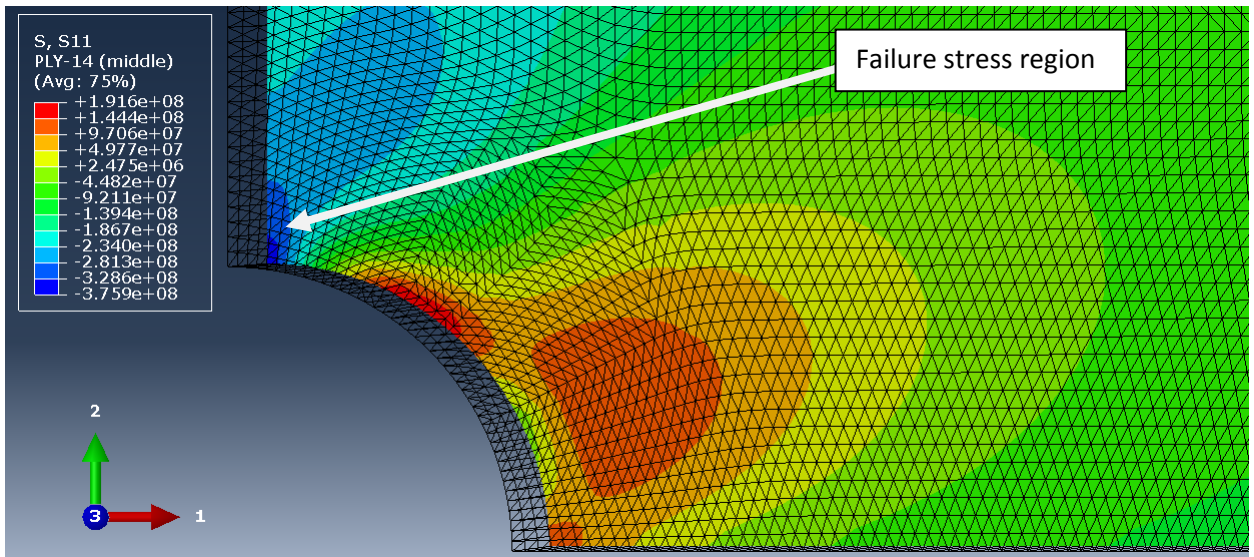


Figure 21: A zoomed view of longitudinal compressive stress variation near the hole at ply-14(Continuum shell model)

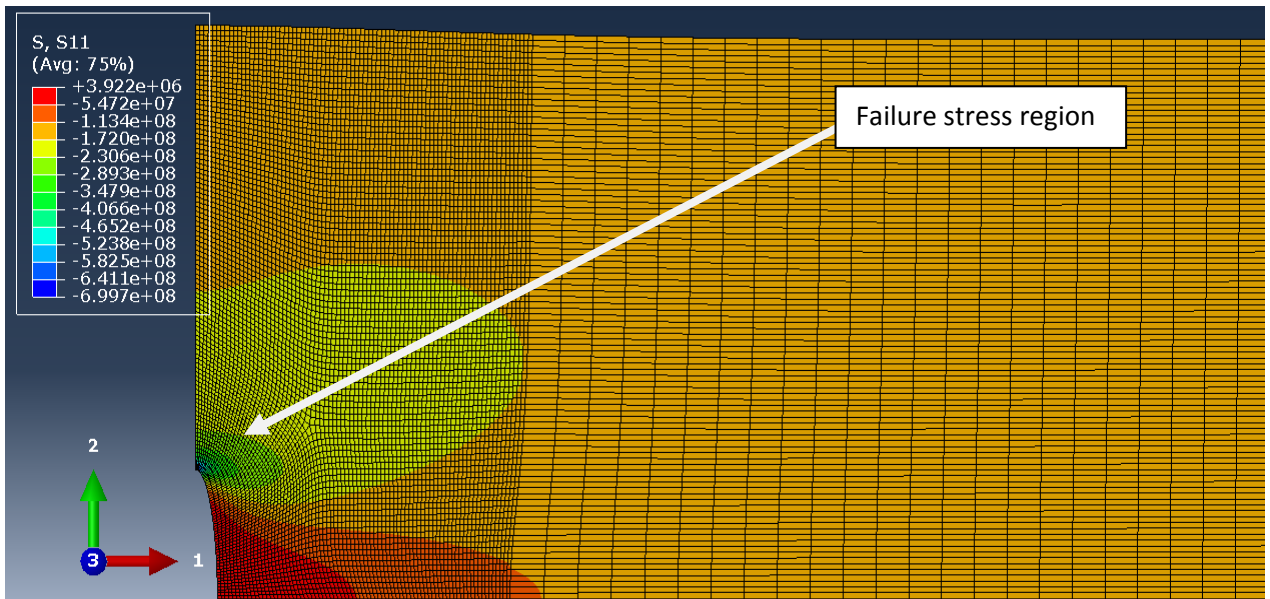


Figure 22: Longitudinal compressive stress variation near the hole (Solid model)

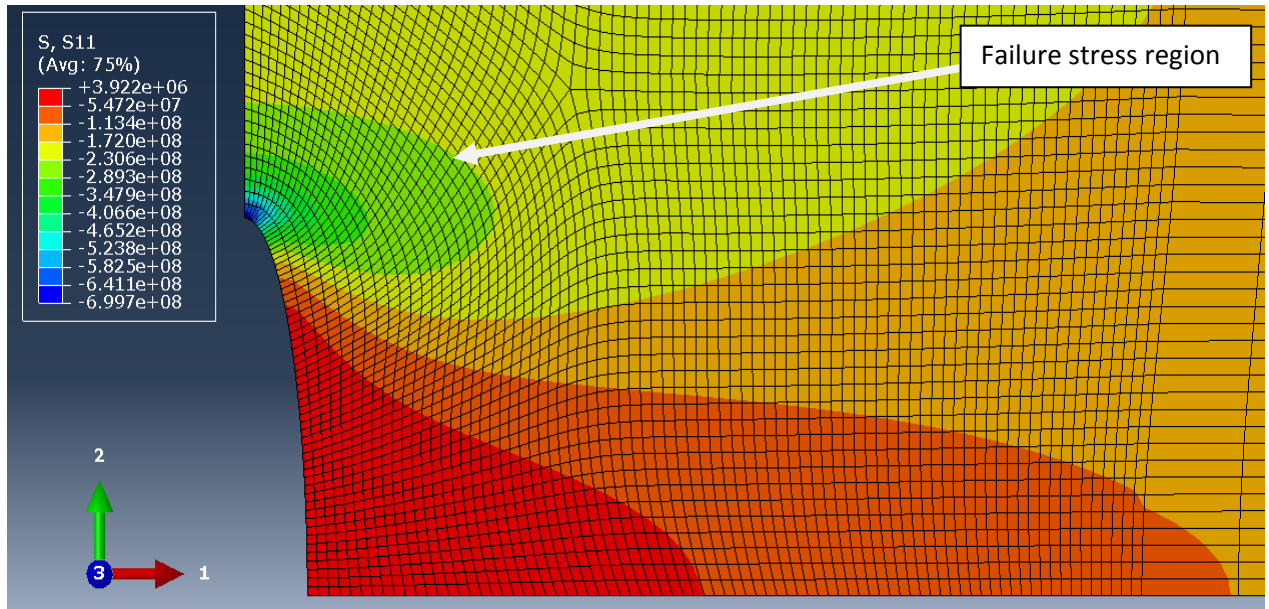


Figure 23: A zoomed view of longitudinal compressive stress variation near the hole (Solid model)

4.2.1.2 Transverse stress, S22

Different magnitude of transverse tensile and transverse compressive stresses was observed in all three models as shown in table. Highest transverse tensile and compressive stresses were observed in solid element model. This occurs due to solid elements as these elements can cater transverse as well as through thickness effects. Table 17 has shown results of conventional shell (ply-14), continuum shell (ply-14) and solid element models.

Table 17: Maximum transverse stress in different models

Model type	S22 tensile, MPa (max)	S22 compressive, MPa (max)
Conventional shell(ply-14)	7.052	20.89
Continuum shell(ply-14)	14.1	46.19
Solid	50.62	33.34

Figs 24, 25 & 26 have shown the transverse stress (S22) variation near the hole of the specimen in all the three models.

High magnitude of transverse tensile stress was observed near the hole in solid element model. This indicated the significant increase in OHC strength of the composite as explained by Fleck et al. In the work of Fleck et al, they also stated that the high magnitude of transverse tension near the hole occurs due to matrix shearing (outward direction) and fibre micro- buckling near the hole [74].

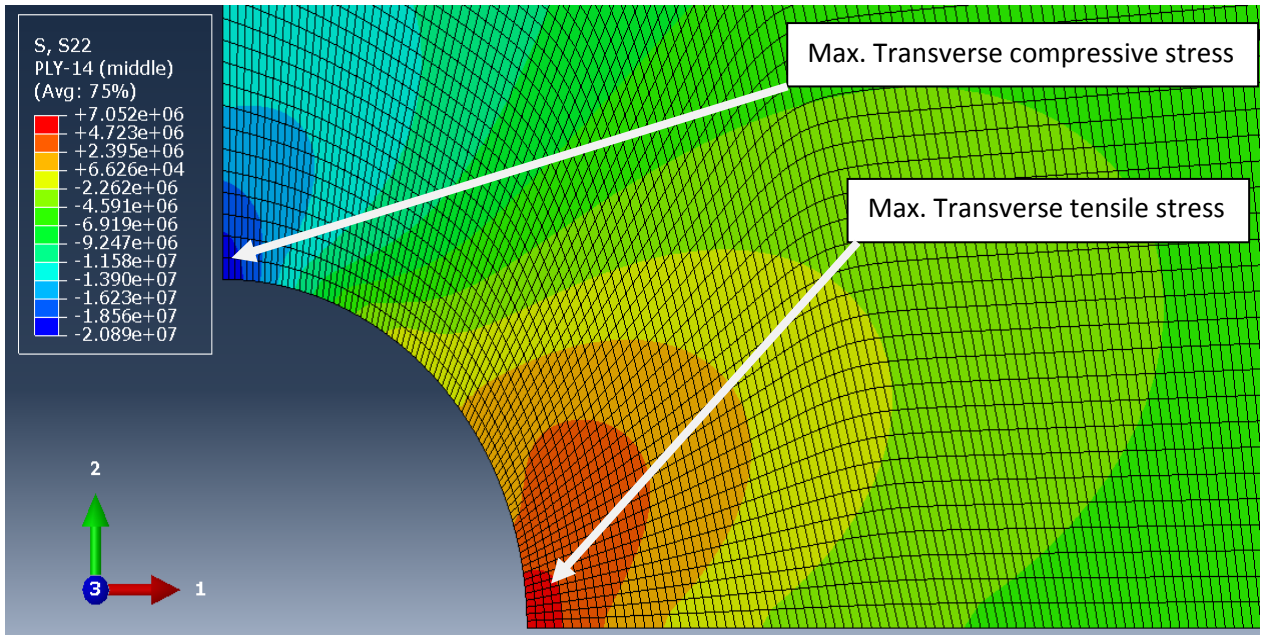


Figure 24: A zoomed view of transverse stress variation near the hole at ply-14(Conventional shell model)

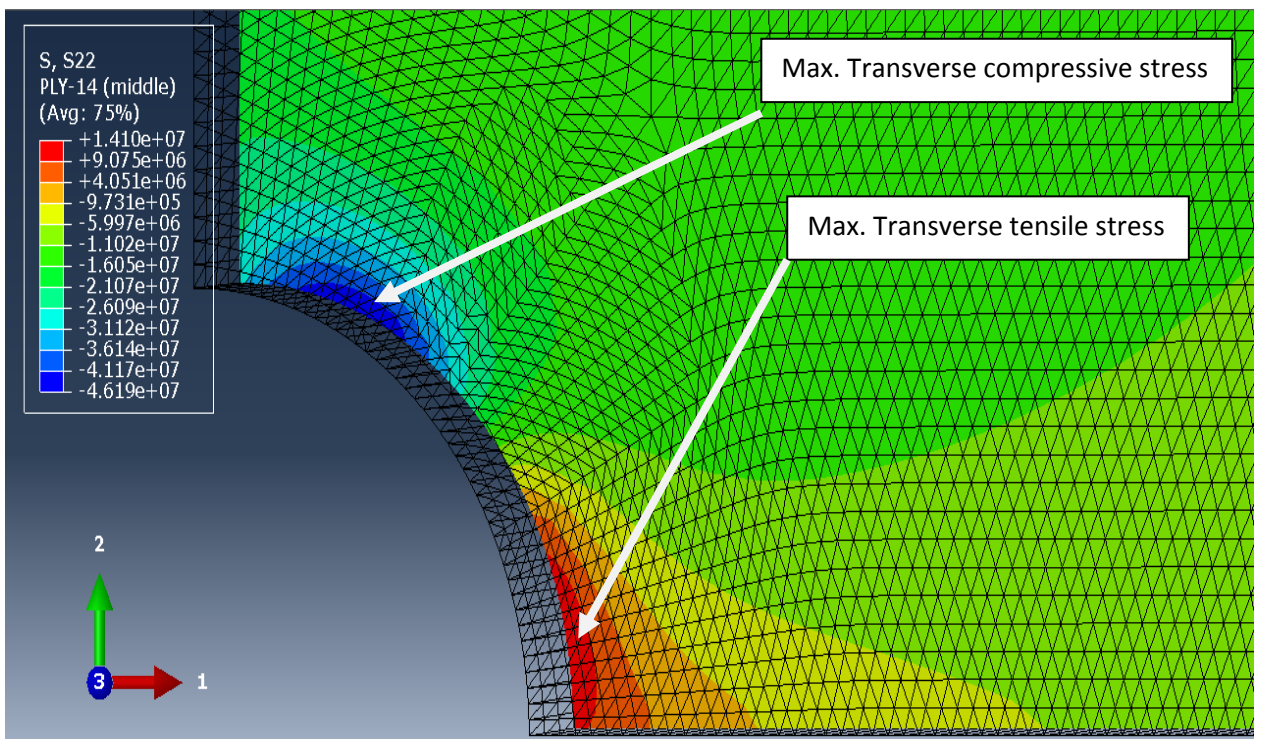


Figure 25: A zoomed view of transverse stress variation near the hole at ply-14 (Continuum shell model)

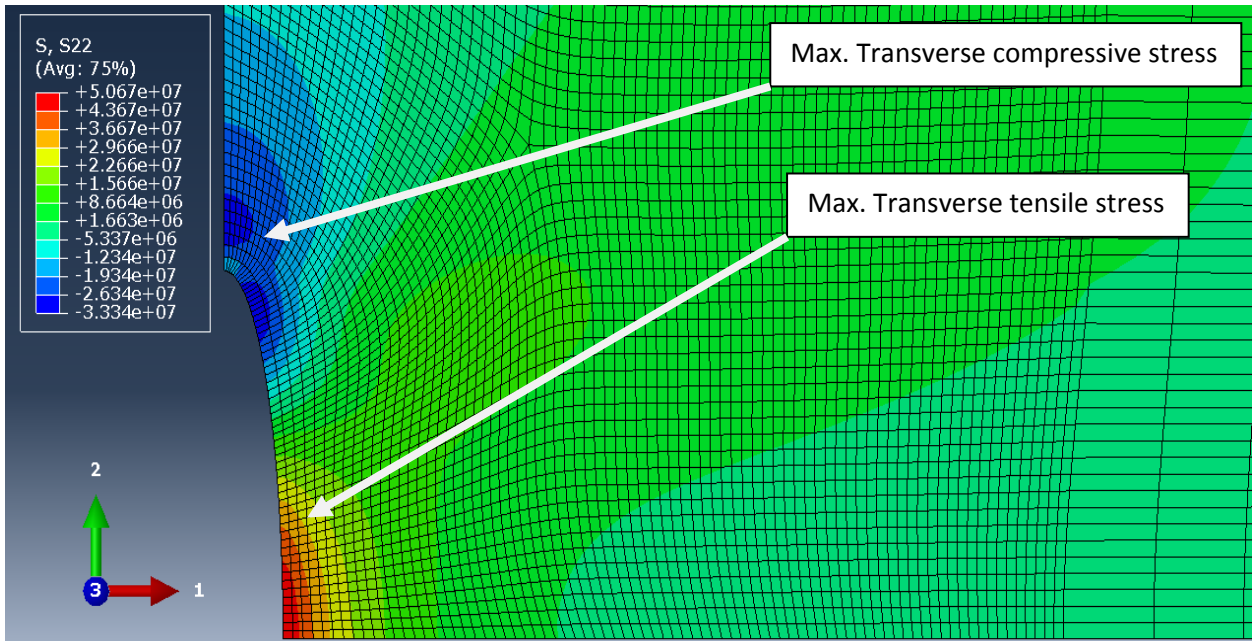


Figure 26: A zoomed view of transverse stress variation near the hole (Solid model)

4.2.1.3 In-plane stresses, S12

Figs 27, 28 & 29 have shown the in-plane shear stress distribution near the hole region of the specimen in all models. In-plane shear stress concentration was also observed near the hole.

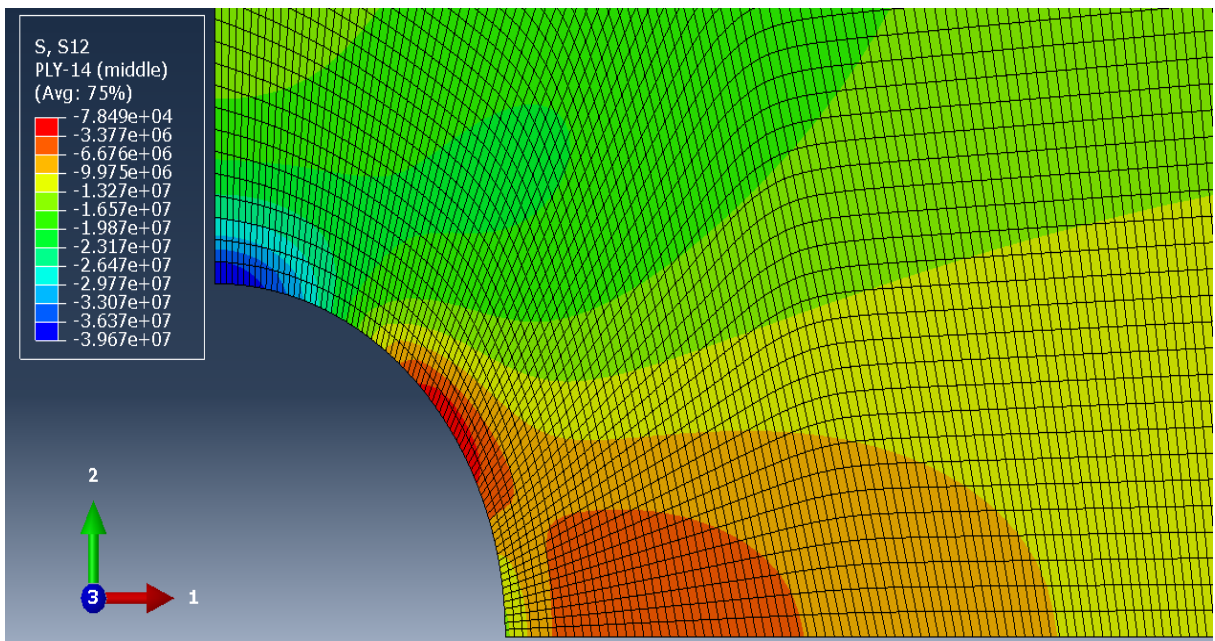


Figure 27: A zoomed view of in-plane stress variation near the hole at ply-14 (Conventional shell model)

Model type	S12, MPa (max)
Conventional shell(ply-14)	39.67
Continuum shell(ply-14)	79.51
Solid	8.94

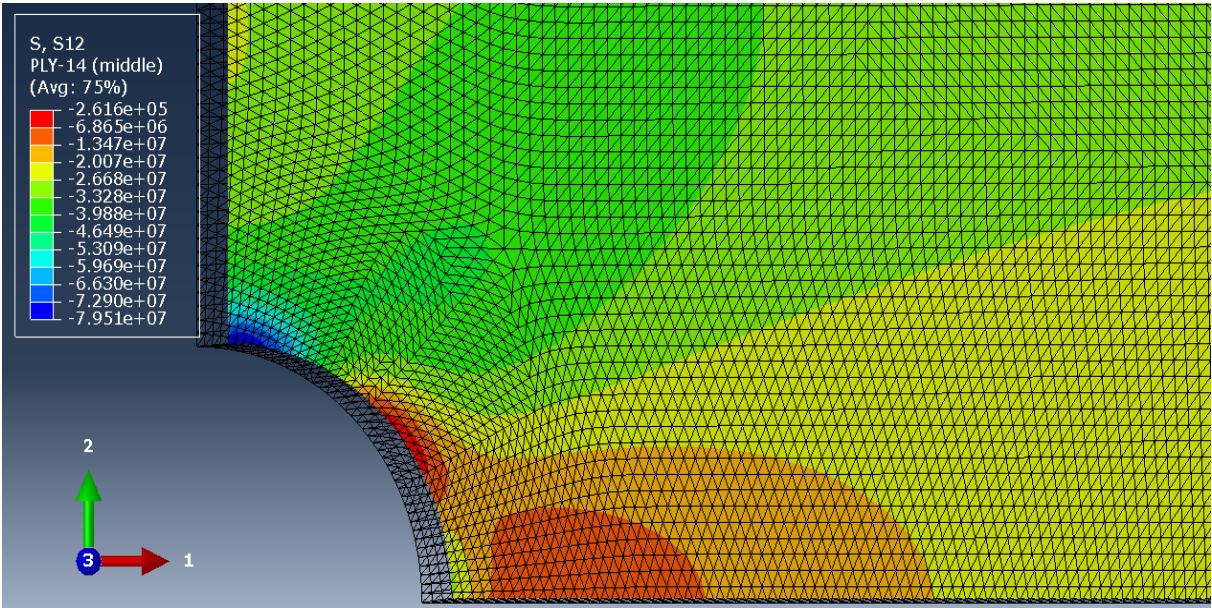


Figure 28: A zoomed view of in-plane stress variation near the hole at ply-14 (Continuum shell model)

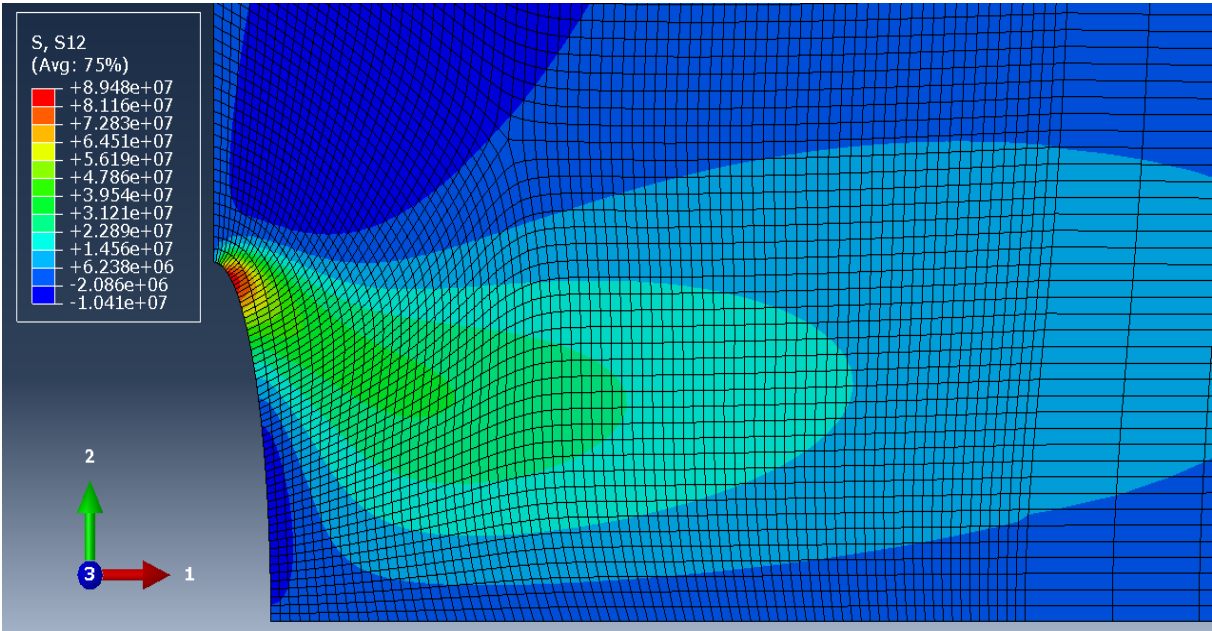


Figure 29: A zoomed view of in-plane stress variation near the hole (solid model)

In conventional shell and solid element models, magnitude of in-plane shear stress was seemed to be lower than in-plane shear strength of the composite. This indicates that the matrix/interface damage is not initiated due to in-plane shear stresses as Camanho et al observed that the high magnitude of in-plane stresses can significantly reduce the matrix properties and can initiate the matrix/interface damage within the specimen. On the other hand, in continuum shell element model, magnitude of in-plane shear stress seemed to be higher than in-plane shear strength of the composite. This indicates that the matrix/interface damage initiation occurs due to in-plane shear stress [75].

4.2.1.4 Through thickness stresses

Continuum and conventional shell elements are not capable of modeling the through thickness response of the specimen. Through thickness stress results of solid element model are as under;

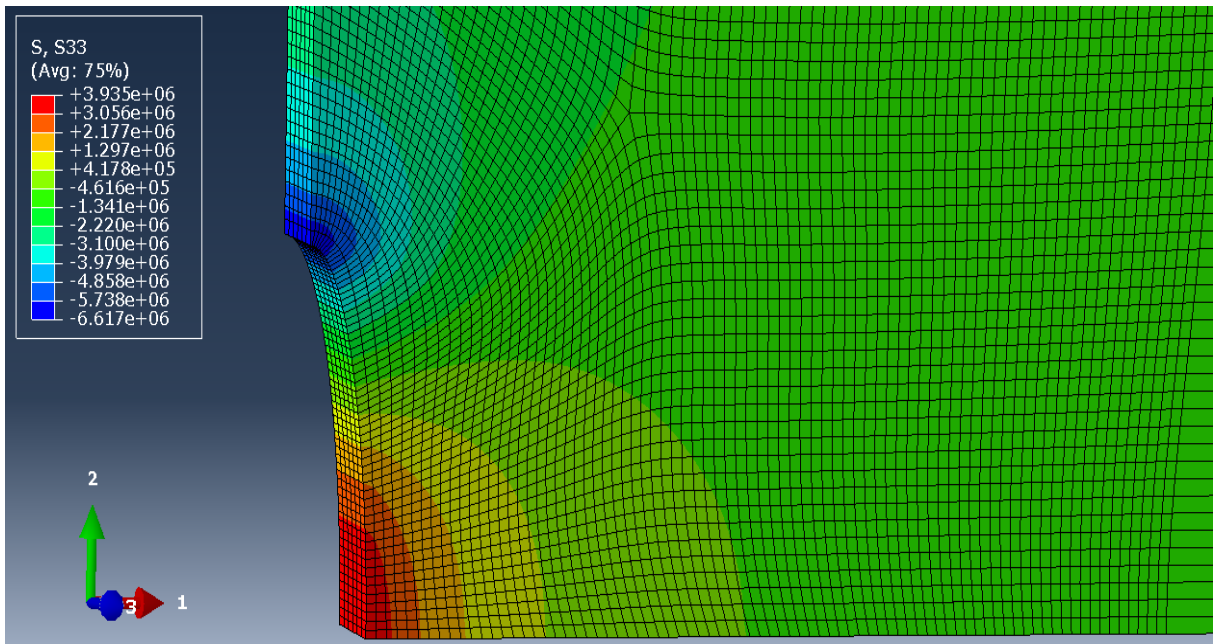


Figure 30: A zoomed view of through thickness stress variation near the hole (solid model)

It was also observed that the magnitude of through thickness stress is much lower than longitudinal compressive stress developed within the specimen. This might occur due to low out of plane moduli of composite.

4.2.2 Damage analysis

4.2.2.1 Conventional and continuum shell element models

In failure modeling of fibre-reinforced composites it was observed that application of failure load causes local matrix/fibre damage of the specimen. Failure mechanics of composites are much more complicated than isotropic materials. Therefore, laws of fracture mechanics cannot be simply implied to do the damage analysis of composites. In this regard, many theories have been proposed to determine the damage initiation and evolution of composites. One of those well known theories is Hashin criterion.

Hashin, a strength based failure criterion was used to predict the damage initiation [76]. In Abaqus 6.10, it can only be applied on conventional shell and continuum shell elements due to plane stress assumption [77,78]. In this work, the aim was to only validate the damage initiation instead of modeling the complete failure. Therefore, four modes of failure were considered i.e. fibre failure in tension, fibre failure in compression, matrix failure in tension and matrix failure in compression [79]. Mathematical formulations are as under:

(a) Fibres rupture in tension: $\hat{\sigma}_{11} \geq 0$

$$F_f^t = (\hat{\sigma}_{11}/X^T)^2 + \alpha (\tau_{12}/S^L)^2$$

(b) Fibre buckling and kinking in compression: $\hat{\sigma}_{11} < 0$

$$F_f^c = (\hat{\sigma}_{11}/X^C)^2$$

(c) Matrix cracking under transverse tension and shearing: $\hat{\sigma}_{22} \geq 0$

$$F_m^t = (\hat{\sigma}_{22}/Y^T)^2 + (\tau_{12}/S^L)^2$$

(d) Matrix crushing under transverse compression and shearing: $\hat{\sigma}_{22} < 0$

$$F_m^c = (\hat{\sigma}_{22}/2S^T)^2 + [(Y^C/2S^T)^2 - 1] \hat{\sigma}_{22}/Y^T + (\tau_{12}/S^L)^2$$

Where,

X^T and X^C are longitudinal tensile and compressive strengths respectively

Y^T and Y^C are transverse tensile and compressive strengths respectively

S^L and S^T are longitudinal and transverse shear strengths respectively

X^T , X^C , Y^T , Y^C , S^L and S^T are the input material properties which are required for Hashin's criterion. α is a constant which measures the overall shear stress contribution in

tensile fibre failure initiation. σ_{11}, σ_{22} and τ_{12} are the effective stress tensor components which are used to evaluate the damage initiation

In this criterion, all modes of damage initiation are associated with output variables to indicate whether the failure is initiated or not. If the magnitudes of output variables reach or exceed 1, the criterion has been met and the damage is initiated. Output variables which are available in Abaqus to relate the damage initiation in composites are shown in table 18.

Table 18: Output variables available in ABAQUS for Hashin damage [80]

HSNFCCRT	Maximum value of the fiber compressive initiation criterion experienced during the analysis.
HSNMTCRT	Maximum value of the matrix tensile initiation criterion experienced during the analysis
HSNMCCRT	Maximum value of the matrix compressive initiation criterion
HSNFTCRT	Maximum value of the fiber tensile initiation criterion experienced during the analysis.

In this section, results of continuum shell elements will be discussed as it was observed that the magnitudes of output variables of conventional and continuum shell elements were almost similar. Therefore, the magnitudes of output variables are presented in table 19.

Table 19: Results of output variables for prediction of damage initiation

Ply layup		Damage model of shell elements			
Sequence	Angle	HSNFCCRT	HSNFTCRT	HSNMCCRT	HSNMTCRT
1	45	1.914	0	11.82	4.179
2	0	5.949	0	3.464	3.772
3	-45	0.94	0	11.8	1.859
4	90	0	0.32	3.674	0
5	45	1.986	0	11.86	4.069
6	0	5.937	0	3.466	3.796
7	-45	2.023	0	11.88	4.015
8	90	0	0.24	3.726	0
9	90	0	0.26	3.739	0
10	-45	0.34	0	11.91	1.966
11	0	5.922	0	3.822	3.432
12	45	2.115	0	11.93	3.208
13	90	0	0.20	3.791	0
14	-45	0.32	0	11.97	2.028
15	0	5.911	0	3.833	3.28
16	45	2.191	0	11.98	3.09

4.2.2.1.1 Hashin's compressive fibre initiation criterion (HSNFCCRT)

In both models, different trends of compressive fibre failure initiation were observed at various plies as shown in table 19. Maximum compressive fibre failure was observed at plies 2, 6, 11 and 15 which are located at 0° i.e. longitudinal fibres. Results of ply-2 are shown in fig 31. On the contrary, minimum/no compressive fibre failure was observed at ply 3, 4, 8, 9, 10, 13 and 14 which are located at 90° i.e. transverse fibres. Results of ply-4 are shown in fig 32. Intermediate compressive fibre failure was observed at plies 7 and plies 1, 5, 12 & 16 which are located at 45° and -45° respectively to the loading direction. Results of ply-1 are shown in fig 33.

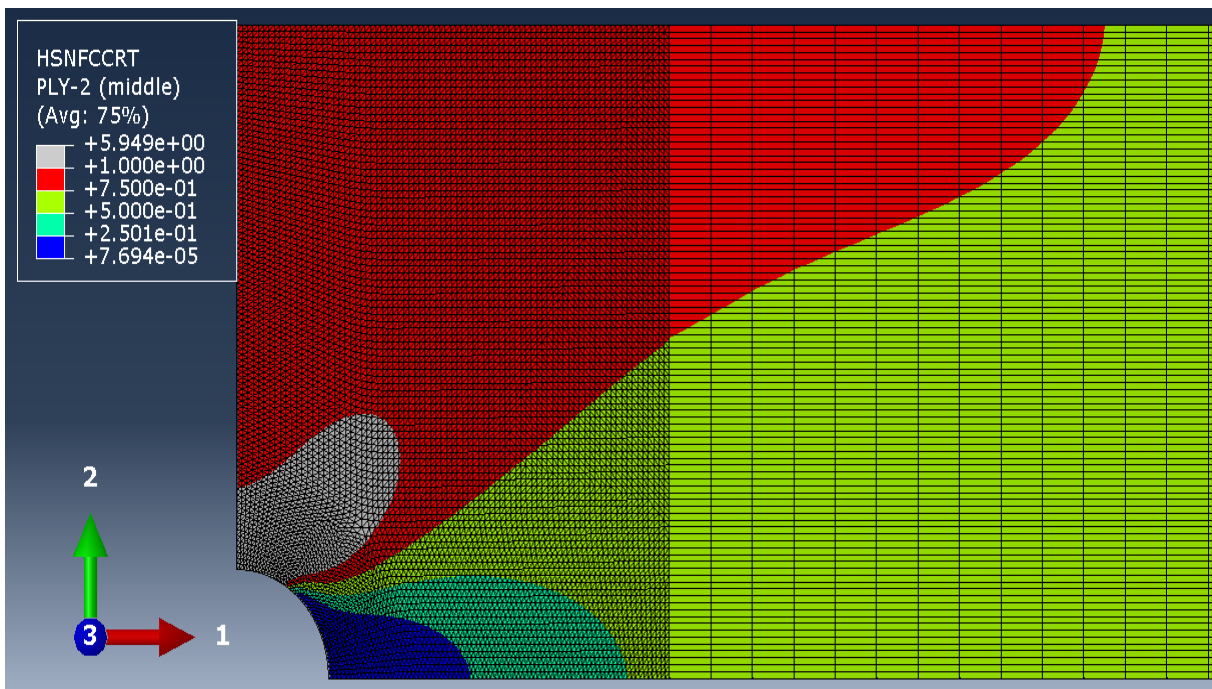


Figure 31: Results of compressive fibre failure at ply-2. A zoomed view near the hole

Initial failure was observed at 0° plies and damage propagates by further increasing the load as shown in table 19. This occurs due to tough interface of the specimen. Similarly, 11.31 times larger stress concentration was observed at 0° plies than the stress applied at transverse fibres as Ishikawa et al reported 11.6 times larger stress concentration at 0° plies than average stress developed in quasi-isotropic laminates. Conclusively, failure initiation was observed at 0° plies as magnitude of longitudinal compressive stress and compressive fibre failure index were maximum at these plies. This may occur due to fibre micro-buckling as Ishikawa et al reported fibre micro-buckling as the major cause of failure initiation in quasi isotropic laminates at 0° plies [24].

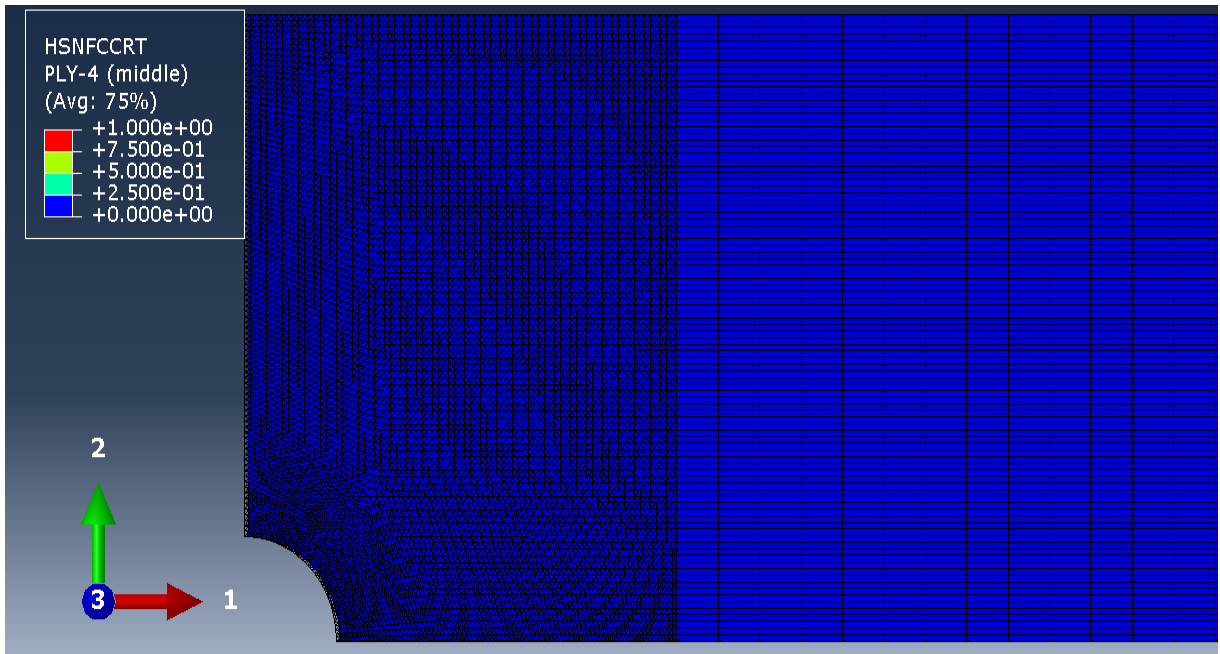


Figure 32: Results of compressive fibre failure at ply-4. A zoomed view near the hole

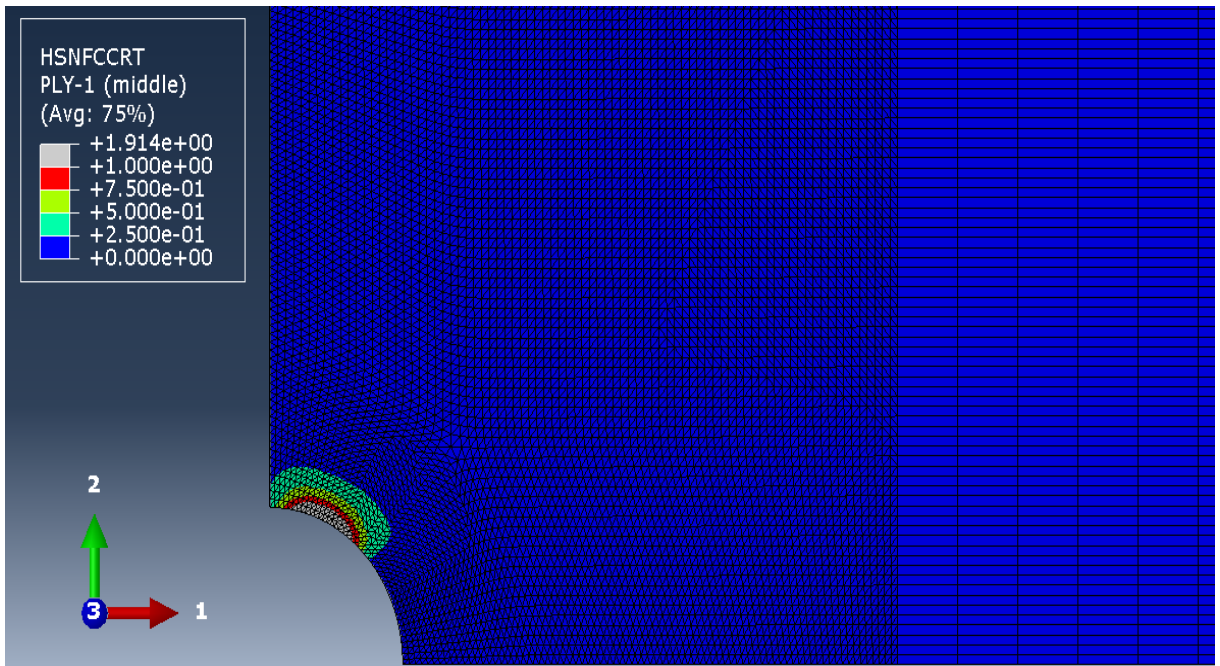


Figure 33: Results of compressive fibre failure at ply-1. A zoomed view near the hole

4.2.2.1.2 Hashin's tensile fibre initiation criterion (HSNFTCRT)

In both models, tensile fibre failure initiation was not observed even at single ply as shown in table 19.

As we know composites are mainly comprised of two constituents i.e. fibre and matrix and the purpose of matrix is to provide the interfacial bonding to fibres. It also provides lateral support which improves the overall stability of composite under longitudinal loading conditions [81]. Therefore, understanding the role of matrix is necessary to accurately predict the failure strength of composite.

It is a fact that the composite failure initiates in matrix and propagates through fibres due to its low elastic modulus. Therefore, it is indispensable to separately model the matrix and fibre failure of composite. Details of tensile and compressive matrix failure are presented below.

4.2.2.1.3 Hashin's compressive matrix initiation criterion (HSNMCRT)

Compressive matrix failure was observed at all plies of the laminate as shown in table 19. Maximum failure was observed at plies 1, 3, 5, 7, 10, 12, 14 and 16 which are oriented at 45° and -45° to the longitudinal fibres. Results of ply-16 are shown in fig 34. On the other hand, intermediate failure was observed at 0° and 90° plies. Minimum damage was observed at ply-2 as shown in fig 35.

Compressive stress concentration near the hole is seemed to be the cause of damage initiation and propagation within matrix. It was observed that the failure is propagated at maximum portion of the specimen at various plies. This may occur due to localized buckling of fibres which initiates due to low modulus of matrix.

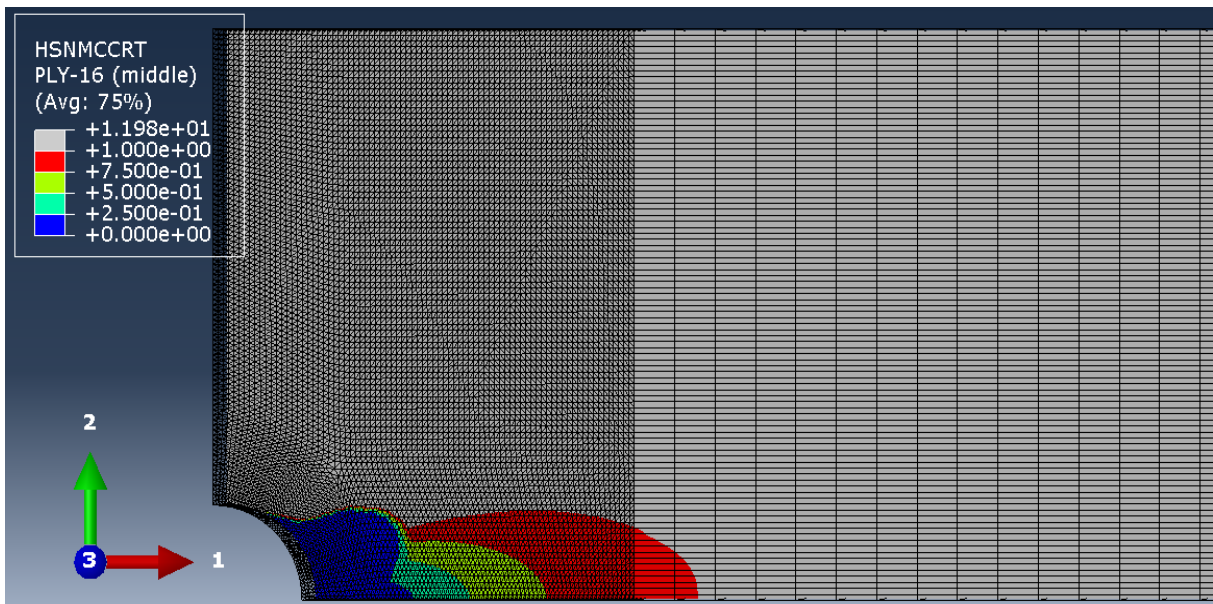


Figure 34: Results of compressive matrix failure at ply-16. A zoomed view near the hole

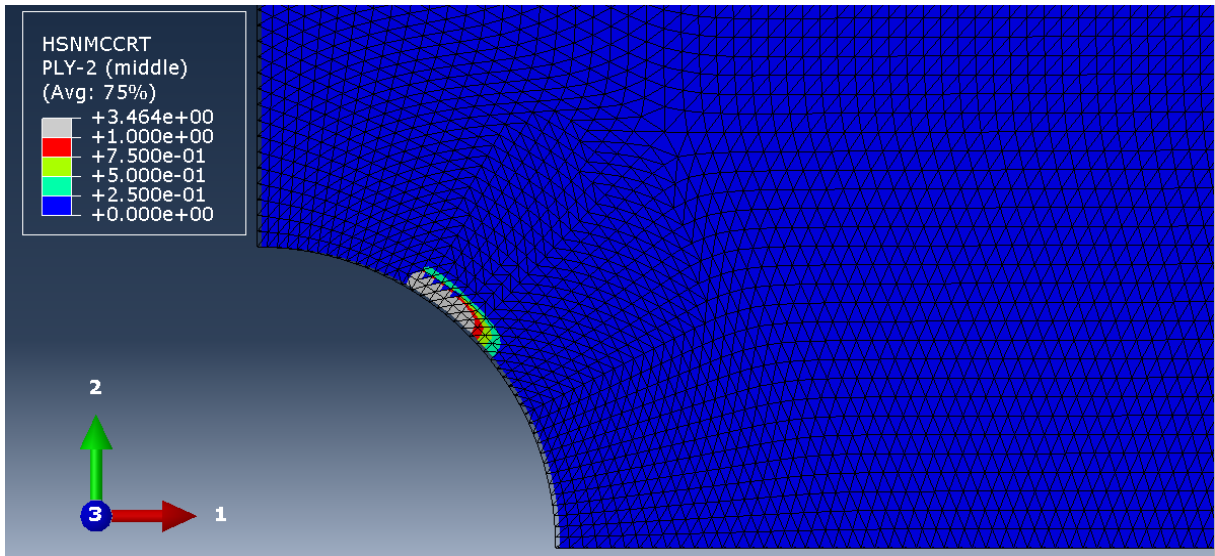


Figure 35: Results of compressive matrix failure at ply-2. A zoomed view near the hole

4.2.2.1.4 Hashin's tensile matrix initiation criterion (HSNMTCRT)

Different trends of tensile fibre failure were observed at various plies as shown in table 19. Maximum tensile matrix damage was observed at ply-1 which is oriented at 45° to the longitudinal fibres. Results of ply-1 are shown in fig 36. On the contrary, minimum/zero damage was observed at ply 4, 8, 9 and 13 which are oriented at 90° to the longitudinal fibres, i.e. transverse fibres. Results of ply-4 are shown in fig 37.

Intermediate compressive fibre failure was observed at plies 2, 3, 5, 6, 7, 10, 11, 12, 14, 15 and 16 which are oriented at 45° and -45° to the loading direction.

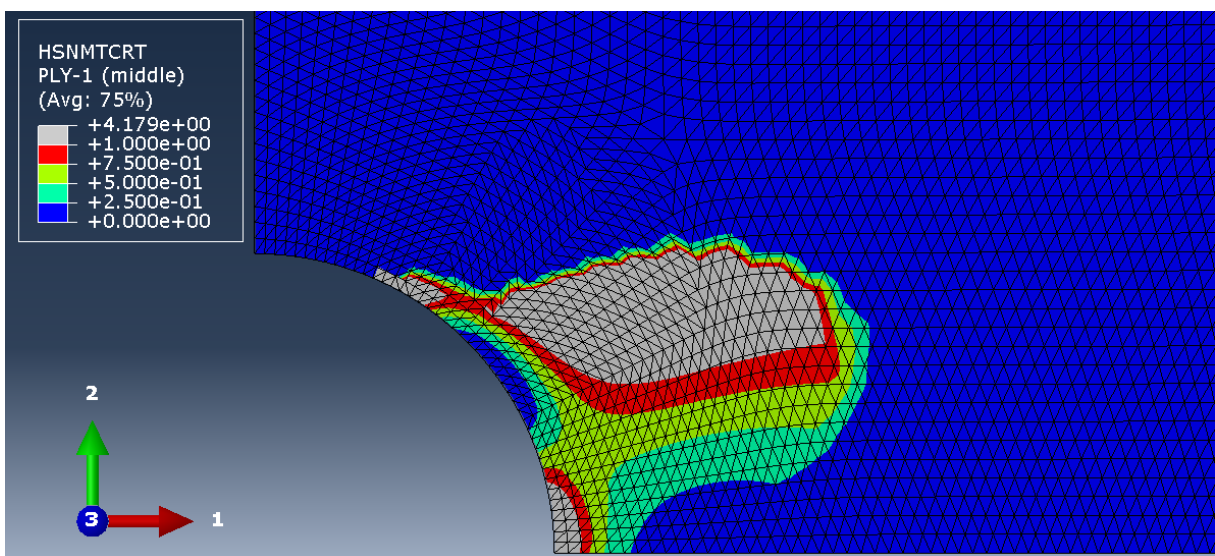


Figure 36: Results of tensile matrix failure at ply-1. A zoomed view near the hole

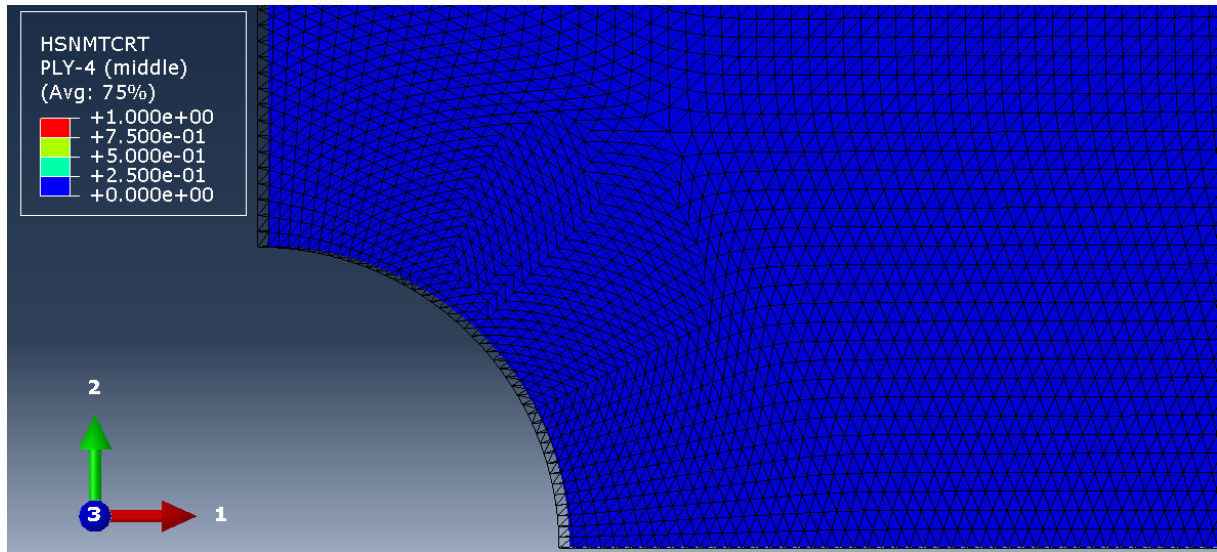


Figure 37: Results of tensile matrix failure at ply-4. A zoomed view near the hole

4.2.2.2 Solid model

Standard available failure criteria for isotropic materials were used to validate the failure initiation within the specimen. Details of the failure criteria which have been used in this work are as under;

4.2.2.2.1 Maximum normal stress criterion

Failure initiation was observed near the hole as the longitudinal compressive stress (i.e. 697 MPa) was much higher than compressive strength (i.e. 398 MPa) of the laminate. Results are shown.

Mathematically, maximum stress criterion can be expressed as

$$\text{Normalized comp. stress (697 MPa)} > \text{Comp. strength of laminate (398 MPa)}$$

Black elements (damaged elements) in fig 38 have shown the failure initiation near the hole as maximum normalized compressive stress in these elements exceeds the compressive strength of composite.

Lau et al proves that, maximum normalized stress criterion provides satisfactory response for determination of notch strength of fabric composites [82]. The only problem in using this criterion for determination of OHC strength of composites is that it ignores the interaction of stresses within the specimen. However, this interaction takes place due to

compression of filling yarns which than increases the strength in warp direction and vice versa.

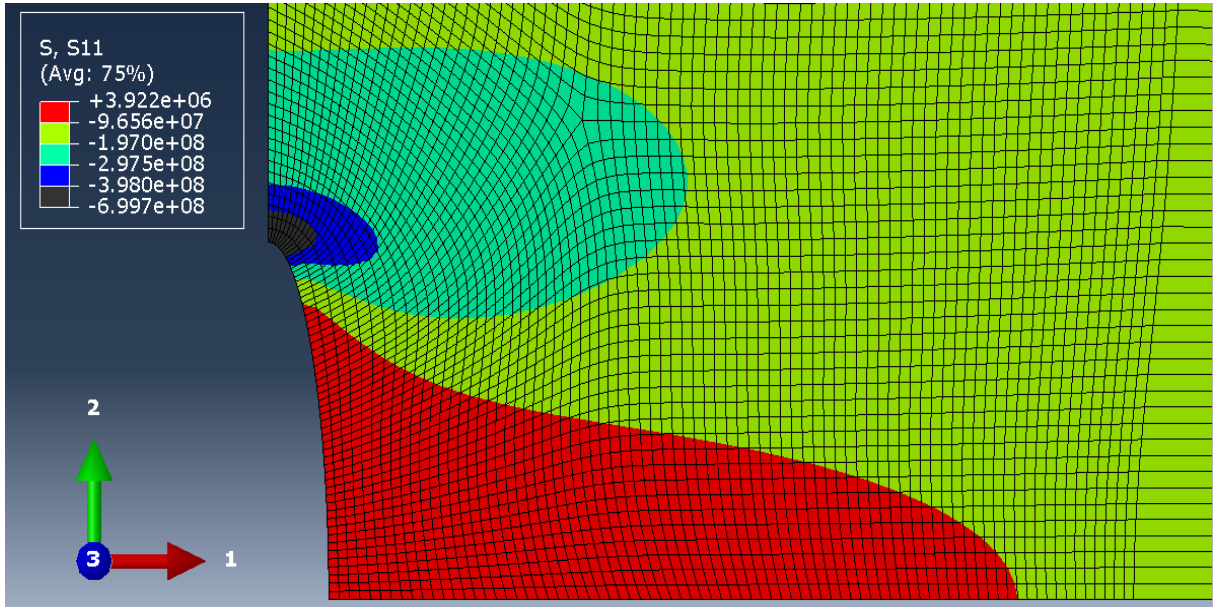


Figure 38: A zoomed view of maximum normalized stress failure near the hole

4.2.2.2.2 Von Mises (VM) criterion

VonMises failure was observed near the hole as the equivalent or VM stress i.e. 689 MPa was higher than the compressive strength i.e. 398MPa of the laminate. Results are shown in fig 39.

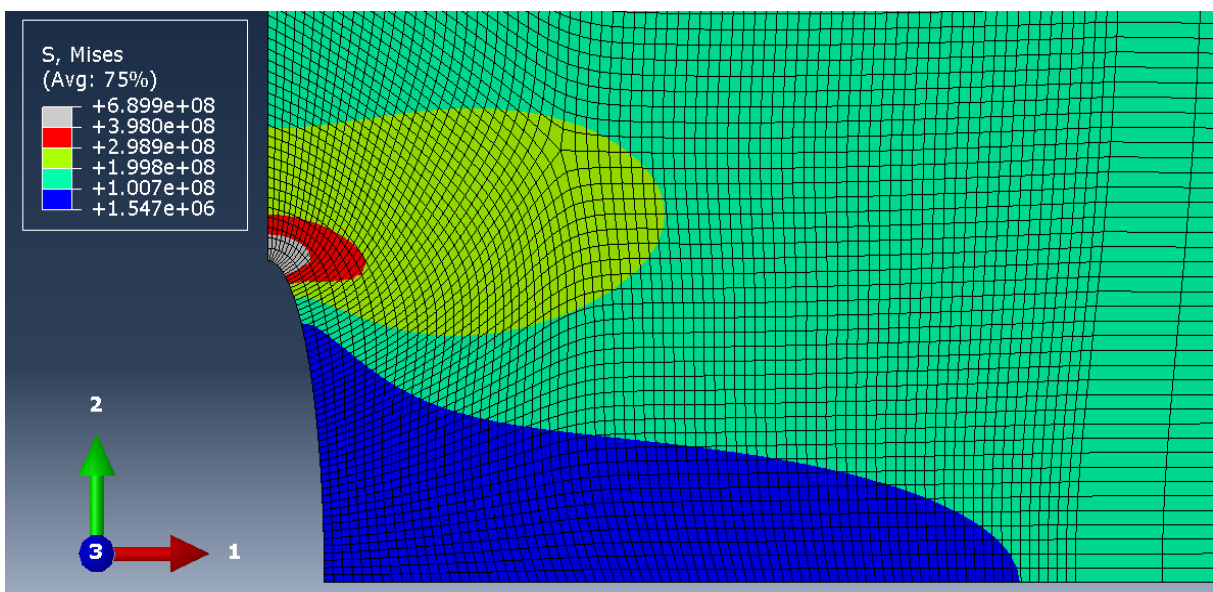


Figure 39: A zoomed view of von-Mises failure near the hole

Grey elements (damaged elements) in fig 39 have shown the failure initiation near the hole as VM stress in these elements exceeds the compressive strength of the composite.

All of these failure criteria have shown that the failure is according to ASTM standard D6484. It was also observed that the failure initiation was at desired stress level and at desired position (i.e. hole).

4.3 2D and 3D woven GFRP composite

As explained in previous sections that the aim of this research is to determine whether ASTM D6484 standard test method is applicable for evaluating open hole compressive properties of 2D and 3D woven composites. To achieve this objective, a detailed numerical and experimental work has been carried out as explained in following sections,

4.3.1 Experimental results

2D and 3D woven GFRP specimens were tested on a 100 KN universal testing machine. The aim was to determine the compressive failure loads, load displacement curves and failure modes of these specimens. Details of experimental results are as under;

4.3.1.1 Failure loads

Fixture was placed vertically between the jaws of the machine and a uni-directional compressive load was then applied on the wedge grips of the fixture. Compression through shear load was then shifted in the specimen and a load was continuously applied till rupture. In order to get the accurate results, factors such as fixture alignment, separation of fixture halves etc must be properly controlled. The aim was to evaluate the failure loads and failure stress of 2D and 3D specimens. Details of 2D and 3D woven GFRP composite specimens are shown in table 20 & 21.

Table 20: Failure loads of 3D specimens

3D specimens	Maximum load(kN)	X-Area of the specimen(mm ²)	Failure stress(MPa)
1	8.36	58.9	141.93
2	8.78	53.2	165
3	11.18	56.9	196.48
4	10.32	56.3	183.3
5	9.44	54.5	173.21
6	11.6	54.8	211.67
Mean	9.94	55.7	178.6
S.D	1.306	1.849	24.470

Table 21: Failure loads of 2D specimens

2D specimens	Maximum load(kN)	X-Area of the specimen(mm ²)	Failure stress(MPa)
1	12.28	60.2	203.98
3	11.98	55.5	215.85
4	10.7	54.1	197.78
5	11.04	54.9	201.09
6	10.38	56.8	182.74
Mean	11.27	56.3	200.29
S.D	0.820	2.39	11.944

For 3D woven composites, mean and standard deviation of failure stress 178.6 and 10.68 was observed respectively. While for 2D woven composites, mean and standard deviation of failure stress 200.2 and 11.94 was observed respectively.

Conclusively, experimental results have shown that the OHC strength of 3D specimens was lower than 2D specimens. This response of 3D material can only be attributed to z-directional fibres. Introduction of z-yarns creates a matrix rich pockets within the composite which significantly reduces the in plane properties of composites[83]. Moreover, this introduces excessive crimping within the fibres which causes reduction in in-plane properties of 3D composites[83].

4.3.1.2 Load-displacement curves

In load transferring, a small slippage between fixture and loading mechanism was observed initially which then causes the strain non linearity in start of test.

For 2D woven fibre reinforced composite specimens, a linear trend was observed initially with increasing load. After a peak load, the material transforms to plastic region and non linearity was observed until the specimen gets fracture. Experimental results of load displacement curves of 2D specimens are shown in fig 41.

For 3D woven fibre reinforced composite samples, a non linear load transfer was observed and it continued till the specimen got failure. This behaviour of 3D samples can be due to 3rd directional fibres as it distributes the loads in all directions.

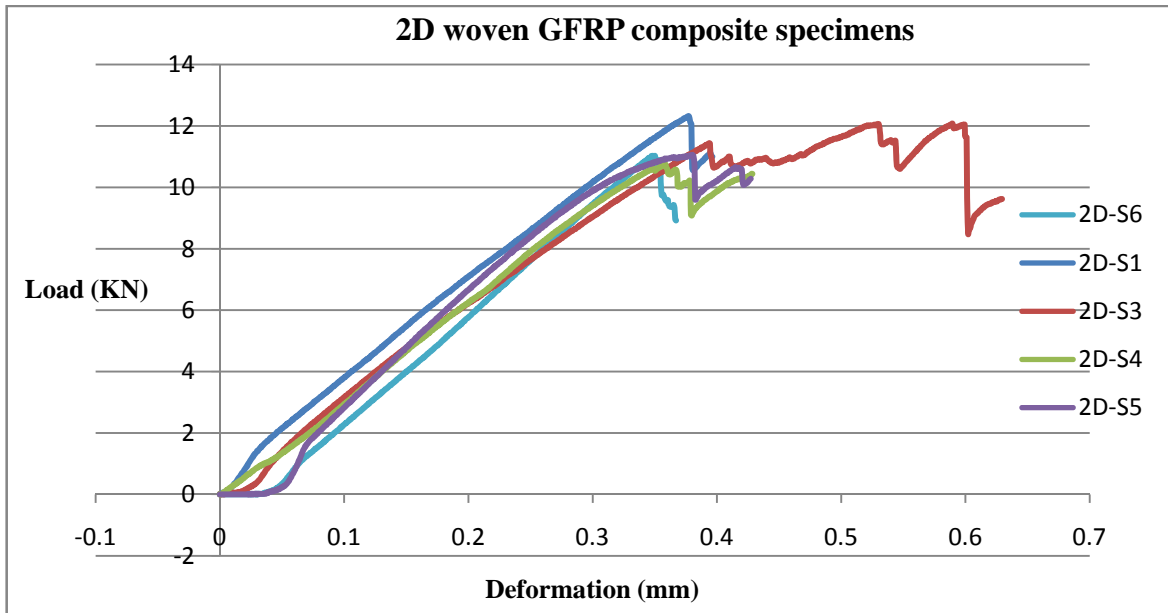


Figure 40: Load displacement curves of 2D woven GFRP composite specimens

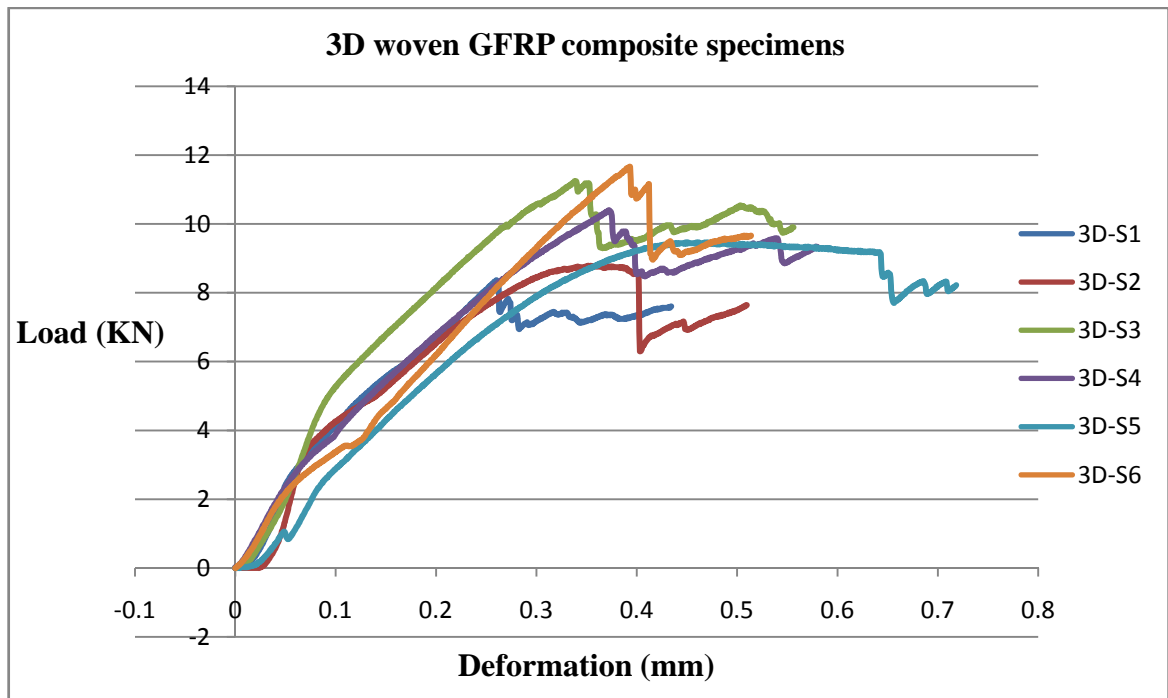


Figure 41: Load displacement curves of 3D woven GFRP composite specimens

4.3.1.3 Stress strain diagrams

For 2D woven fibre reinforced composite specimens, a linear trend was observed initially with increasing stress. After a peak stress, the material transforms to plastic region

and non linearity was observed until the specimen gets fracture. Therefore, it was concluded that the catastrophic damage was observed in all 2D specimens. Experimental results of stress vs. strain curves of 2D specimens are shown in fig 43.

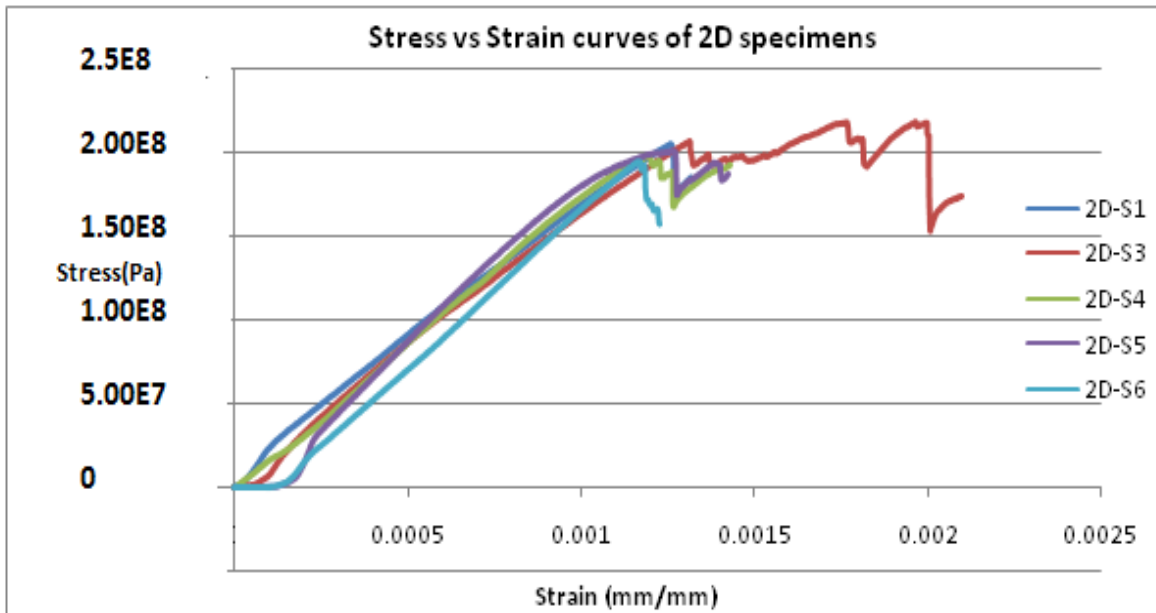


Figure 42: Stress strain diagram of 2D woven GFRP composite specimens

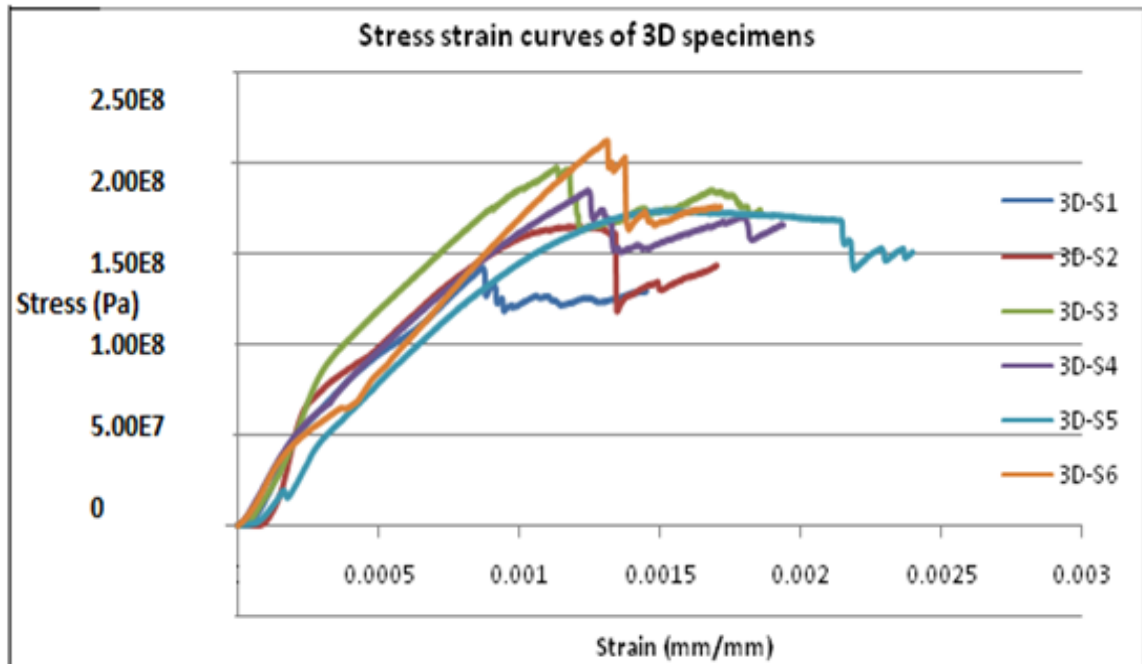


Figure 43: Stress strain diagram of 3D woven GFRP composite specimens

For 3D woven fibre reinforced composite samples, a non linear trend i.e. a plastic region was observed and it continued till the specimen gets ruptured. This response of 3D composite can be due to the fact that stresses are also transferred in z-yarns. On the other hand, this may occur due to geometrical flaws within the composite because geometrical flaws can increase the strains to ultimate failure by distributing the damage throughout the specimen [84]. Experimental results of stress vs. strain curves of 3D specimens are shown in fig. 44.

Compressivestrength of 3D woven notched composite specimens was lower than 2D woven notched composite specimens as observed by Fleck et al [85]. This reduction in in-plane strength properties can be attributed to excessive crimping, matrix rich channels and low fibre volume fraction of 3D composites as compared to 2D composites[86]. Furthermore, it was also concluded that the resultsobtained through experimentation were similar as observed by Walter et al i.e. 3D composites have lower damage resistance than 2D composites and 3D composites have higher damage tolerance than 2D composites [87].

4.3.1.4 Damage modes

Similar trend of failure was observed in 2D and 3D woven GFRP composite specimens. Failure initiation occurs at the hole and propagates laterally towards the edges. Out of plane displacement, splitting of axial yarns and displacement of hole edges was also not observed in damaged specimens. Therefore it was concluded that, Lateral gauge middle (as defined in standard open-hole compression test method i.e. ASTM standard D 6484), a purely compressive failure mode was observed as a dominant damage mode in all specimens[47]. Zoomed view of 2D and 3D woven damaged specimens are shown in fig 45 &46 and fig. 47 & 48 respectively.



Figure 44: Damaged specimens of 2D woven GFRP composites-A zoomed view

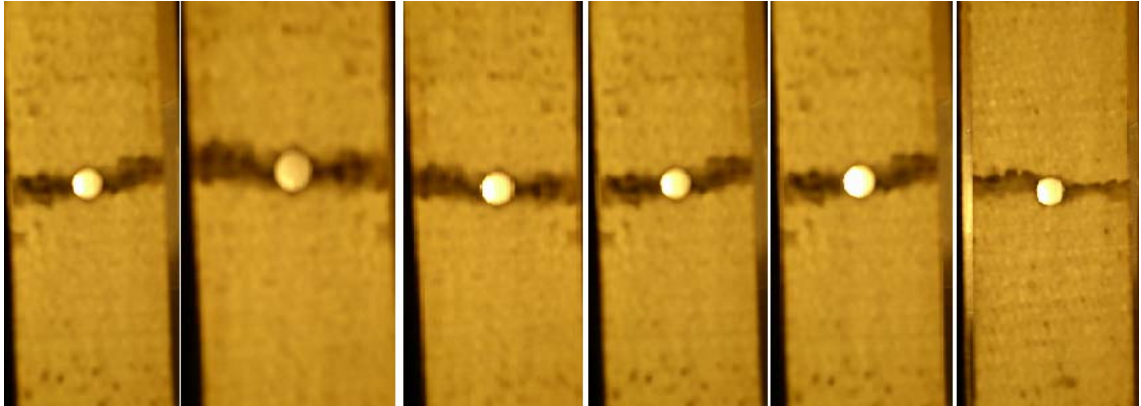


Figure 45: Damaged specimens of 2D woven GFRP composites- Zoomed views are taken by using overhead projector



Figure 46: Damaged specimens of 3D woven GFRP composites-A zoomed view

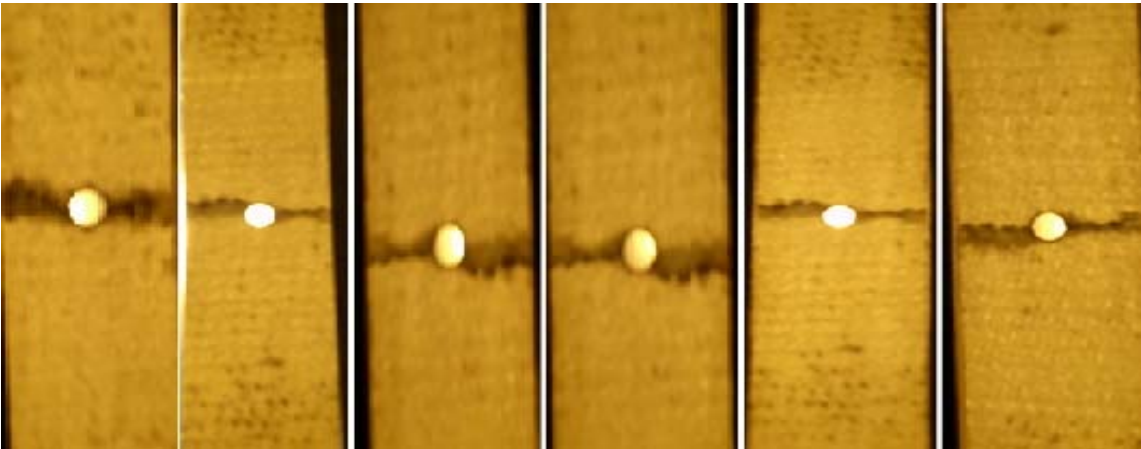


Figure 47: Damaged specimens of 3D woven GFRP composites- Zoomed views are taken by using overhead projector

4.3.2 Numerical findings

A detailed experimental work was carried out in which failure loads, load displacement curves and failure modes of 2D and 3D specimens has been evaluated. As the aim of this work was to analyze and compare the stress state of 2D and 3D open-hole compressive specimens. Therefore a detailed numerical study was also performed.

4.3.2.1 Stress analysis

Knowledge of stress field around the hole is necessary to understand the compressive stress variation in 2D and 3D woven GFRP composite specimens. In order to achieve this purpose, four paths of varying lengths (i.e. 5-12mm) have been created near the hole (As discussed in chapter 3). Longitudinal, transverse, through thickness and in-plane stresses were plotted against true distance along the path. Details are as under;

4.3.2.1.1 Longitudinal stress variation

Similar trend of longitudinal compressive stress variation was observed near the hole in 2D and 3D woven GFRP composite specimens. Initially, lower stresses were observed in 3D specimens than 2D specimens along the length of all paths but the magnitudes of longitudinal stresses were found almost similar in all paths as shown in fig. 49, 50, 51 & 52.

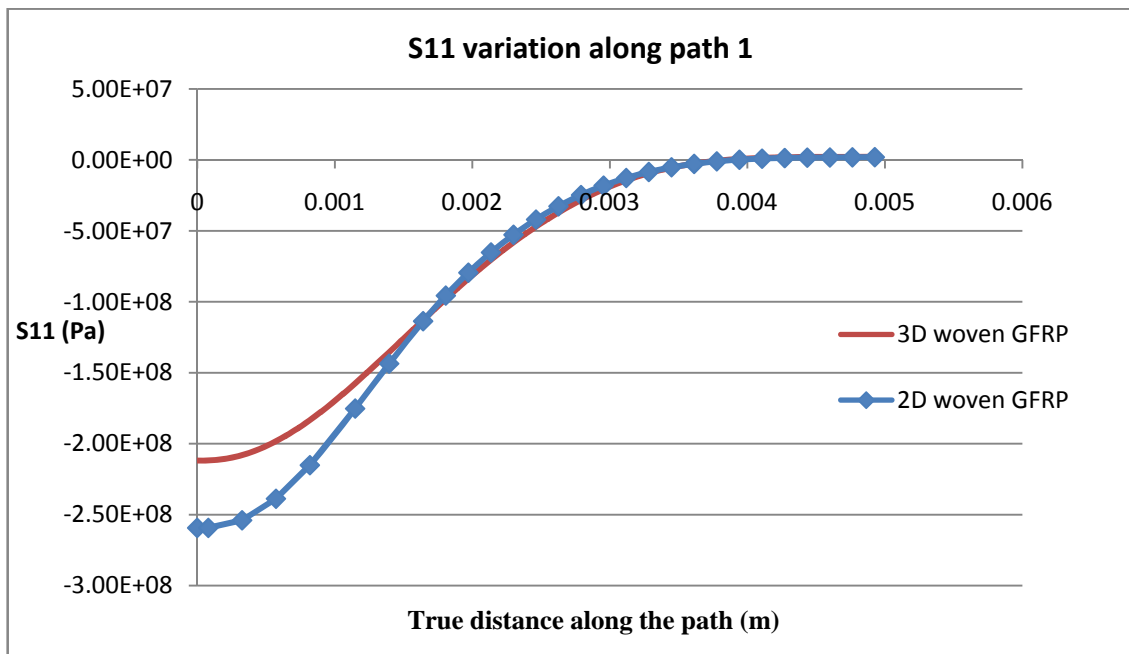


Figure 48: Longitudinal stress variation along path-1

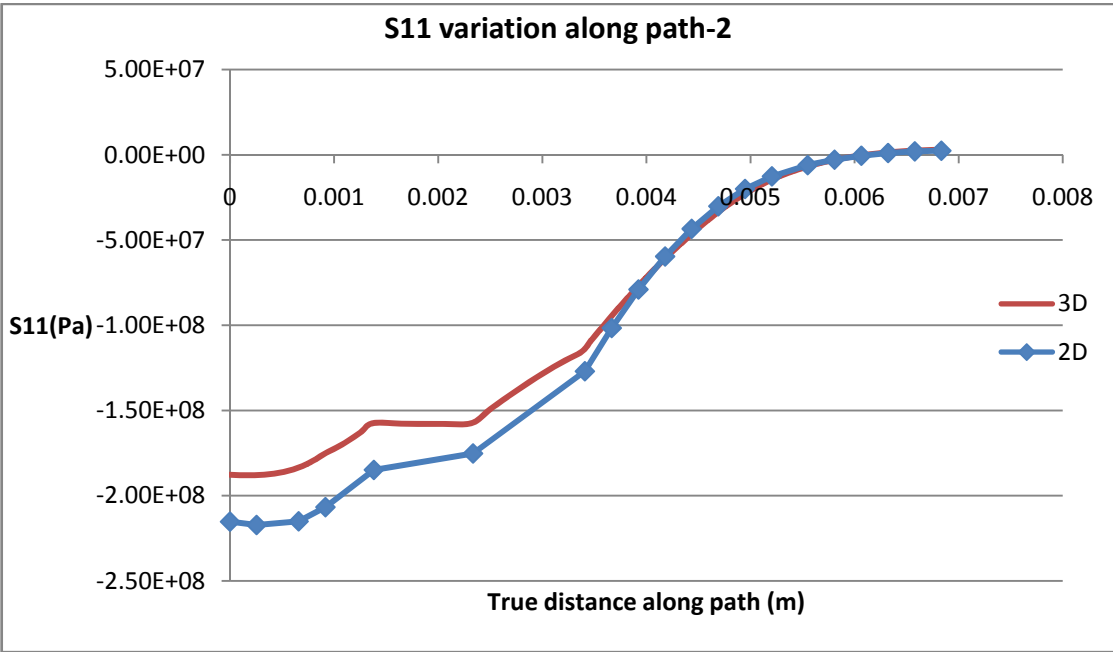


Figure 49: Longitudinal stress variation along path-2

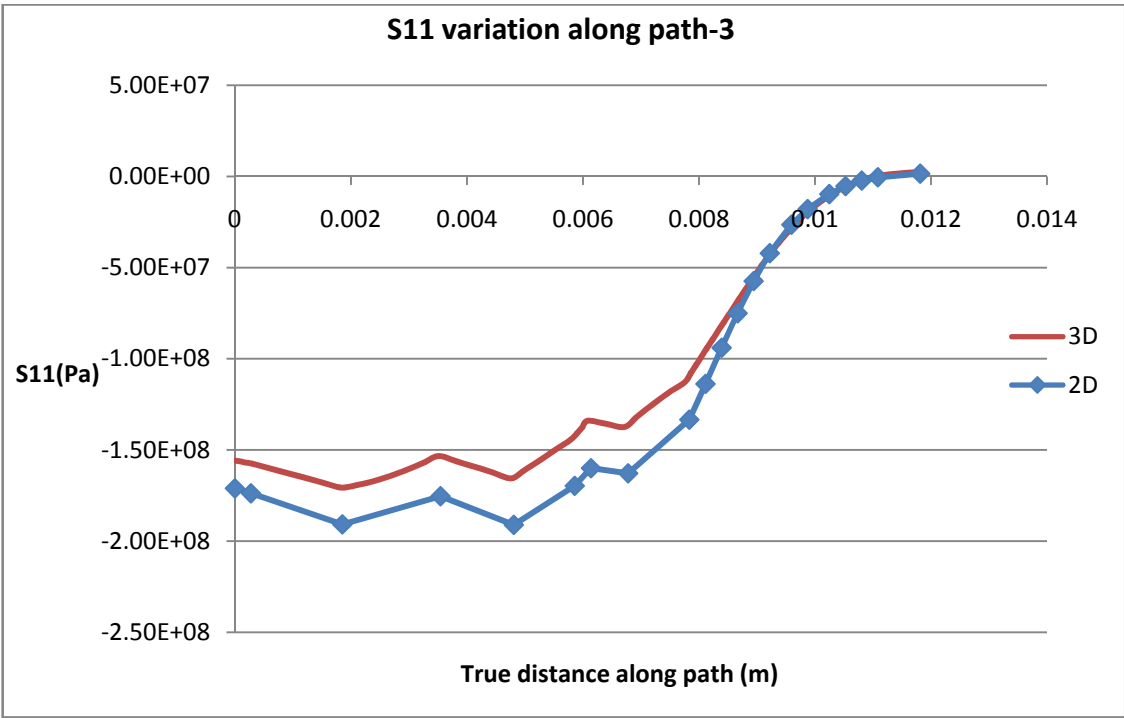


Figure 50: Longitudinal stress variation along path-3

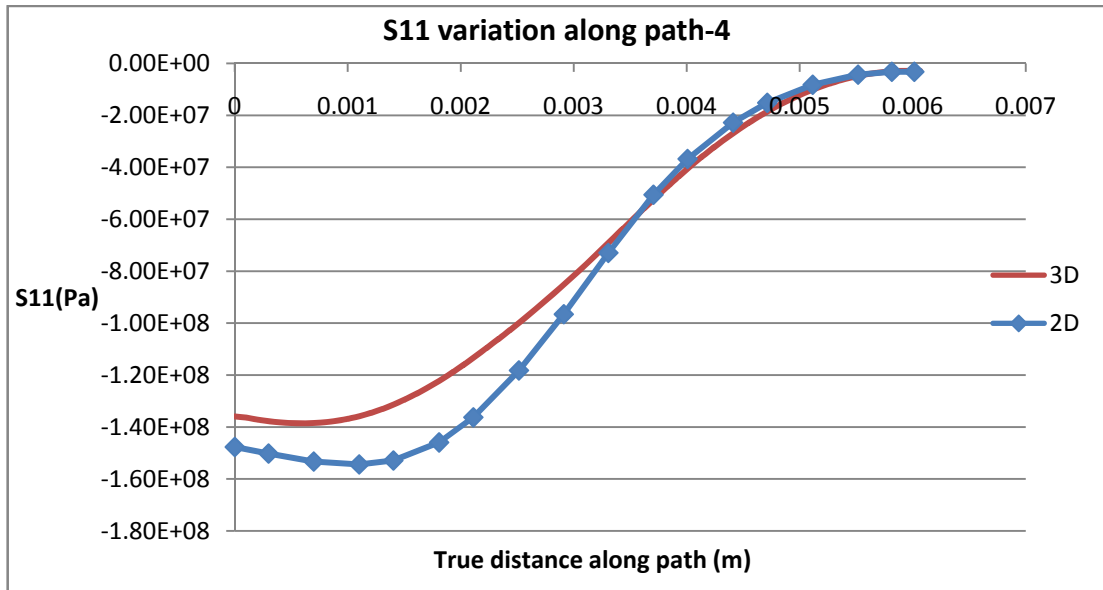


Figure 51: Longitudinal stress variation along path-4

4.3.2.1.2 Transverse stress variation

Similar trend of transverse tensile and compressive stress variation was observed near the hole in 2D and 3D woven GFRP composite specimens. Magnitudes of transverse stresses were also found similar on all four paths around the circle as shown in fig 53, 54, 55 & 56.

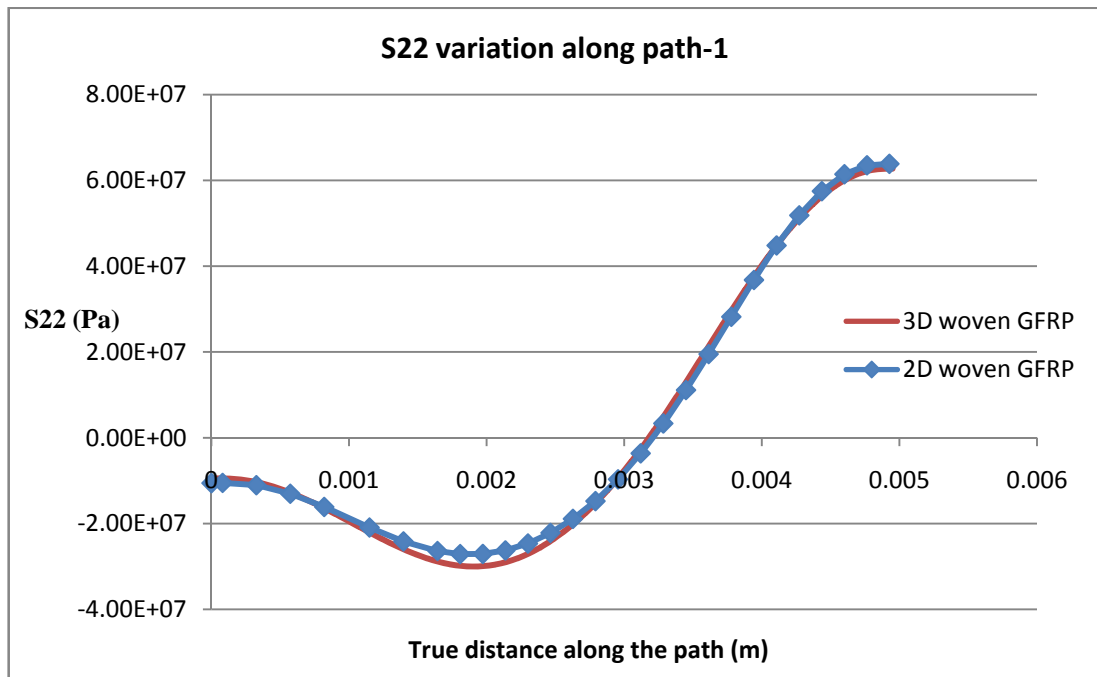


Figure 52: Transverse stress variation along path-1

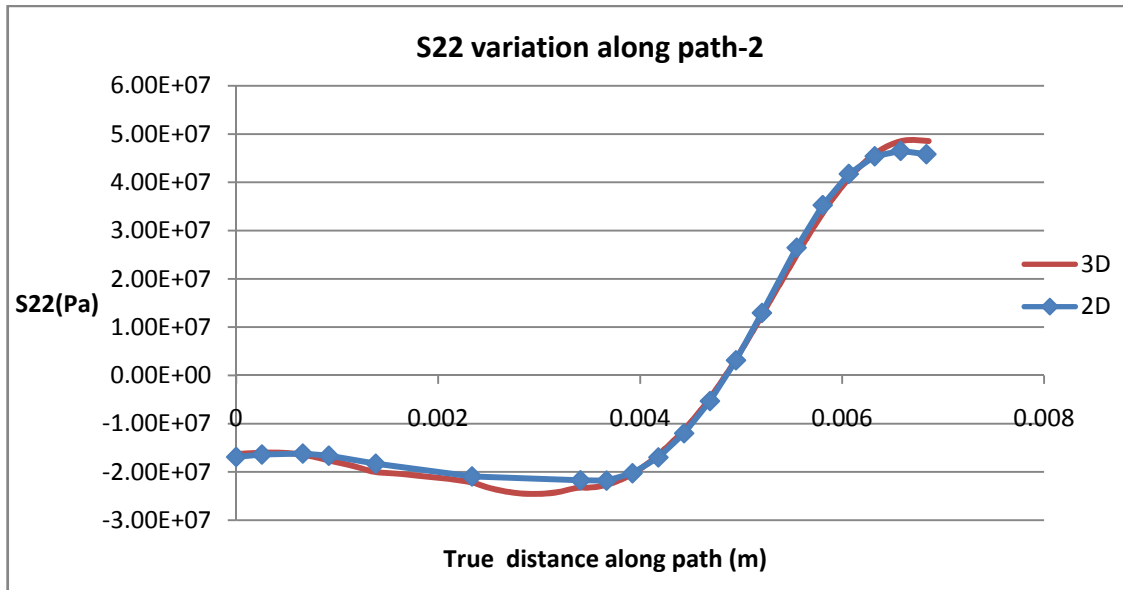


Figure 53: Transverse stress variation along path-2

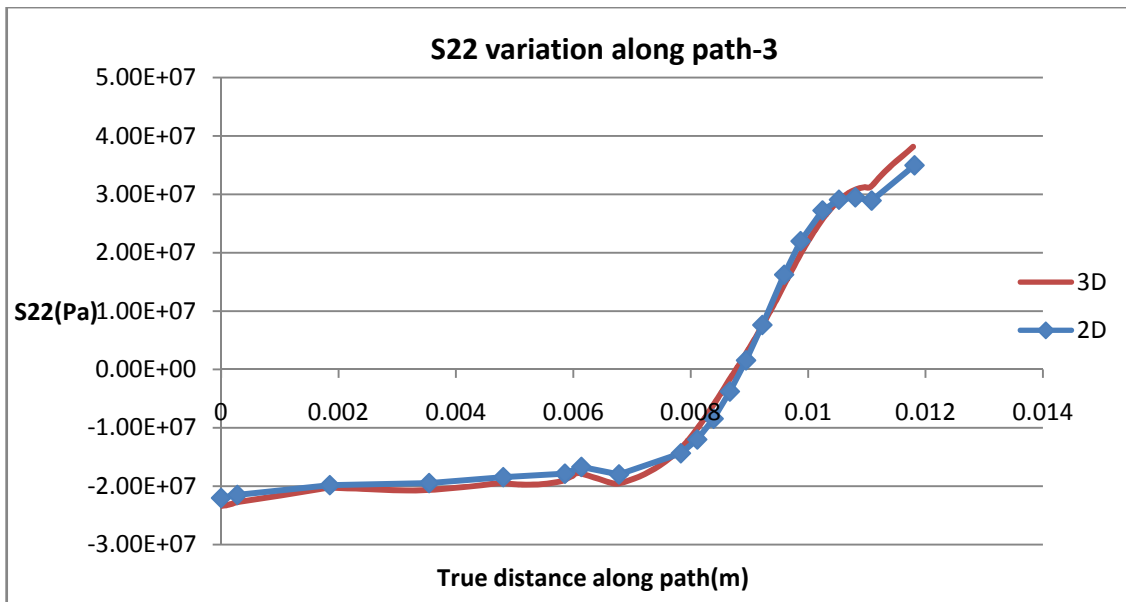


Figure 54: Transverse stress variation along path-3

Magnitude of transverse stresses was seemed to be much lower than failure strength of relative composites. Therefore, it was concluded that the transverse stress was not involved in failure mode mixing.

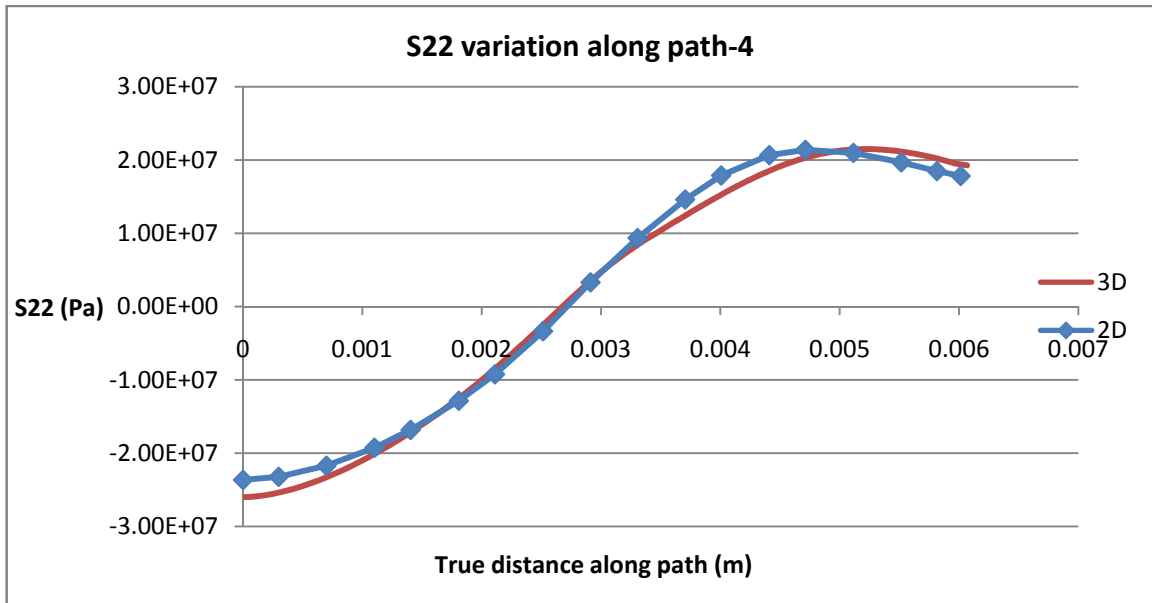


Figure 55: Transverse stress variation along path-4

4.3.2.1.3 Through thickness stress variation

Magnitudes of out of plane compressive and tensile stresses were observed near the hole and found significantly higher in 3D specimens as compared to 2D specimens. This difference can be attributed to involvement of z yarn as it causes distribution of stresses in third direction. On the other hand, it was concluded that the overall trend of through thickness stress variation was found similar in both types of composites as shown in fig. 57, 58, 59 & 60.

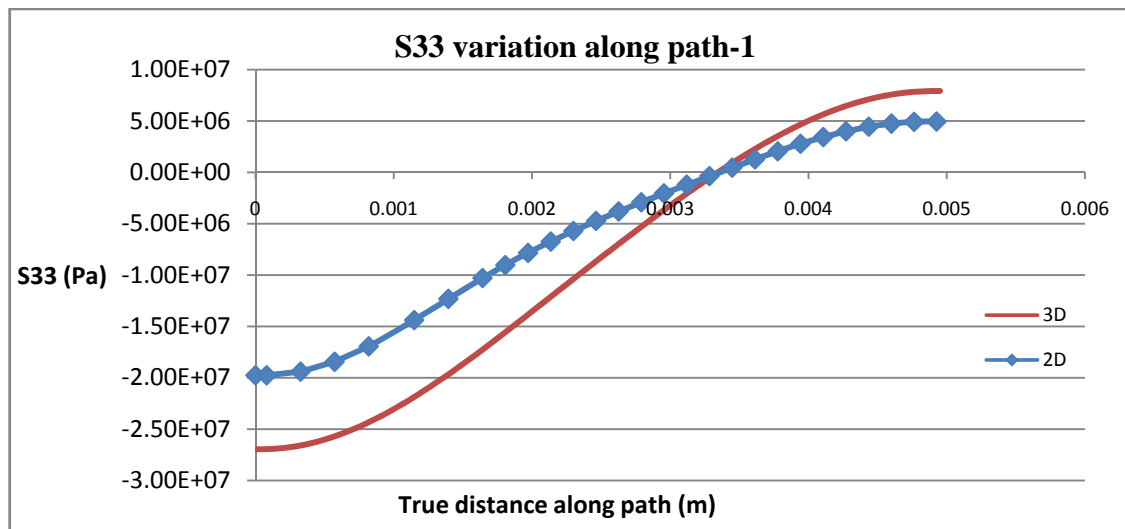


Figure 56: Through thickness stress variation along path-1

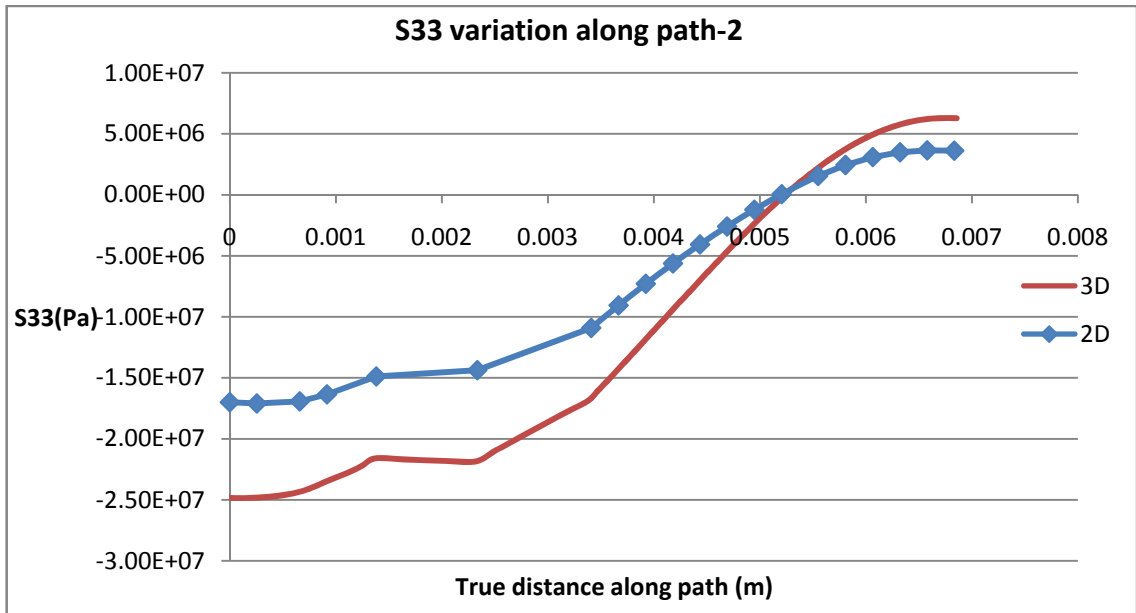


Figure 57: Through thickness stress variation along path-2

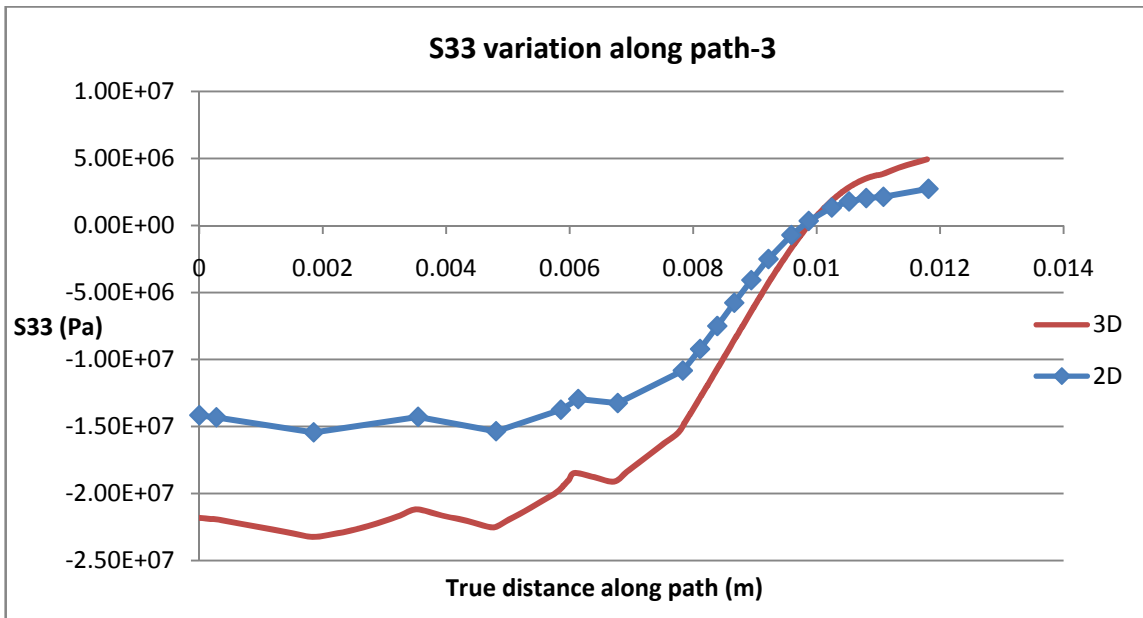


Figure 58: Through thickness stress variation along path-3

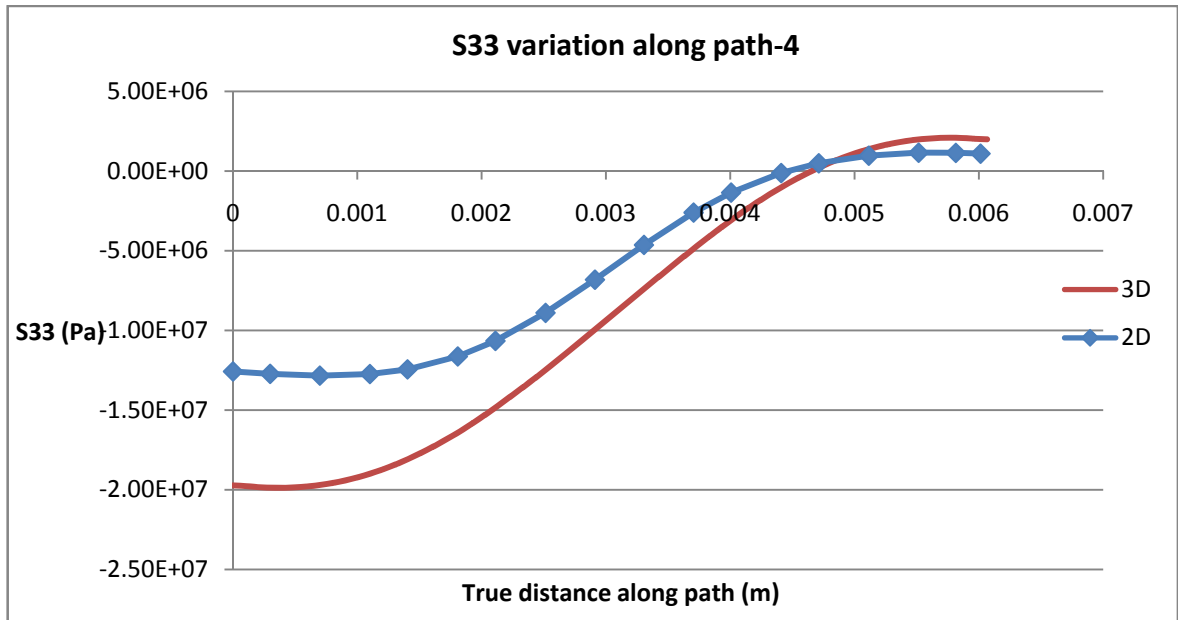


Figure 59: Through thickness stress variation along path-4

4.3.2.1.4 In- plane shear stress variation

Similar trend of in-plane stress variation was observed near the hole in 2D and 3D woven GFRP composite specimens. Magnitudes of in-plane stresses were also seemed to be similar on all four paths as shown in fig 61, 62, 63 & 64.

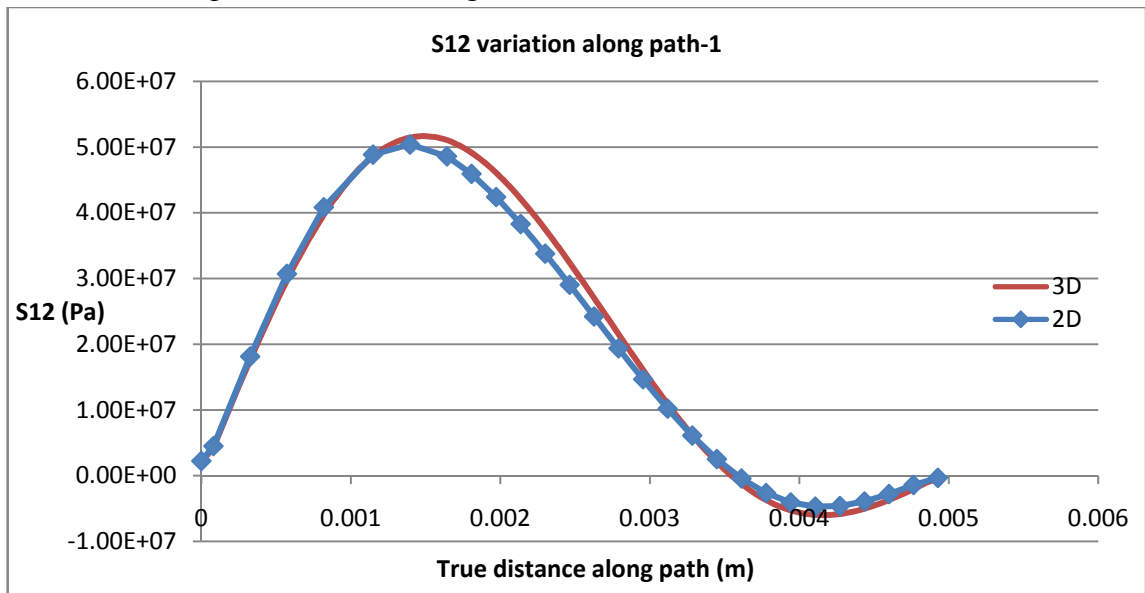


Figure 60: In-plane stress variation along path-1

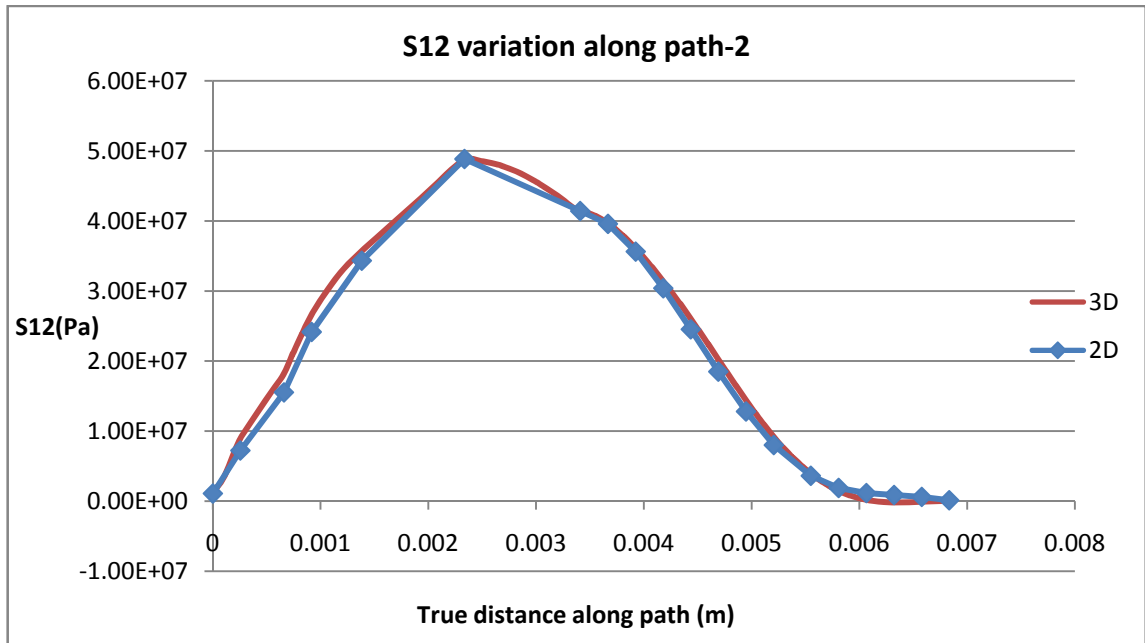


Figure 61: In-plane stress variation along path-2

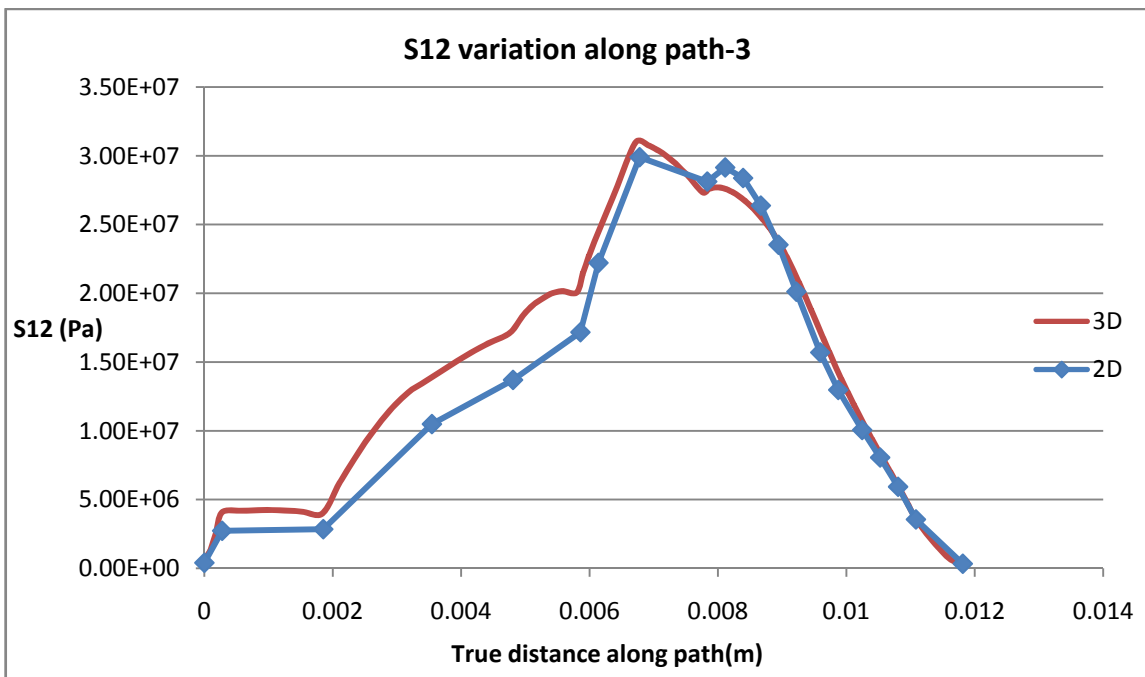


Figure 62: In-plane stress variation along path-3

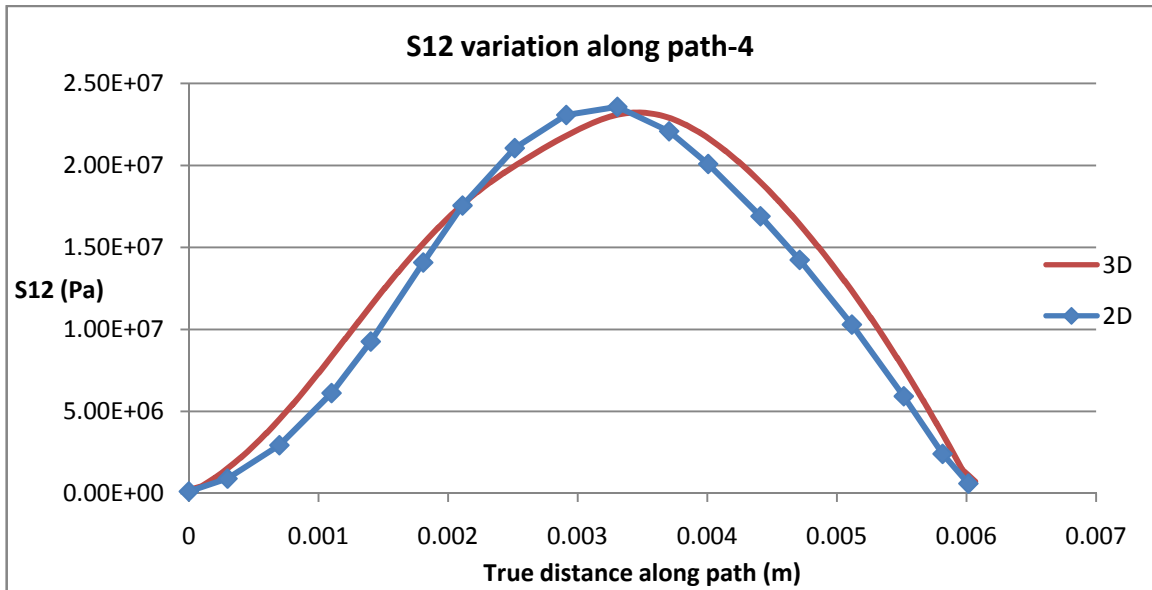


Figure 63: In-plane stress variation along path-4

4.3.2.2 Parametric study using hole size variation

A parametric study was carried out in Abaqus 6.10 in order to determine the effect of hole diameter on compressive stress developed in 3D woven composite as shown in fig.65. Numerical investigation has shown that similar effect of hole diameter was observed on 3D woven GFRP composites as observed by Saha et al [32]. It was observed that the strength of composite decreases with increasing the hole size. Saha et al explained this trend by Couple stress theory as it states that the bending resistance of fibres increases by decreasing the hole size which predominantly increases the hole strength [32].

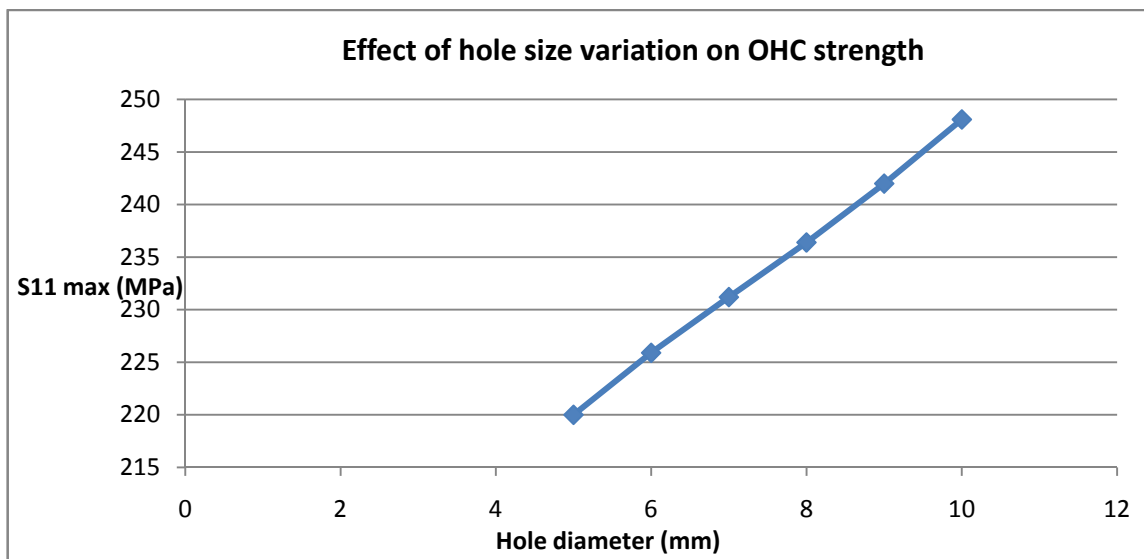


Figure 64: Effect of hole diameter variation on OHC strength of 3D woven GFRP composites

4.4 Concluding remarks

Conventional shell, continuum shell and solid element models were developed to validate the loading and boundary conditions of standard OHC test method i.e. ASTM D6484. A good agreement was observed between numerical and experimental results. In order to capture the through thickness response of 2D and 3D woven composites, solid element model was used. Longitudinal, transverse, in-plane and through thickness stress variation was examined near the hole and it was concluded that the similar trend of variation was observed in all stresses except the through thickness stress. Through thickness stresses seemed to be higher in 3D composites as compared to 2D composites due to the influence of z-yarns.

In the meantime, a detailed experimental analysis was also carried out to get the failure loads, load-displacement curves and stress-strain curves of 2D and 3D woven GFRP composites specimens. Experimental results have clearly shown that the failure loads of 3D composites are lower as compared to 2D composites. Similarly, the failure strength of 3D specimens is lower than 2D specimens. In this research work, it was also concluded that the lateral gauge middle is the dominant failure mode in 2D and 3D woven GFRP composite specimens.

CHAPTER 5: CONCLUSIONS AND FUTURE RECOMMENDATIONS

5.1 Introduction

This chapter discusses the conclusions based on a numerical and experimental study of OHC strength of 2D and 3D woven composites. A detailed comparison of 2D and 3D woven composites is also being made. It also describes the limitations of currently developed FE models and the limitations of experimental work being carried out in this research. Future recommendations for improvement of FE model and discrepancies in the current ASTM standard D6484 in determining the OHC strength of 3D woven composites will also be discussed. Therefore, the aim is to provide some healthy suggestions to further improve the testing method for 3D woven composites.

5.2 Comparison of 2D and 3D woven composites

Following are the conclusions which have been drawn on the basis of numerical and experimental investigation of OHC strength of 2D and 3D woven composites;

- 3D woven composites have lower failure loads than 2D woven composites. This decrease in apparent failure loads is due to reinforcements in through thickness direction which can cause excessive crimping.
- 3D woven composites exhibits higher strains to failure than 2D woven composites. This occurs mainly due to through thickness yarns as they are capable of capturing crack propagation between the yarns.
- LGM, a pure compressive failure mode (as defined by the standard test method i.e. ASTM D6484) was observed in 2D and 3D woven composite specimens. In this mode of damage, failure initiates at the hole and propagates lateral toward the edges.
- Standard deviations observed in 3D woven composites were significantly lower than 2D woven composites. This proves that the results obtained from experimental analysis were repeatable for 3D woven composites.
- The failure stress state of 2D and 3D woven GFRP composite specimens were examined and similar trend of longitudinal, transverse and in-plane stress variation was observed in 2D and 3D woven composites except through thickness stresses as they were significantly higher in 3D specimens as compared to 2D specimens. This

occurs due to presence of 3rd yarn as it increases the through thickness stress component of the composite.

- Similar trend of failure stress concentration was observed near the hole in 2D and 3D woven GFRP composite specimens.

5.3 Limitations

Number of limitations was observed during the numerical and experimental investigation of 2D and 3D woven GFRP composite specimens and is discussed as under;

5.3.1 Numerical modeling

Limitations which were observed in numerical simulations are as under;

- FE model which is being used to analyze the stress state of 2D and 3D woven GFRP composites is not able to separately model the properties of the constituents. 3D orthotropic material properties have been used to define the material model. The drawback of this assumption is that the model is unable to capture the localized damage modes occurring due to the interaction of fibres, matrix and fibre-matrix interface.
- FE model made of solid elements is neither able to predict the failure region nor the desired failure mode. A reasonable approximation can only be made by using the built-in failure criteria which have been developed for isotropic materials e.g. max. Normal stress, von Mises, Tresca etc. This FE model is also not capable of predicting the delamination failure within 2D or 3D damage modes.
- Contact elements are not used between the contact regions of loading and specimens which may cause high localized stresses in the model.
- The current analysis is performed as linear static analysis with the applied load at constant amplitude, so non linear effects have not been taken into account.
- Progressive damage analysis was not performed so failure propagation can't be predicted in the model.
- Current model can only predict failure on the basis of failure index defined by various strength based failure criteria. The built-in failure criteria in ABAQUS 6.10 are based on 2D (plane) stress state and thus cannot be used with 3D solid elements.

- Quarter FE model was developed with symmetric loading and boundary conditions due to homogeneous material properties. This assumption may or may not be applicable for 3D woven composites. Therefore, detailed micromechanics based model is needed which will be able to predict the complete failure stress state.
- Implicit damage modeling scheme was used in FE model in which failed elements are removed from the analysis. A scheme which can accurately predict the stiffness degradation of damaged elements is needed to be used.

5.3.2 Experimental work

Limitations which were observed in experimental work are as under;

- Some suitable experimental technique such as acoustic emission analysis technique is needed to be used to physically examine the failure initiation and propagation within the specimens.
- A detailed parametric study such as hole size, thickness, specimen size etc is needed to be carried out to experimentally study the influence of these parameters on OHC strength of the composites.
- SEM (Scanning electron microscopy) of broken specimens is needed to be performed to better visualize the damage modes of 2D and 3D woven composite specimens.
- Size of RVE is one of the major problems in testing of 3D composites as it may increase or decrease the standard size of specimen. Larger size of specimen may increase the failure loads and take the specimen into non linear stress state or vice versa [88]. Therefore, a detailed X-ray tomography of 3D composites is needed to be performed for examining the actual size of RVE. This will later help in micromechanical modeling of 3D composites.

5.4 Future recommendations

Numerical simulations & experimental results have shown that the existing specimen size, loading configuration and test method are sufficient to induce desired failure stress state within 3D woven composites. There are some possible futures works which can be done to take this research to the lead and are as under;

- In this research work, stress variation is investigated by using macro-mechanical model in which composite is considered as a 3D orthotropic lamina, which is not able to distinct the effect of fibre, matrix and interface. Therefore, micromechanics based FE model is needed which can completely model the failure stress state developed within 3D woven composites. The model will also be capable of predicting the localized damage modes and determining the material properties for 3D woven composites. Similarly, it would be able to include the effect of undulation and crimping of fibres in the analysis.
- The present FE model can only predict the material response in elastic region as non linearities are not included. Therefore, a detailed non linear analysis is needed to be modeled to investigate the failure initiation and propagation within the 3D woven composite specimens.
- Solid model is used to study the stress state response of 2D and 3D woven composites as it considers composite as a whole laminate thus neglecting the effect of stacking sequence of different layers (as in conventional shell and continuum shell element modes). Therefore, FE based model is needed which can cater the effect of stacked layers of 3D composites by examining the properties through failure theories available in literature. The contact of loading and fixture is recommended to be made by using contact elements to examine the effect of actual contact.
- Cohesive elements are also recommended to be used for determining the effect of fibre-matrix interface on OHC response of 3D woven composites.
- A dynamic analysis is needed to be performed with actual loadings as the present solid model is unable to predict the point of damage initiation and peakload at which failure initiates.
- Physics based criterion such as LaRC04 (Langley Research Center) is needed to be implemented in FE model to better visualize the influence of 3D stress developed within the model. The criterion has the ability to individually examine the various damage modes of fibre and matrix.
- In this study, it is concluded that the existing ASTM standard D6484 can reliably be used to determine the OHC strength of 3D woven interlock composites but these results cannot be simply implemented on all weave architectures of 3D composites such as 3D woven (orthogonal), stitched, braided and knitted fabrics. Therefore, effect of fibre architecture is needed to be investigated by using numerical and experimental techniques.

- In 3D composites, size of specimen varies with the size of unit cells included in the sample. Therefore, the size of unit cells for various weave architectures of 3D composites is needed to be investigated for better understanding of failure modes of 3D composites.
- Experimental technique such as Moiré interferometry, strain gauging and birefringent coating is needed to be used to accurately determine the stress concentration factor of composite plates [89].
- In currently FE model and fixture, out of plane displacement was constrained. Thus, model must be modified to cater the out of plane response of the 3D composite.

Publication

Engr. Muhammad Kamran, Dr. RizwanSaeedChoudhry, Dr. S. Kamran Afaq,
An Investigation of “Open-hole Compression” testing method for use with 3D woven
composites in Proceedings of Pakistan Composites Show, 5th Dec 2012, Islamabad Hotel,
Islamabad, ISBN: 978-969-8535-13-1

References

- [1]. Kamiya, R., B.A. Cheeseman, P. Popper and T.-W. Chou, Some recent advances in the fabrication and design of three-dimensional textile preforms: a review. *Composites Science and Technology*, 2000. 60(1): p. 33-47.
- [2]. Gu, Pu, and Mansour Hussein Mohamed. "Shaped three-dimensional engineered fiber preforms with insertion holes and rigid composite structures incorporating same, and method therefor." U.S. Patent No. 6,283,168. 4 Sep. 2001.
- [3]. Masters, J.E. and M.A. Portanova, Standard Test Methods for Textile Composites, NASA Contractor Report 4751, September 1996
- [4]. M.H. Mohamed and A.E. Bogdanovich, Comparative analysis of different 3D weaving processes, machines and products, 17th International Conference on Composite Materials. 2009. Edinburgh International Convention Centre (EICC), Edinburgh, UK.
- [5]. Bannister, Michael. "Challenges for composites into the next millennium—a reinforcement perspective." *Composites Part A: Applied Science and Manufacturing* 32.7 (2001): 901-910.
- [6]. Yang, Jenn-Ming, Chang-Long Ma, and Tsu-Wei Chou. "Fiber inclination model of three-dimensional textile structural composites." *Journal of Composite Materials* 20.5 (1986): 472-484.
- [7]. Nehme, Samer, et al. "Numerical/analytical methods to evaluate the mechanical behavior of interlock composites." *Journal of Composite Materials* 45.16 (2011): 1699-1716.
- [8]. Pochiraju, Kishore, and Tsu Wei Chou. "Three-dimensionally woven and braided composites. I: A model for anisotropic stiffness prediction." *Polymer composites* 20.4 (1999): 565-580.
- [9]. Whitcomb, John, Kyeongsik Woo, and Sitaram Gundapaneni. "Macro finite element for analysis of textile composites." *Journal of composite materials* 28.7 (1994): 607-618.
- [10]. Cox, B. N., W. C. Carter, and N. A. Fleck. "A binary model of textile composites—I. Formulation." *Acta Metallurgica et Materialia* 42.10 (1994): 3463-3479.

-
- [11]. Naik, Rajiv A. "TEXCAD: TEXile Composite Analysis for Design." In NASA, Langley Research Center Mechanics of Textile Composites Conference p 587-596(SEE N 96-17705 04-24). Vol. 1995. 1995.
- [12]. Stig, F. and S. Hallström, Assessment of the mechanical properties of a new 3D woven fibre composite material. *Composites Science and Technology*, 2009. 69(11–12): p. 1686-1692.
- [13]. ASTM Standard D 4762 – 2004, " Historical Standard: ASTM D4762-04 Standard Guide for Testing Polymer Matrix Composite Materials", ASTM International West Conshohocken, PA, 2008, DOI: 10.1520/D4762-04, www.astm.org
- [14]. ASTM Standard D6856 / D6856M - 2003(2008)e1, "Standard Guide for Testing Fabric-Reinforced 'Textile' Composite Materials", ASTM International West Conshohocken, PA, 2008, DOI: 10.1520/D6856_D6856M-03R08E01, www.astm.org
- [15]. Pankow, M., A. Salvi, A.M. Waas, C.F. Yen, and S. Ghiorse, Split Hopkinson pressure bar testing of 3D woven composites. *Composites Science and Technology*, 2011. 71(9): p. 1196-1208.
- [16]. Ansar, Mahmood, Wang Xinwei, Zhou Chouwei. Modeling strategies of 3D woven composites, a review." *Composite Structures* 93.8 (2011): 1947-1963.
- [17]. Kuo, W.S., J. Fang, and H.W. Lin, Failure behavior of 3D woven composites under transverse shear. *Composites Part A: Applied Science and Manufacturing*, 2003. 34(7): p. 561-575.
- [18]. Tarnopol'skii, Y.M., V.L. Kulakov, and A.K. Aranautov, Measurements of shear characteristics of textile composites. *Composites & Structures*, 2000. 76(1-3): p. 115-123.
- [19]. B. Dambrine, J-N Mahieu, J. Goering and K. Ouellette, Development of 3D Woven, Resin Transfer Molded Fan Blades, *TexComp 9*, Newark, DE, October 13-15, 2008.
- [20]. Iarve, E. V., and N. J. Pagano. "Singular full-field stresses in composite laminates with open holes." *International journal of solids and structures* 38.1 (2001): 1-28.
- [21]. Iarve, E. V. "Spline variational three dimensional stress analysis of laminated composite plates with open holes." *International Journal of Solids and Structures* 33.14 (1996): 2095-2118.

-
- [22]. Soutis, C., N. A. Fleck, and P. A. Smith. "Failure prediction technique for compression loaded carbon fibre-epoxy laminate with open holes." *Journal of Composite Materials* 25.11 (1991): 1476-1498.
- [23]. Hatta, Hiroshi, Keisuke Taniguchi, and YasuoKogo."Compressive strength of three-dimensionally reinforced carbon/carbon composite." *Carbon* 43.2 (2005): 351-358.
- [24]. Suemasu, H., H. Takahashi, and T. Ishikawa. "On failure mechanisms of composite laminates with an open hole subjected to compressive load." *Composites science and technology* 66.5 (2006): 634-641.
- [25]. Tan, P., L. Tong, G.P. Steven, and T. Ishikawa, Behavior of 3D orthogonal woven CFRP composites. Part I. Experimental investigation. *Composites Part A: Applied Science and Manufacturing (Incorporating Composites and Composites Manufacturing)*, 2000. 31(3): p. 259-271.
- [26]. Whitney, J. M., and R. J. Nuismer. "Stress fracture criteria for laminated composites containing stress concentrations." *Journal of Composite Materials* 8.3 (1974): 253-265.
- [27].Hatta, Hiroshi, Keisuke Taniguchi, and YasuoKogo."Compressive strength of three-dimensionally reinforced carbon/carbon composite." *Carbon* 43.2 (2005): 351-358.
- [28]. Davim, J. Paulo, J. Campos Rubio, and A. M. Abrao. "A novel approach based on digital image analysis to evaluate the delamination factor after drilling composite laminates." *Composites science and technology* 67.9 (2007): 1939-1945.
- [29]. Kambiz, Iraj and Farhad, "Investigation of stress concentration factor for finite width orthotropic rectangular plates with a circular opening using 3D finite element model", *Journal of mechanical engineering, UDK-UDC 539.319:624.073*
- [30]. Waas, Anthony M., AhnJunghyun, and Amir R. Khamseh. "Compressive failure of notched uniply composite laminates." *Composites Part B: Engineering* 29.1 (1998): 75-80.
- [31].Goutianos, S., C. Galiotis, and T. Peijs."Compressive failure mechanisms in multi-fibre microcomposites." *Composites Part A: Applied Science and Manufacturing* 35.4 (2004): 461-475.
- [32]. Saha, M., R. Prabhakaran, and W. A. Waters Jr. "Compressive behavior of pultruded composite plates with circular holes." *Composite structures* 65.1 (2004): 29-36.

-
- [33]. Poon, C., et al. Damage Progression Under Compressive Loading in Composite Laminates Containing an Open Hole. NATIONAL RESEARCH COUNCIL OF CANADA OTTAWA (ONTARIO) INST FOR AEROSPACE RESEARCH, 1992.
- [34]. Wang, J., P. J. Callus, and M. K. Bannister."Experimental and numerical investigation of the tension and compression strength of un-notched and notched quasi-isotropic laminates." *Composite Structures* 64.3 (2004): 297-306.
- [35]. Schultheisz, Carl R., and Anthony M. Waas. "Compressive failure of composites, part I: testing and micromechanical theories." *Progress in Aerospace Sciences* 32.1 (1996): 1-42.
- [36]. Lee, J., and C. Soutis."Measuring the notched compressive strength of composite laminates: Specimen size effects." *Composites Science and Technology* 68.12 (2008): 2359-2366.
- [37]. Basu, Shiladitya, Anthony M. Waas, and Damodar R. Ambur."Compressive failure of fiber composites under multi-axial loading." *Journal of the Mechanics and Physics of Solids* 54.3 (2006): 611-634.
- [38]. Hahn, H. Thomas and Jerry G. Williams."Compression failure mechanisms in unidirectional composites." *Composite Materials: Testing and Design (Seventh Conference)*, ASTM STP. Vol. 893. 1986.
- [39]. Moran, P. M., X. H. Liu, and C. F. Shih."Kink band formation and band broadening in fiber composites under compressive loading." *Actametallurgicaetmaterialia* 43.8 (1995): 2943-2958.
- [40] Naik, N. K., and Rajesh S. Kumar. "Compressive strength of unidirectional composites: evaluation and comparison of prediction models." *Composite structures* 46.3 (1999): 299-308.
- [41]. Dadkhah, M. S., B. N. Cox, and W. L. Morris."Compression-compression fatigue of 3D woven composites." *Actametallurgicaetmaterialia* 43.12 (1995): 4235-4245.
- [42]. Masters, John E. "Improved impact and delamination resistance through interleaving." *Key Engineering Materials* 37 (1991): 317.
- [43]. Waas, Anthony M., and Carl R. Schultheisz. "Compressive failure of composites, part II: experimental studies." *Progress in Aerospace Sciences* 32.1 (1996): 43-78.
- [44].Fleck, N. A. and Budiansky, B. "Compressive failure of fiber composites", *Journal of the Mechanics and Physics of Solids*, Vol. 41, No. 1 (1993) 183-211 .

-
- [45].Saha, M., R. Prabhakaran, and W. A. Waters Jr. "Compressive behavior of pultruded composite plates with circular holes." *Composite structures* 65.1 (2004): 29-36.
- [46]. Schultheisz, Carl R., and Anthony M. Waas. "Compressive failure of composites, part I: testing and micromechanical theories." *Progress in Aerospace Sciences* 32.1 (1996): 1-42.
- [47]. Fleck, N. A., P. M. Jelf, and P. T. Curtis."Compressive failure of laminated and woven composites." (1995): 212-220.
- [48]. Zako, Masaru, Yasutomo Uetsuji, and Tetsusei Kurashiki."Finite element analysis of damaged woven fabric composite materials." *Composites Science and Technology* 63.3 (2003): 507-516.
- [49].Carvalho, N. V., S. T. Pinho, and P. Robinson."Compressive failure of 2D woven composites." *ICCM-17 Conference proceedings*. 2009.
- [50]. K. Mohamed Kaleemulla, B. Siddeswarappa, K. G. Satish, "Investigations to Model and Analyse the OHC Strength of Hybrid Composites, *SOURCE, Journal of Engineering Science & Technology Review*;2009, Vol. 2 Issue 1, p91.
- [51]. Tan, Ping, et al. "Behavior of 3D orthogonal woven CFRP composites. Part I. Experimental investigation." *Composites Part A: Applied Science and Manufacturing* 31.3 (2000): 259-271.
- [52].Sohn, Min-Seok, and Xiao-ZhiHu."Processing of carbon-fibre/epoxy composites with cost-effective interlaminar reinforcement." *Composites science and technology* 58.2 (1998): 211-220.
- [53].Mouritz, A. P., et al. "Review of applications for advanced three-dimensional fibre textile composites." *Composites Part A: applied science and manufacturing* 30.12 (1999): 1445-1461.
- [54]. Sun, Baozhong, Yuankun Liu, and Bohong Gu. "A unit cell approach of finite element calculation of ballistic impact damage of 3-D orthogonal woven composite." *Composites Part B: Engineering* 40.6 (2009): 552-560.
- [55] Cox, B. N., et al. "Mechanisms of compressive failure in 3D composites." *Acta Metallurgica et Materialia* 40.12 (1992): 3285-3298.
- [56].Cox, B. N., et al. "Failure mechanisms of 3D woven composites in tension, compression, and bending." *Acta Metallurgica et Materialia* 42.12 (1994): 3967-3984.

-
- [57]. Sankar, Bhavani V., and Ramesh V. Marrey. "Analytical method for micromechanics of textile composites." *Composites Science and Technology* 57.6 (1997): 703-713.
- [58] Tan, P., L. Tong, and G. P. Steven. "Modelling for predicting the mechanical properties of textile composites—a review." *Composites Part A: Applied Science and Manufacturing* 28.11 (1997): 903-922.
- [59] Nurhaniza, M., et al. "Finite element analysis of composites materials for aerospace applications." *IOP Conference Series: Materials Science and Engineering*. Vol. 11.No. 1. IOP Publishing, 2010.
- [60] Schuecker, Clara, and Heinz E. Pettermann. "Constitutive ply damage modeling, FEM implementation, and analyses of laminated structures." *Computers & Structures* 86.9 (2008): 908-918.
- [61] Rao, Subba, and VinaySagar. Evaluation of mechanical properties of laminated composites using Multi-Continuum Theory in ABAQUS. Diss. Wichita State University, 2010.
- [62] Lin, H. J., C. C. Tsai, and J. S. Shie. "Failure analysis of woven-fabric composites with moulded-in holes." *Composites science and technology* 55.3 (1995): 231-239.
- [63]. ASTM D6484 / D6484M - 09 Standard Test Method for Open-Hole Compressive Strength of Polymer Matrix Composite Laminates, ASTM International West Conshohocken, PA, 2009, DOI: 10.1520/D6484_D6484M-09, www.astm.org
- [64]. Kyriakides, S., et al. "On the compressive failure of fiber reinforced composites." *International Journal of Solids and Structures* 32.6 (1995): 689-738.
- [65]. Yang, B., et al. "Bending, compression, and shear behavior of woven glass fiber–epoxy composites." *Composites Part B: Engineering* 31.8 (2000): 715-721.
- [66]. Whitney, J. M., and R. Y. Kim. "Effect of stacking sequence on the notched strength of laminated composites." *Composite Materials: Testing and Design (Fourth Conference)*. ASTM STP. Vol. 617. 1976.
- [67]. Chapter 2, *Mechanics of composite materials* book by autar.k. kaw
- [68]. Zhang, Yan, Ping Zhu, and XinminLai. "Finite element analysis of low-velocity impact damage in composite laminated plates." *Materials & design* 27.6 (2006): 513-519.

-
- [69]. Soutis, C., and N. A. Fleck. "Static compression failure of carbon fibre T800/924C composite plate with a single hole." *Journal of Composite Materials* 24.5 (1990): 536-558.
- [70]. Bahei-El-Din, Yehia A., and Mohammed A. Zikry. "Impact-induced deformation fields in 2D and 3D woven composites." *Composites science and technology* 63.7 (2003): 923-942.
- [71]. Pahr, D.H., et al., A study of short-beam-shear and double-lap-shear specimens of glass fabric/epoxy composites. *Composites Part B: Engineering*, 2002. 33(2): p. 125-132.
- [72]. Scida, D., et al. "A micromechanics model for 3D elasticity and failure of woven-fibre composite materials." *Composites Science and Technology* 59.4 (1999): 505-517.
- [73]. Bahei-El-Din, Yehia A., and Mohammed A. Zikry. "Impact-induced deformation fields in 2D and 3D woven composites." *Composites science and technology* 63.7 (2003): 923-942.
- [74]. N.A. Fleck, D. Liua, J.Y. Shu, Micro buckle initiation from a hole and from the free edge of a fibre composite, *International journal of solids and structures*, PERGAMON Elsevier, Received 17 April 1998
- [75]. Dávila, Carlos G., and Pedro P. Camanho. "Failure criteria for FRP laminates in plane stress." *Proceedings of the AIAA/ASME/ASCE/AHS/ASC 44th Structures, Structural Dynamics and Materials (SDM) Conference*, Norfolk, VA. 2003.
- [76]. Davila, Carlos G., Pedro P. Camanho, and Cheryl A. Rose. "Failure criteria for FRP laminates." *Journal of Composite materials* 39.4 (2005): 323-345.
- [77]. Hashin, Zvi. "Failure criteria for unidirectional fiber composites." *Journal of applied mechanics* 47 (1980): 329.
- [78]. Hashin, Zvi, and Assa Rotem. "A fatigue failure criterion for fiber reinforced materials." *Journal of composite materials* 7.4 (1973): 448-464.
- [79]. Lin, H. J., C. C. Tsai, and J. S. Shie. "Failure analysis of woven-fabric composites with moulded-in holes." *Composites science and technology* 55.3 (1995): 231-239.
- [80]. ABAQUS help files
- [81]. Valadez-Gonzalez, A., et al. "Effect of fiber surface treatment on the fiber-matrix bond strength of natural fiber reinforced composites." *Composites Part B: Engineering* 30.3 (1999): 309-320.

-
- [82]. Ng, S-P., K. J. Lau, and P. C. Tse. "3D finite element analysis of tensile notched strength of 2/2 twill weave fabric composites with drilled circular hole." *Composites Part B: Engineering* 31.2 (2000): 113-132.
- [83]. Bogdanovich, Alexander E. "Advancements in manufacturing and applications of 3D woven preforms and composites." *Proceeding of the 16th International Conference on Composites Materials (ICCM-16)*. 2007
- [84] Cox, B. N., et al. "Mechanisms of compressive failure in 3D composites." *Actametallurgicaetmaterialia* 40.12 (1992): 3285-3298.
- [85]. Fleck, N. A., P. M. Jelf, and P. T. Curtis. "Compressive failure of laminated and woven composites." *Journal of composites technology & research* 17.3 (1995): 212-220.
- [86] Cox, B. N., et al. "Mechanisms of compressive failure in 3D composites." *Actametallurgicaetmaterialia* 40.12 (1992): 3285-3298.
- [87]. Walter, T. R., et al. "Monotonic and cyclic short beam shear response of 3D woven composites." *Composites Science and Technology* 70.15 (2010): 2190-2197.
- [88]. Callus, P. J., et al. "Tensile properties and failure mechanisms of 3D woven GRP composites." *Composites Part A: Applied Science and Manufacturing* 30.11 (1999): 1277-1287.
- [89]. Patterson, E. A., and E. J. Olden. "Optical analysis of crack tip stress fields: a comparative study." *Fatigue & Fracture of Engineering Materials & Structures* 27.7 (2004): 623-635.